Production and use of H_2O_2 for atom-efficient functionalization of hydrocarbons and small molecules

Neil M. Wilson,† Daniel T. Bregante,† Pranjali Priyadarshini and David W. Flaherty*

DOI: 10.1039/9781788010634-00122

H_2O_2 is a relatively benign and selective oxidant, which has motivated research into scalable methods for H_2O_2 production and the design of catalysts to perform oxidations with H_2O_2. The energy intensive anthraquinone oxidation process is the standard for H_2O_2 production, however, alternatives such as electrocatalytic oxygen reduction and the direct synthesis of H_2O_2 have significant potential. Recent publications have investigated the reactor design, the mechanism for H_2O_2 formation, and the synthesis of increasingly selective catalysts and have demonstrated the role of proton–electron transfer in H_2O_2 formation and improving selectivities by alloying transition metals. H_2O_2 is a relatively unstable molecule which readily decomposes over a catalyst, making it difficult to use H_2O_2 for many oxidation reactions selectively. As such, there is extensive research on the use of H_2O_2 for different oxidation reactions, with the most common being olefin epoxidation. Olefin epoxidation is readily catalyzed by transition metal substituted zeolites, polyoxometallates, metal oxides, and homogeneous coordination compounds. These catalysts activate H_2O_2 to form many reactive intermediates, which possess selectivities for the epoxidation of olefins that reflect electronic properties of the reactive intermediate and the substrate. Ideally, H_2O_2 could be used for epoxidations within a single reactor (*i.e.*, tandem catalysis), which would reduce costs from purification and transportation of H_2O_2. However, performing these reactions together typically provides poor epoxidation selectivities due to over-oxidation products. These chemistries are industrially relevant and present many unanswered questions of fundamental interest that warrant future investigation.

1 Overview of H_2O_2 production and use

1.1 H_2O_2 as a green oxidant to replace chlorine

Selective oxidations are used at the industrial scale in the manufacture of many familiar products used today. The activation of strong C–H bonds in alkanes and the epoxidation of alkenes by selective oxidants are involved in the synthesis of building block chemicals (*e.g.*, ethylene oxide, propylene oxide, adipic acid) used to produce indispensable materials (*e.g.*, polyurethane, nylon, and polyethylene terephthalate).[1,2] Oxidations are important also in the non-destructive bleaching of paper,[3] the disinfection of wastewater,[4,5] and the deactivation of chemical warfare agents.[6] Many of these oxidations are currently accomplished through the use of chlorinated oxidizers; however, their potential for severe environmental impact motivate the replacement of Cl containing oxidants with those derived from O_2 such as H_2O_2 (the focus of this review) as well as O_2 and O_3, which are more environmentally benign.

Department of Chemical and Biomolecular Engineering, University of Illinois Urbana-Champaign, Urbana, IL 61801, USA. E-mail: dwflhrty@illinois.edu
†Contributed equally.

However, as discussed below, there are significant environmental and economic barriers to overcome before chlorinated oxidants can be replaced.

Chlorine containing compounds (*e.g.*, Cl_2, NaClO) are often used for oxidations[3,4] because they are not only selective but also inexpensive and available in large quantities from the chlor-alkali process. This well-established process converts brine (NaCl solution) into Cl_2, H_2, and caustic soda (NaOH) by electrolysis and is practiced on an incredible scale (4.5×10^7 tons Cl_2 produced and 1.5×10^{11} kWh energy consumed annually).[7,8] Consequently, the use of Cl_2 has become engrained in many industrial processes, such as oxidations, despite the difficulties and dangers associated with use and storage of large quantities of Cl_2.[7,9] Cl_2 can be insidious, and even when proper care is taken, it may be released into the environment where it forms carcinogenic and corrosive residues (*e.g.*, chlorinated dioxins, chloroform).[10–12] Figure 1 shows that environmental dioxin contamination near Lake Huron increased roughly in proportion to the scale of the chlor-alkali industry in the United States during the past century. While there is evidence for the negative impact of Cl contamination (Fig. 1), there is still much that is unknown about the scale and potential environmental impact of the contamination in the air and soil.[13,14] United States federal regulation standards require that potential contaminants be proven undoubtedly hazardous prior to implementing regulatory actions (or changes in regulations),[15] therefore, little governmental regulation has been put in place to limit environmental Cl exposure. Currently, only 65% of all Cl consumed is used in the

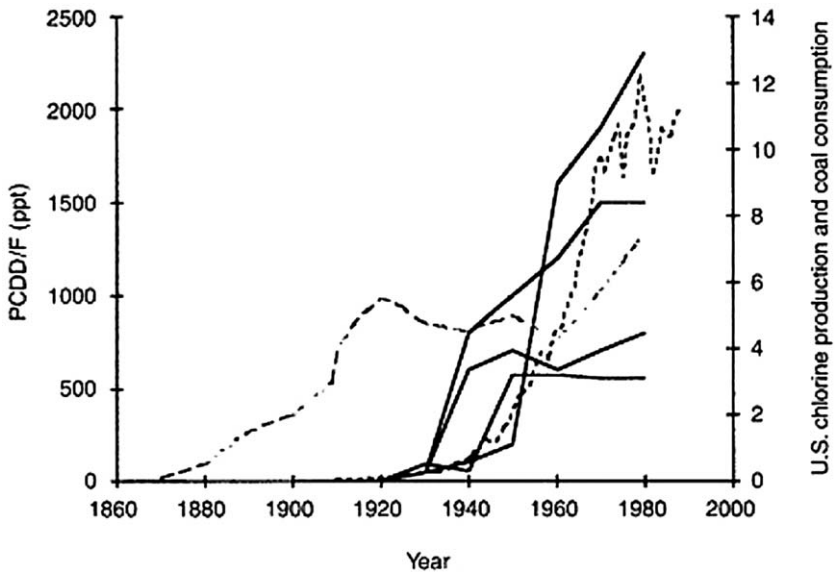

Fig. 1 Concentration of dioxin contamination in four separate samples from Lake Huron (solid lines) and total chlorine (short dash) and coal (long dash) output in the U.S. in millions of tons between 1870 and 1980. Reproduced from J. Thornton, *Pandora's Poison: Chlorine, Health, and a New Environmental Strategy*, Figure 5.2; © 2000 Massachusetts Institute of Technology, by permission of the MIT Press.

manufacture of Cl-containing products (*i.e.*, those that must necessarily use Cl, which include polyvinyl chloride (PVC), inorganics such as HCl, chlorofluorocarbons, pesticides, *etc.*).[15] Thus, nearly 35% of all Cl produced is used needlessly in oxidations whose products do not contain Cl.[15] Moreover, demand for Cl_2 (and not NaOH) drives the volume of production in the chlor-alkali industry.[16] Finally, many Cl-mediated oxidations use basic solutions (*e.g.*, NaOH) downstream to eliminate Cl from intermediates but produce large amounts of salt and organic wastes. Consequently, these processes are far from being atom-efficient and following the tenants of green chemistry. Thus, large-scale implementation of alternative oxidants in industrial processes may dramatically decrease the overall amount of Cl_2 produced and thereby reduce its environmental impact.

The substitution of Cl_2 with an alternative oxidant, however, is non-trivial because of numerous practical and economic demands of industrial oxidants, in addition to considerable investment in the design and construction of existing processes. Aside from Cl_2, acids (*e.g.*, HNO_3, H_2SO_4, $HClO_4$) and NO_x compounds are effective oxidants, but these compounds are also environmentally noxious and highly corrosive, and consequently present similar problems with emission control and safe-handling that plague chlorinated oxidants. Molecular oxygen (O_2) is a potential alternative that is both benign and abundant. Unfortunately, O_2 lacks the reactivity and selectivity to be useful for functionalizing hydrocarbons in many cases (one notable exception being the epoxidation of ethylene (C_2H_4) on Ag catalysts),[17,18] and so O_2 is an unlikely candidate to directly replace chlorinated oxidizers in current processes.[1] O_2 can, however, be converted into more reactive species such as ozone or hydrogen peroxide. Ozone (O_3) is formed by exposing O_2 to an electrical discharge or UV-light, but this method is both expensive and slow. Further, O_3 tends to react non-specifically and is highly toxic.[19] Hydrogen peroxide (H_2O_2) is a strong oxidizer with significant potential to replace Cl_2 because H_2O_2 possesses desirable chemical selectivity, forms benign byproducts (*e.g.*, H_2O), and is more safely stored and transported.[19,20] Consequently, the volume of H_2O_2 consumed has increased by a factor of five over a 20 year period (Table 1). Unfortunately, the current cost of

Table 1 Consumption of H_2O_2 in North America in 10^3 t.[a]

Use area	1980	1990	1995	2000[b]
Pulp and paper	32	144	340	410
Textile	28	34	40	63
Chemical[c]	44	52	59	75
Environmental[d]	10	23	31	66
Other	30	39	41	67
Total	*144*	*292*	*511*	*681*

[a] Recreated from W. Eul, A. Moeller and N. Steiner, *Kirk-Othmer Encyclopedia of Chemical Technology: Hydrogen Peroxide*, Chapter 10 Uses; Copyright © 2001 John Wiley and Sons Inc., by permission of John Wiley & Sons Inc.
[b] Estimate.
[c] Includes captive use.
[d] Includes mining industry.

H_2O_2 (\$52 $kmol^{-1}$) is greater than that for Cl_2 (\$20 $kmol^{-1}$),[21] which together with stoichiometric arguments (*i.e.*, one mole of Cl_2 can oxidize two moles of reactant while H_2O_2 can only oxidize one) demonstrates that economic considerations favor the continued use of Cl_2. Thus, the high cost of H_2O_2 is the predominant factor that has limited its implementation in new chemical plants, therefore, reducing the cost of H_2O_2 is a necessary first step to begin the process of replacing chlorinated oxidants.

1.2 Current H_2O_2 production methods and future directions

Currently more than 95% of all H_2O_2 is produced *via* the anthraquinone auto-oxidation process (AO).[20,22] This process is well-established and forms H_2O_2 with high selectivity (≥99%),[23] however, AO suffers from several economic and environmental drawbacks. AO requires a significant number of unit operations.[24] First, H_2O_2 forms as dilute solutions (0.8–1.9 wt%)[20] in an organic solvent using two sequential reactors for the reduction and oxidation of the anthraquinone substrate. Second, crude aqueous H_2O_2 solutions are generated by liquid–liquid extraction (to 15–40 wt%) and these are subsequently purified and concentrated by energy-intensive distillation steps (to 50–70 wt%).[24] Additionally, the insolubility of anthraquinones in aqueous solutions requires the use of hazardous organic solvents (*e.g.*, benzene, xylene, alkyl phosphates).[24] These requirements cause AO to only be economically viable for large-scale production ($>4\times10^4$ tons $year^{-1}$),[25] and therefore, make on-site production of H_2O_2 (a desirable option for reducing transportation costs) infeasible in many applications. The hydrogen peroxide–propylene oxide (HPPO) process is one notable exception which demonstrates the potential for on-site H_2O_2 production to transform industrial oxidations, as discussed later in Section 2.1.[26]

Alternative approaches for the formation of H_2O_2, which do not face the challenges of AO and might be feasible for small on-site facilities, include electrochemical O_2 reduction, photocatalytic O_2 reduction, and direct synthesis of H_2O_2. The electrocatalytic two-electron oxygen reduction reaction (ORR, $O_2 + 2H^+ + 2e^- \rightarrow H_2O_2$) is one such approach.[27–30] This reaction has the advantage that the chemical energy lost from non-selective H_2 conversion to H_2O can be partially recovered as electrical energy,[31] but the reaction is driven by applying an electrical over-potential across a proton exchange membrane and requires corrosive alkali solutions for proton conductivity.[32] While electrochemical processes could possibly be scaled up, they require electrical energy derived from a source higher in energy (*e.g.*, chemical energy derived from shale gas or renewable sources), therefore, direct use of chemical energy in the form of H_2 may be a more energy efficient method for producing H_2O_2. Another alternative approach is the absorption of UV light by a semiconductor (typically TiO_2), which leads to the excitation of electrons to the conduction band and subsequent reduction of O_2, followed by reaction with protons from the solution to form H_2O_2.[33,34] Unfortunately, photon-mediated methods give low rates and produce only micromolar concentrations of H_2O_2, which are useful primarily for environmental remediation of dilute contaminants *in situ* and other niche applications. Therefore, photoelectrochemical H_2O_2

production could not easily be intensified and coupled with an industrial oxidation process. Similarly low H_2O_2 formation rates and yields plague a number of other H_2O_2 synthesis approaches including electrical discharge (*i.e.*, plasma) driven reactions of O_2 with H_2[35] and the oxidation of CO in the presence of water and a catalyst ($CO + O_2 + H_2O \rightarrow H_2O_2 + CO_2$).[36]

One of the most promising alternatives to the AO process is the direct synthesis of H_2O_2 ($H_2 + O_2 \rightarrow H_2O_2$), which can achieve high yields (up to 10 wt% H_2O_2),[37] requires less energy to operate than AO (*i.e.*, fewer separation and concentration steps), and may be reasonably scaled to small facilities for on-site use.[25] In addition, the price of H_2 has decreased substantially over the past 10 years due to the concomitant drop in the price of shale gas (from \$10.5 $MBTU^{-1}$ in 2005 to \$2.6 $MBTU^{-1}$ in 2015),[38,39] which makes direct synthesis of H_2O_2 formation more appealing than the other alternatives to AO. The selectivity to H_2O_2 in direct synthesis, however, is much lower on benchmark Pd catalysts (~60%)[40,41] than that of the AO process (>99%).[23] As such, wide-spread use of H_2O_2 will likely follow the development of significantly more selective catalysts and efficient processes for the direct synthesis of H_2O_2.[37] Recent progress towards understanding the mechanism of the direct synthesis reaction, the influence of the composition and structure of metal cluster catalysts, and the effects of solvents and supports are discussed in Section 3.

1.3 Applications for H_2O_2 as an industrial oxidant

Oxidation reactions are ubiquitous in the chemical industry. These reactions play an integral role in the production of a number of products used in everyday life, such as epoxy resins, plastics, fuel additives, surfactants and medicines.[42,43] However, many oxidizers such as heavy metals,[44] HNO_3,[45,46] permanganates,[47] and organic (*e.g.*, *t*BuOOH) and chlorinated (*e.g.*, NaClO and ClO_2) molecules produce toxic or corrosive byproducts which require additional separation and purification steps, and thus have high capital and operating costs.[48–50] In contrast, H_2O_2 is a green oxidant, which can produce precursors for high value chemicals, agricultural products, pharmaceuticals, and electronic products where high purity products are desired.[42,51–57] Importantly, oxidation reactions that use H_2O_2 are selective and produce only H_2O as a byproduct, therefore, H_2O_2 also finds applications in oxidative removal of compounds from the environment.[42]

Various categories of reactants can be oxidatively functionalized by H_2O_2 (perhaps at large scales) including alkanes,[51,52,58–61] alkenes,[54–56,62–66] alcohols,[42,57,67,68] aldehydes,[69] sulfides,[43] thioethers,[70] and sulfoxides.[70] Oxidation of small alkanes and alkenes provide useful building block oxygenates. Specifically, activation of methane and ethane leads to the formation of important products like methanol, ethanol, acetic acid and acetaldehyde.[58,71] Current production methods, however, use harsh reaction conditions, require high energy input, and give non-selective oxidations that indirectly form the desired small oxygenates.[51] For example, steam reforming of methane to produce synthesis gas mixtures used to form small alcohols requires high temperatures (800–1400 K).[72] Ethylene, a precursor for ethanol production by hydration, is produced by cracking

of ethane or mixed hydrocarbons.[51] These indirect methods of oxygenate production require massive amounts of energy and result in high emissions of greenhouse gases like CO_2.[51] Hence, significant effort has been directed towards one-step selective methods for the conversion of lower alkanes to useful oxygenates.[53,59,73] Aldehydes, ketones, carboxylic acids, and epoxides are obtained by oxidations of alcohols and alkenes and are important building blocks for polymers, fuel additives, and platform chemicals.[42,68] Work by Davy in 1820 involved the oxidation of ethanol with air over a Pt catalyst and was among the first in this area.[74] Alcohols are often oxidized using Cr or Mn catalysts[75] in toxic organic solvents (*e.g.*, dimethylsulfoxide (DMSO), chloroform)[76] and with halogen-containing organic oxidizers (*e.g.*, NaOCl and (2,2,6,6-tetramethylpiperidin-1-yl)oxyl (TEMPO)).[77] However, many of these reactions are non-selective, yielding a myriad of by-products, which require extensive separation.[68,75–77] H_2O_2 is effective for oxidations of primary and secondary alcohols[42,68,78] as well as benzylic alcohols[57,67] and eliminate the need for halides and organic solvents. Oxidations of sulfides to sulfoxides and sulfones (*i.e.*, common moieties in commodity chemicals and pharmaceuticals)[79–81] traditionally use chlorinated oxidants,[80] permanganates,[47] or organic oxidants.[82,83] However, none of these processes have been found to be scalable to high capacities because of low O_2 content, unwanted by-products, and high costs.[43] H_2O_2 is a potential oxidant for this chemistry, as shown by previous results that demonstrate the success of H_2O_2 in combination with a W catalyst and a phase transfer catalyst for the oxidation of sulfides to sulfoxides and sulfones.[43] Apart from these activities, ongoing research aims to use transition metal based catalysts (*e.g.*, Nb, W, Ti) to deactivate chemical warfare agents *via* oxidation of the alkyl and aromatic sulfides to the corresponding sulfoxides and sulfones.[84] Yet, overall, the most important category of industrial chemicals which can be produced by oxidation by H_2O_2 are likely epoxides, which have been the focus of significant study among researchers.[65,85–87]

1.4 Catalysts for activating H_2O_2 for epoxidation reactions

Epoxides are an important class of commodity and specialty chemicals that are widely used in the production of epoxy resins, plastics, surfactants, fragrances, and pharmaceutical agents.[88,89] Many epoxides are currently produced on an industrial scale using oxidants which are either toxic or lead to toxic by-products such as with the chlorohydrin process and the hydroperoxide process using styrene monomers[90] and adipic acid production by HNO_3 oxidation.[91] H_2O_2 can be an environmentally benign and economic replacement for these harmful oxidants, as demonstrated by the success of the HPPO process.[54,66] However, H_2O_2 will only replace halogenated compounds in epoxidations if catalysts used for H_2O_2 activation can achieve sufficiently high selectivities, rates, and stabilities while being easily removed from the product stream for catalyst recovery. Previous reviews have focused on olefin epoxidation catalysts that use H_2O_2 as the oxidant,[86,87,89,92] and so, this review highlights selected classes of epoxidation catalysts, spectroscopic evidence for the critical

active intermediates (*i.e.*, reactive forms of oxygen) stabilized by these materials, and recent improvements in catalyst design.

Catalysts for epoxidations can largely be classified as transition-metal substituted zeolites,[89,93] supported and unsupported metal oxides,[94] polyoxometalates,[1,87] and coordination compounds.[92] Substituted zeolites are formed by the incorporation of metal atoms into a microporous, crystalline framework comprised mainly of tetrahedral silica units (*i.e.*, $[SiO_4]$) and can possess incredible chemical and thermal stability.[95] Unfortunately, there has been limited success in creating zeolite catalysts that are regioselective for epoxidation when multiple types of C=C bonds (*e.g.*, cyclic *vs.* terminal) are present.[96] Furthermore, the vast majority of the active sites of substituted zeolites are located within small pores (typically <0.7 nm), which inhibit the diffusion of molecules with relatively large kinetic diameters from accessing the H_2O_2-activated metal centers.[97,98] Metal oxide epoxidation catalysts consist of either homogeneous organometallic compounds (*e.g.*, methyltrioxorhenium)[99] or heterogeneous metal oxide clusters (*e.g.*, Al_2O_3,[100] ZrO_2,[101] TiO_2,[66,102] Nb_2O_5[103,104]), typically grafted onto a mesoporous support (*e.g.*, SiO_2, glassy carbon).[105] Homogeneous metal oxides are highly active for epoxidation reactions, but require subsequent separation steps to remove the catalyst from the product stream.[106,107] Heterogeneous metal oxides have been synthesized to achieve atomically dispersed metal centers,[108] increasing the utilization of the metal used. However, the catalyst's activity can vary over orders of magnitude depending on the metal identity.[89] Polyoxometalates (POMs) are polyatomic ions (most typically anions) that form three-dimensional structures (*e.g.*, Dawson-, Keggin-clusters) by the coordination of multiple transition metal atoms *via* bridging oxygen atoms.[87,109–111] The most common POMs investigated for epoxidation are W-based POMs, due to their high intrinsic propensity to react with H_2O_2, forming an activated complex.[87] The first POMs discovered for epoxidation chemistries were soluble peroxotungstates that required extraction from the reactant pool to recover the products and catalyst.[112] Since then, many researchers have either immobilized the POMs onto a support[113] or created catalytic systems from which the inactive complex precipitates.[114] Homogeneous coordination complexes (generally organometallic compounds) tend to be the most active and selective catalysts used for H_2O_2 activation in olefin epoxidation. Coordination compounds consist of neutral or ionic ligand molecules covalently bound to a central metal atom.[115] Additionally, careful ligand design allows for the enantioselective epoxidation of olefins, which is necessary for the production of pharmaceutical active ingredients.[88] Among these, this review will discuss three classes of coordination compounds, methyltrioxorhenium, transition metal porphyrin, and Schiff-base complexes.[86,92,116]

2 Processes for the production of H_2O_2

2.1 Anthraquinone auto-oxidation

The first commercial AO process for H_2O_2 production was implemented by the German company IG Farben in the 1940s with a production

capacity of one ton H_2O_2 per day.[20] Since then, many more AO process facilities have been commissioned by companies such as Solvay,[117] Evonik,[118] and Arkema,[119] which give a combined production capacity of over 3×10^3 kt H_2O_2 $year^{-1}$.[119–121] These modern facilities produce H_2O_2 through a complex series of steps that can be classified roughly by the type of unit operation: hydrogenation, oxidation, extraction, and concentration.[20,24] Figure 2 shows these primary unit operations as well as several necessary auxiliary units (*e.g.*, catalyst regeneration, working solution recovery).

The anthraquinone substrates are first hydrogenated using molecular hydrogen (H_2) in the presence of a catalyst (Pd black,[24] RANEY® Ni[20,24]), which is suspended in solution or supported on a fixed bed. Organic solvents are needed to solvate the reactants in each reactor; quinones (*i.e.*, oxidized anthraquinones) require potentially toxic solvents such as benzene[122] or xylene,[123] while hydroquinones (*i.e.*, hydrogenated anthraquinones) need complex alkyl phosphates,[124] carbamates,[125] or carbonamides.[126] During hydrogenation, the conversion of the quinones is kept below 60% to minimize secondary hydrogenation of the aromatic ring, which would need to be subsequently re-aromatized.[20] Suspended RANEY® Ni has been commonly used for the hydrogenation process, however, Ni readily hydrogenates the aromatic ring of 2-alkylanthraquinone, is easily deactivated by oxygen and H_2O_2,[127] and is pyrophoric.[22] As such, Pd black (*i.e.*, highly porous Pd supported on SiO_2 or Al_2O_3) now replaces RANEY® Ni as a hydrogenation catalyst in several AO facilities.[22] Pd black

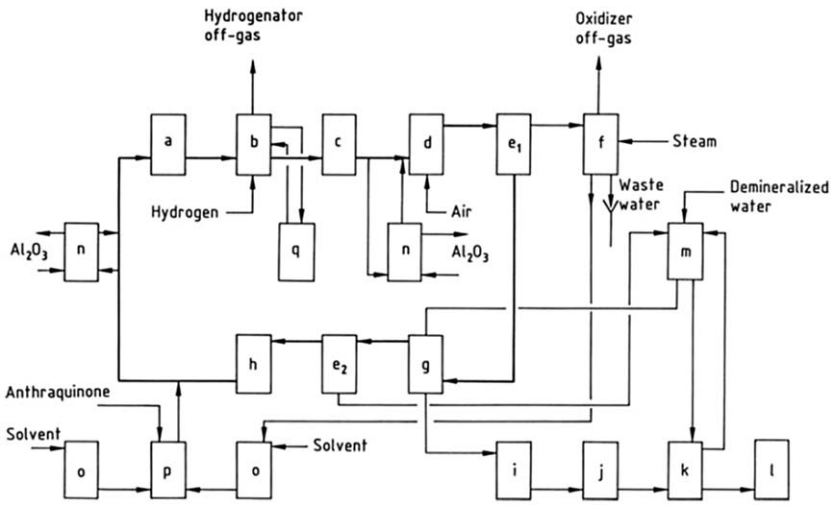

Fig. 2 Block-flow diagram for the production of H_2O_2 by the AO process. (a) Storage tank for working solution or hydrogenator feed tank; (b) hydrogenator; (c) safety filtration; (d) oxidizer; (e) separator; (f) activated carbon adsorber; (g) extraction; (h) drying; (i) pre-purification; (j) crude product storage tank; (k) hydrogen peroxide concentration; (l) hydrogen peroxide storage tank; (m) demineralized water feed tank; (n) regeneration and purification; (o) solvent storage tank; (p) working solution make up tank; (q) catalyst regeneration. Reproduced from G. Goor, J. Glennberg and S. Jacobi, *Ullmann's Encyclopedia of Industrial Chemistry: Hydrogen Peroxide*, 2007, p. 401. Copyright Wiley-VCH Verlag GmbH & Co. KGaA. Reproduced with permission.

is more stable and easier to handle than RANEY® Ni, but Pd still catalyzes the ring saturation of 2-alkylanthraquinone, albeit to a lesser extent.[22,24] Both RANEY® Ni and Pd deactivate with time on stream, presumably by accumulation of surface carbon, and consequently, these catalysts are regenerated periodically by high temperature (523–973 K) oxidative treatments with steam, strong oxidants, inorganic acids, or air.[22]

Hydrogenation of the aromatic rings on substituted anthraquinones can be mitigated by adding inhibiting molecules (*e.g.*, NH_3, water-soluble amines, or ammonium salts)[22] to the reduction-reaction solution or by using functionalized resin supports (*e.g.*, lipophilic resins like poly-(decyl methacrylate)-methyl methacrylate (PDMA-MMA) and polystyrene-divinylbenzene (PS-DVB))[128] instead of metal oxides (*e.g.*, SiO_2, Al_2O_3). More selective hydrogenation catalysts for AO are still being identified, and nano-sized amorphous alloys such as Ni/B[129,130] and Ni/Cr/B[131] show promise. Ni-B supported on SBA-15[129,130] and Ni–Cr–B[131] gives nearly 100% H_2O_2 yield, and suppresses nearly all secondary hydrogenation reactions. Evidence from X-ray diffraction (XRD), transmission electron microscopy (TEM), and H_2 temperature programmed desorption (TPD), suggest that hydrogen atoms bind more strongly to Ni atoms on these Ni–B surfaces, which may help prevent the hydrogenation of the aromatic rings and increase H_2O_2 yields.[129,131]

Hydroquinones produced by hydrogenation are then oxidized using air in the absence of a catalyst in order to regenerate the quinones and form H_2O_2 in a separate reactor.[20,22,24] This oxidation process occurs spontaneously (*i.e.*, in the absence of a catalyst) and proceeds through a free radical chain mechanism (Scheme 1).[20] Overall H_2O_2 yields decrease significantly if the metallic hydrogenation catalyst is not completely removed from the working solution, because the metal surfaces readily

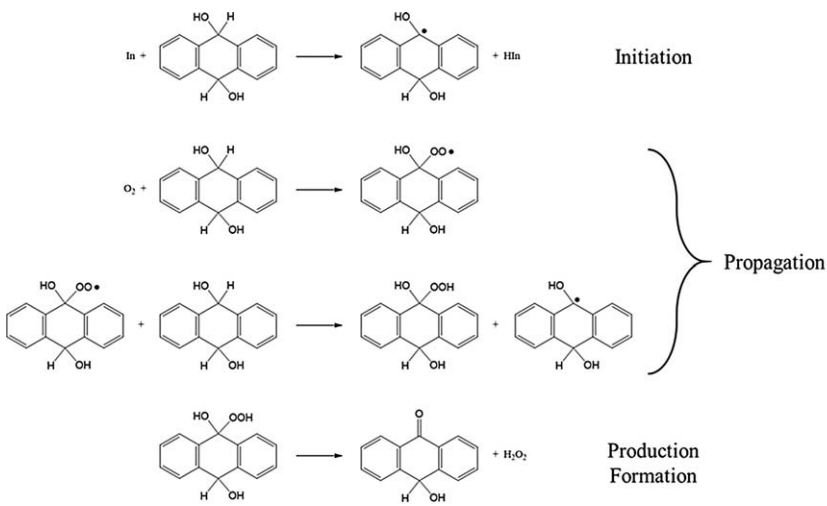

Scheme 1 Free-radical chain mechanism for the oxidation step in the AO process. Adapted from J. M. Campos-Martin, G. Blanco-Brieva and J. L. G. Fierro, Hydrogen Peroxide Synthesis: An Outlook beyond the Anthraquinone Process, *Angew. Chem., Int. Ed.*, 2006, **45**, 6962. Copyright 2006 WILEY-VCH Verlag GmbH & Co. KGaA, Weinheim.

decompose H_2O_2 to H_2O and O_2. Therefore, the hydrogenation catalyst is thoroughly filtered from the hydroquinone working solution prior to entering the oxidation reactor.[20,24] H_2O_2 yields during oxidation increase with the rate of O_2 transport into the working solution,[132] therefore, venturi tubes[133] or static mixers are used to thoroughly mix the working solution with a reactant air stream to increase concentrations of dissolved O_2.[134]

After oxidation is complete, the working solution containing the H_2O_2 product is sent to a liquid–liquid extractor where H_2O_2 is extracted into an aqueous stream. Residual H_2O is removed from the working solution by adsorption onto activated carbon,[24] and the working solution is then cleaned of degradation products by treatment with an alkaline substrate,[135] alkali hydroxide,[136] aluminum oxide, or liquid CO_2.[24] The clean, dry working solution is then recycled to the hydrogenation reactor.[24] Additional anthraquinones are added to this stream to compensate for anthraquinone losses due to non-selective hydrogenation and imperfect H_2O_2 concentration and purification.[24] A countercurrent liquid–liquid extractor contacts the working solution (0.8–1.9 wt% H_2O_2) with H_2O, which recovers approximately 95% of the H_2O_2 and produces a crude aqueous product stream of 25–40 wt% H_2O_2.[20] For off-site applications, the crude H_2O_2 product is concentrated further by distillation to a 50–70 wt% H_2O_2 solution,[22,24] which is then stabilized against decomposition by the addition of sodium pyrophosphate and sodium stannate, either separately[137] or together.[138] The final H_2O_2 product is stored in inert tanks (*e.g.*, polyethylene or HNO_3-passivated aluminum) to avoid corrosion and H_2O_2 decomposition.[22,24] A significant amount of energy is required to concentrate H_2O_2 by distilling off excess H_2O, which contributes in part to the high cost of H_2O_2 produced by AO ($550 ton^{-1} of 50 wt% H_2O_2).[139] As a result of this energy cost and the large capital cost of the complex process, AO is viable only at large scales ($>40\times10^3$ tons year^{-1}).[25] Notably, on-site H_2O_2 production (such as for the HPPO process)[140,141] can avoid the need to concentrate the crude aqueous H_2O_2, and in fact, can use more dilute streams based on the H_2O_2 concentrations (*e.g.*, 2–10 wt%) needed at the adjacent PO production plant.[142]

The world's first HPPO plant, a joint venture by Dow and BASF in Belgium, was completed in 2009 and possessed a propylene oxide production capacity of 3×10^5 tons year^{-1}.[143] The H_2O_2 produced on-site is used to epoxidize propylene oxide (PO),[142] which reduces wastewater production by 70–80%, energy usage by 35%, and capital investment by 25%.[144,145] Overall, the integration of an economically feasible, large-scale AO facility (2.3×10^5 tons H_2O_2 year^{-1})[145] with a propylene epoxidation plant of similar size (3×10^5 tons PO year^{-1}) leveraged economies of scale to make this otherwise economically impossible venture feasible.[37] To date, an additional three HPPO facilities have been constructed or commissioned in locations throughout the world (Evonik and SKC in South Korea,[146] Dow and SGC in Thailand,[144] and Evonik and Uhde in China[121]). Such schemes are not currently possible at the smaller scales typical of many other oxidation chemistries (*e.g.*, paper bleaching,[3] disinfection of wastewater[4,5]), however, the development of an alternative to

Scheme 2 Alcohol oxidation (Shell) process for the production of H_2O_2.

AO would enable the cost-effective use of H_2O_2 as an oxidant for these small scale processes.

2.2 Alcohol oxidation (shell process)

Shell Chemical pioneered the production of H_2O_2 by oxidation of 2-propanol with an oxygen enriched gas stream (80–90% O_2, Scheme 2) in 1957, and the process was used to produce 1.5×10^4 tons of H_2O_2 annually until 1980.[20,22] The reaction is auto-catalyzed by H_2O_2, and therefore, does not require a metal catalyst, which reduces the rate of secondary decomposition of H_2O_2. Instead, a small amount of H_2O_2 is added to the 2-propanol and O_2 reactant mixture to initiate the reaction. While simple decomposition of H_2O_2 is minimal, the H_2O_2 selectivity is diminished by secondary oxidation reactions that convert 2-propanol to acetone.[20,24] These secondary reactions may be reduced by operating at differential conversion (<15%), and the process can achieve high overall H_2O_2 yields (87–98%).[24] The 2-propanol reactant is highly soluble in the peroxide phase, which makes the recovery of the H_2O_2 by distillation more energy intensive, and therefore, more expensive than AO.[20] As a result, the alcohol oxidation (*i.e.*, Shell) process has been mostly discontinued. As an alternative to 2-propanol, the high temperature (393–453 K) oxidation of methylbenzyl alcohol (a co-product from the styrene process for propylene oxide production)[147] was investigated and was found to give H_2O_2 selectivities in the range of 80–97% at approximately 30% alcohol conversion.[147] The use of a methylbenzyl alcohol facilitates the separation of H_2O_2 from the working solution, however, the unit operations needed for this process are similar to AO (oxidation, extraction, distillation units). No plants based on methylbenzyl alcohol oxidation are operating currently, to the best of our knowledge. At the present time, AO remains the dominant method for industrial scale production of H_2O_2.

2.3 Direct synthesis

The direct synthesis of H_2O_2 ($H_2+O_2\rightarrow H_2O_2$) is promising for future commercial H_2O_2 production, because proposed designs for direct synthesis plants do not require the use of toxic organic solvents, require fewer separations, and could be feasible at a smaller scale that enables on-site H_2O_2 production for a number of applications.[20,22,24,37,41,148] No direct synthesis facilities for commercial H_2O_2 production are operating currently, in large part, because the selective formation of H_2O_2 by this pathway remains a challenge. Below, we briefly summarize a few critical aspects of proposed direct synthesis processes, as discussed by Salmi *et al.*[37,41,149]

Researchers have used a number of different types of reactor designs for direct synthesis of H_2O_2 (*e.g.*, batch,[150–152] semi-batch,[153,154] packed bed,[41,148,155,156] microreactors,[157–159] and membrane reactors[160–163]), and upon review, packed bed reactors (PBRs) seem best suited for industrial direct synthesis facilities due to their ease of operation and scalability.[37,41] Salmi *et al.* determined that PBRs could minimize secondary decomposition of H_2O_2 (by reaction with H_2) when operated with co-current (as opposed to counter-current) downward flow (*i.e.*, trickle bed) of the liquid (aqueous methanol) and gas (mixtures of H_2, O_2, and a diluent such as N_2) streams.[41] Figure 3 shows a lab-scale example of the proposed trickle bed reactor for the direct synthesis of H_2O_2.[37,41] This system consists of a gas and a liquid inlet, a packed catalyst bed, and a gas–liquid separator at the outlet.[37,41] The catalyst bed is immobilized by means of glass wool and metal filters. The liquid flows down through the bed, wets the catalyst particles, turbulently mixes the gas and liquid streams, and provides large gas–liquid interfacial area, which results in facile mass transport and greater H_2O_2 formation rates. [37] The down-flow configuration (Fig. 3) also minimizes gas hold-up, which helps to avoid high pressure drop and H_2–O_2 mixtures that may fall within the explosive regime.[164] Packed and trickle bed reactors would be viable options for industrial direct synthesis, yet, the costing must be considered in more detail in order to get an accurate comparison of the viability of DS to AO.

Highly detailed cost analyses for AO and direct synthesis are not readily available in widely accessible publications, however, Biasi *et al.* has developed a general cost analysis in 2014.[37] A Chemical Engineering Plant Cost Index (CEPCI) analysis showed that the initial capital

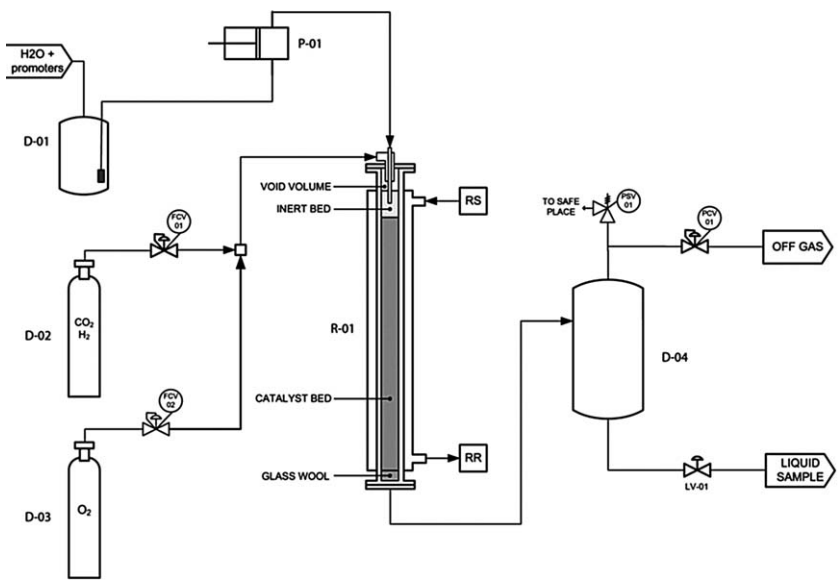

Fig. 3 Schematic of a lab-scale trickle bed reactor (TBR) for direct synthesis of hydrogen peroxide. Reproduced from J. García-Serna, T. Moreno, P. Biasi, M. J. Cocero, J.-P. Mikkola and T. O. Salmi, *Green Chem.*, 2014, **16**, 2320, with permissions from the Royal Society of Chemistry.

investment for a 10 kton year^{-1} direct synthesis plant would be $\$4.3 \pm 1.2 \times 10^7$, which is comparable to capital investments for similarly sized AO plants.[37] At these scales (10 kton year^{-1}) the combined operating costs (*i.e.*, utilities, labor, maintenance, and raw materials such as H_2, O_2, catalysts, and promoters) for a direct synthesis plant were estimated to be less than those for an AO facility, mainly due to the need for ~50% fewer operators. A significant portion of the operating costs for both processes are the cost of H_2 ($2.6 MBTU^{-1}),[38,39] therefore, achieving high selectivities for the conversion of H_2 to H_2O_2 remains important and is the primary area of research regarding direct synthesis. Biasi *et al.* did not specify a value for the H_2O_2 selectivity above which direct synthesis plants would be competitive with those for AO, but it can be safely assumed that direct synthesis would be more economically attractive if it gave selectivities comparable to that of AO. Despite significant research, selectivities obtained by DS are only comparable under specific laboratory conditions,[165–169] and significant improvements are needed before direct synthesis could be practiced at scale. Recent efforts to better understand direct synthesis, enable more flexible operating conditions, and reach high H_2O_2 selectivities on stable catalysts are reviewed below.

3 Direct synthesis of H_2O_2

3.1 The history of direct synthesis

The first patent for the direct synthesis of H_2O_2[170] was published in 1914 (25 years prior to the first AO patent)[171] by German scientists Hugo Henkel and Walter Weber as a replacement for the electrolysis of ammonium sulfate (the primary method for H_2O_2 formation at the time).[25] Notably, the original patent identifies specific catalysts and suggests process conditions that are still used today (*e.g.*, Pd catalysts[172] and aqueous solvents). Despite these initial achievements, the process was never fully implemented at an industrial scale primarily due to safety concerns about the explosive H_2–O_2 reactant mixtures[25] and low selectivities towards H_2O_2 on Pd catalysts (<70%).[40,41] Few patents for direct synthesis on Pd catalysts have been filed and maintained subsequently, and many of these claim only moderate selectivities (~70%) and require the use of potentially hazardous additives such as acids and halides.[173–176] As such, the most significant advancements in the industrial production of H_2O_2 include the integration of AO with other processes, such as the development of HPPO plants (see Section 2.1).[145,177] Such facilities underline the emerging need for cheaper and environmentally benign industrial oxidants in order to both satisfy the needs of a growing population and reduce the environmental impact of those processes. AO is, however, only viable at large scales[25] and therefore cannot fully meet the needs of many smaller processes (*e.g.*, pulp and paper bleaching, wastewater treatment) at cost-effective prices. These considerations and the current low price of shale gas, and related cost of H_2 ($2.6 MBTU^{-1})[38,39] motivate current interest in improving the selectivity and practicality of the direct synthesis reaction.

The initial discovery that the titanium silicalite zeolite (TS-1)[178] catalyzed the selective epoxidation of small alkenes (in addition to alkylation, cracking, isomerization, and polymerization reactions) renewed interest in the use of H_2O_2 for industrial oxidations. Epoxidations with TS-1 catalyst involved co-feeding H_2O_2 with organic reactants such as styrene[179] and phenol[180] and motivated interest in finding uses for H_2O_2 in other large scale oxidation processes. The merits of such processes were recognized widely when the HPPO process received a Presidential Green Chemistry Challenge Award in 2010.[181] Researchers have studied the use of H_2O_2 in other industrially relevant oxidations, especially those practiced at small scales, which would be enabled by on-site H_2O_2 production by direct synthesis. In 2002, Hutchings *et al.* demonstrated that AuPd clusters supported on Al_2O_3 catalyze the direct synthesis of H_2O_2 in mixtures of methanol and supercritical CO_2 at H_2O_2 formation rates (4.5 (mol H_2O_2)($g_{catalyst}$ h)$^{-1}$) higher than on Pd (0.4 (mol H_2O_2)($g_{catalyst}$ h)$^{-1}$) and Au (1.5 (mol H_2O_2)($g_{catalyst}$ h)$^{-1}$) clusters.[182] This work was followed shortly by a pivotal study showing that the bimetallic AuPd clusters supported on Al_2O_3 gave selectivities (14%) that were 10-fold greater than monometallic Pd (1%).[151] Subsequent investigations have focused on the effects of the catalyst support,[167,168,183–185] the method of reducing and combining precursors for the AuPd clusters, and the presence and identity of various additives[168,186,187] and have improved H_2O_2 selectivities significantly from 14% on AuPd–Al_2O_3[151] to 98% on AuPd–carbon (Table 2).[168] Table 2 shows also that Pd-based bimetallic and intermetallic catalysts such as PdPt[188] and PdSn[169] give higher H_2O_2 selectivities and rates than pure Pd. Over the past two decades, notable studies have probed the mechanism of H_2O_2 formation,[148,172,189–191] developed more productive and selective catalysts,[151,168,169] and optimized the design of reactors for direct synthesis.[37,155,192]

3.2 Experimental considerations for studies of direct synthesis

Despite the apparent simplicity of the reaction network for direct synthesis (Scheme 3), accurate rate measurements for H_2O_2 formation are difficult to acquire at many conditions. One of the primary challenges of this chemistry is that H_2O_2 is an unstable molecule that readily decomposes to form H_2O by secondary pathways in the presence of most metal catalysts.[25,151,172,193,194] Among these pathways, secondary decomposition of H_2O_2 by reaction with H_2 ($H_2 + H_2O_2 \rightarrow 2H_2O$) is thermodynamically favored over spontaneous decomposition ($2H_2O_2 \rightarrow 2H_2O + O_2$).[153,156,167,168] The decomposition of H_2O_2 in the presence of H_2, which must be present for direct synthesis, makes it difficult to differentiate between primary and secondary H_2O formation rates and can obscure H_2O_2 formation rates, too. In addition, direct synthesis occurs at the solid–liquid interface within a three phase system (*i.e.*, gaseous reactants, liquid solvent, and solid catalyst),[189] and transport restrictions can easily introduce experimental artifacts from poor liquid–gas mixing and slow intra-particle diffusion that lead to uncertain concentrations of the reactants throughout the system (*i.e.*, large Thiele moduli and low effectiveness factors). These interactions between phases are especially complicated in continuous flow systems,

Table 2 H_2O_2 selectivity and formation rates with various catalysts, supports, solvents, and additives.

Ref.	Catalyst[a]	Support	Solvent	Additives	H_2O_2 selectivity (%)	H_2O_2 formation rate[e] (mol H_2O_2) (mol_{metal} h)$^{-1}$
168	5% Pd	Carbon	66 wt% CH_3OH[d]	—	42	106[g]
168	5% Pd	Carbon treated in 2% HNO_3	66 wt% CH_3OH[d]	—	42	110[g]
168	5% Au	Carbon	66 wt% CH_3OH[d]	—	—[c]	2[g]
168	5% Au	Carbon treated in 2% HNO_3	66 wt% CH_3OH[d]	—	—[c]	2[g]
168	2.5% Au–2.5% Pd	Carbon	66 wt% CH_3OH[d]	—	80	302[g]
168	2.5% Au–2.5% Pd	Carbon treated in 2% HNO_3	66 wt% CH_3OH[d]	—	>98	440[g]
168	2.5% Au–2.5% Pd	Carbon treated in 2% CH_3COOH	66 wt% CH_3OH[d]	—	>98	481[g]
169	2% Sn–3% Pd	SnO_x/TiO_2	66 wt% CH_3OH[d]	—	96	215[g]
197	5% Pd	SiO_2	C_2H_5OH	0.12 M H_2SO_4	0	0[h]
197	5% Pd	SiO_2	C_2H_5OH	0.12 M H_2SO_4 0.4 mM HCl	51	257[f,h]
153	5% Pd	Carbon	H_2O	0.05 M H_2SO_4	0	0[h]
153	5% Pd	Carbon	H_2O	0.05 M H_2SO_4 2.7 mM KF	0	0[h]
153	5% Pd	Carbon	H_2O	0.05 M H_2SO_4 2.7 mM KCl	26	1[f,h]
153	5% Pd	Carbon	H_2O	0.05 M H_2SO_4 2.7 mM KBr	27	0.7[f,h]
153	5% Pd	Carbon	H_2O	0.05 M H_2SO_4 2.7 mM KI	0	0[h]
188	1% Pd	K2621[b]	CH_3OH	—	37	904[g]
188	1% Pd–0.1% Pt	K2621[b]	CH_3OH	—	43	571[g]
188	1% Pd–0.25% Pt	K2621[b]	CH_3OH	—	30	845[g]
188	1% Pd–0.5% Pt	K2621[b]	CH_3OH	—	36	1218[g]
188	1% Pd–1% Pt	K2621[b]	CH_3OH	—	38	946[g]

[a] All metal loadings are reported as wt%.
[b] Sulfonated polystyrene-divinylbenzene macroreticular ion-exchange resin from Lanxess.
[c] Not determined due to low yields.
[d] Balance H_2O.
[e] Units converted to (mol H_2O_2)(mol_{metal} h)$^{-1}$ from reported metal loadings and mass of catalyst added.
[f] Rates not reported, but estimated from reported H_2 conversion and selectivity with a known amount of catalyst and assuming the pseudo steady-state hypothesis.
[g] Experiments were carried out in a batch reactor.
[h] Experiments were carried out in a semi-batch reactor.

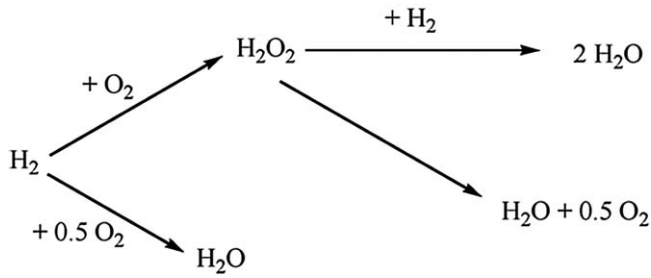

Scheme 3 Direct synthesis reaction network for H_2O_2 and H_2O formation by direct synthesis and including secondary decomposition and hydrogenation of H_2O_2. Reprinted from C. Samanta, Direct synthesis of hydrogen peroxide from hydrogen and oxygen: An overview of recent developments in the process, *Appl. Catal., A,* **350**, 133. Copyright 2008 with permission from Elsevier.

because a number of complex flow regimes exist and depend on the independent flows rates of both the gas and liquid streams (details of these effects are discussed below). Finally, direct synthesis involves mixtures of H_2 and O_2 reactants, which can form explosive mixtures unless proper safety precautions are followed. Typically, direct synthesis studies are performed in the presence of a diluent (*e.g.*, N_2, CO_2)[41,168,195] so that the concentrations of H_2 and O_2 in the reactor lie outside of the flammability limit (<5 vol.% of either H_2 or O_2).[164,196] Selected studies have been performed using H_2 and O_2 mixtures within the explosive regime,[195,197–199] and in these conditions the catalyst should be mixed first with the solvent before being exposed to the H_2–O_2 reactant stream. Even when this procedure is followed, laboratory reactors have exploded,[195] therefore, diluted reactant gases (*e.g.*, O_2–N_2 mixtures) should be used to reduce safety risks during these experiments.

Stirred batch[150–152] and semi-batch[153,154] reactors are commonly employed for screening catalysts and performing kinetic measurements, because they are inexpensive and easily built, minimize inter-particle mass transport restrictions with rapid stirring, and give good thermal control.[37] However, the hydrodynamics and operation of these batch-type reactors differ significantly from the packed bed reactors that appear most promising for the implementation of direct synthesis.[37] Batch reactors are typically fashioned from glass or made from stainless steel autoclaves and are fed gaseous reactants at constant pressure or controlled flow rates (*via* mass flow controllers (MFCs)) to control H_2–O_2 ratios (Fig. 4 shows a representative semi-batch reactor used by Lunsford *et al.*). Concentrations of H_2O_2 are usually determined by titration with a chemical indicator until the solution changes color (*e.g.*, KI–H_2SO_4, $KMnO_4$–H_2SO_4, $Ce(SO_4)_2$–ferroin)[200] or by performing UV-vis spectroscopy after addition of a given quantity of a spectrophotometric indicator (*e.g.*, $CuSO_4$–neocuproine).[200,201] The concentration of the reactant (*i.e.*, H_2, O_2) is typically measured using a gas chromatograph equipped with a thermal conductivity detector, however, the concentration of dissolved H_2 in batch experiments can be analyzed directly with a hydrogen analyzer.[150] The concentrations of both reactants and products change throughout the course of these reactions and long residence times can lead to significant

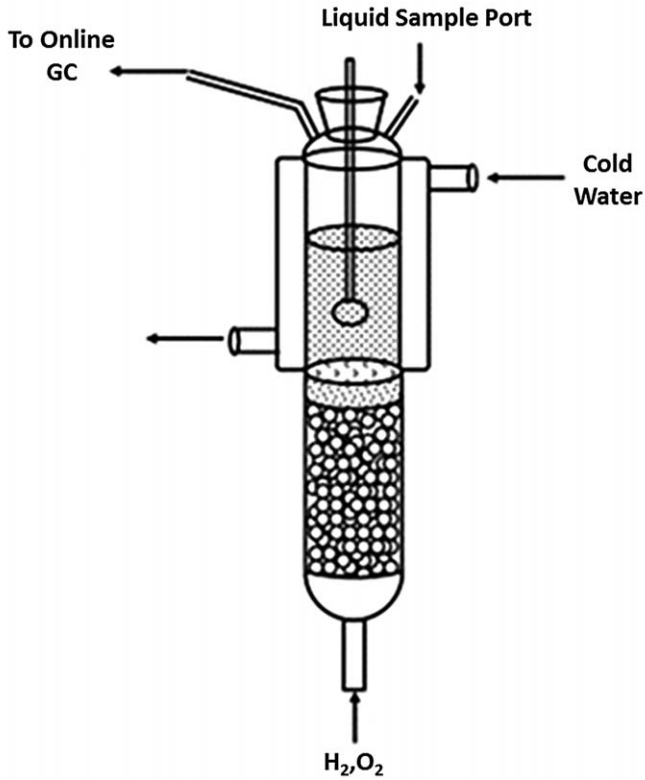

Fig. 4 A representative semi-batch reactor for direct synthesis experiments. Reprinted from S. Chinta and J. H. Lunsford, A mechanistic study of H202 and H20 formation from H2 and O2 catalyzed by palladium in an aqueous medium, *J. Catal.*, 2004, **225**, 249. Copyright 2004 with permissions from Elsevier.

secondary decomposition of H_2O_2. Together these changes require that the kinetics of both H_2O_2 formation and decomposition pathways be analyzed simultaneously. Such calculations are certainly possible, however, this approach leads to greater uncertainties in the final H_2O_2 formation and decomposition rates than if primary rates were measured in the absence of secondary decomposition of H_2O_2. The primary advantages of batch-type reactors are their low cost and the related ability to operate many reactors simultaneously, which enables researchers to screen H_2O_2 rates and selectivities on a number of different combinations of catalysts, solvents, and additives.

Packed bed reactors (PBRs) have also been used to study direct synthesis,[41,148,155,156] and are useful particularly for kinetic studies because they operate at steady state and minimize secondary decomposition of H_2O_2 at short liquid residence times.[148] Unfortunately, complex flow regimes, due to hydrodynamic interactions between the three phases, can result in mass transport limitations that are more significant than in the well-stirred batch and semi-batch reactors. Mass transport coefficients depend on the gas–liquid flow regime within the reactor and increase with turbulence.[202] Figure 5 shows that the flow regime depends, in turn,

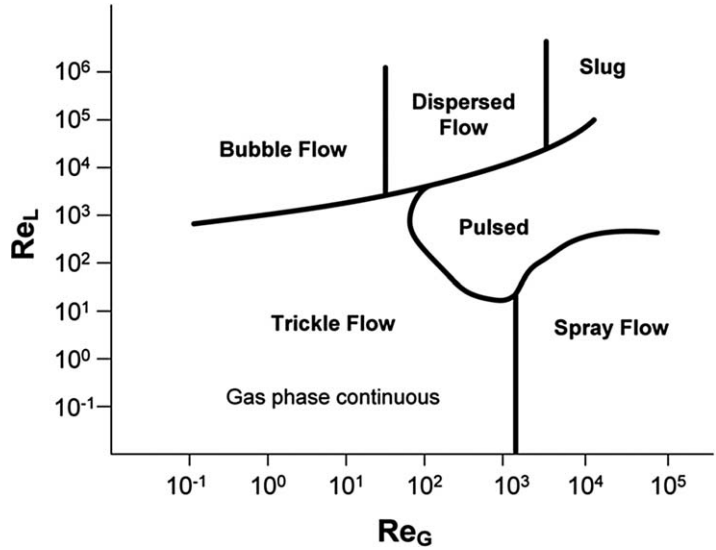

Fig. 5 Flow regime in a downward-flow packed bed reactor as a function of liquid (Re_L) and gas (Re_G) Reynold's numbers. Reproduced from J. García-Serna, T. Moreno, P. Biasi, M. J. Cocero, J.-P. Mikkola and T. O. Salmi, *Green Chem.*, 2014, **16**, 2320; with permission from the Royal Society of Chemistry.

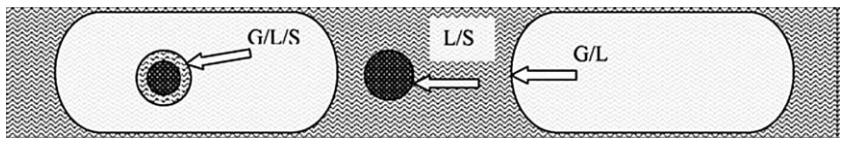

Fig. 6 Three different mass transport steps relevant to Taylor flow; (1) H_2 diffusion from the gas phase through a thin layer of liquid and then into the catalyst (G/L/S), (2) dissolved H_2 diffusing from the liquid into the catalyst (L/S), and (3) H_2 dissolving from the gas phase into the liquid (G/L). Reproduced from Y. Voloshin, R. Halder and A. Lawal, Kinetics of hydrogen peroxide synthesis by direct combination of H2 and O2 in a microreactor, *Catal. Today*, **125**, 40. Copyright 2007 with permissions from Elsevier.

on the Reynolds numbers of both the gas and the liquid phases, which are a function of the flow rate, catalyst particle packing, reactor diameter, and the density and viscosity of the solvent and gas streams.[189] Consequently, the type of flow can be difficult to predict, however, it may be observed experimentally (*e.g.*, with a transparent reactor) to allow rough estimates of mass transport coefficients and for the potential for mass transfer limitations.[189] Lawal *et al.* performed an analysis of mass transport on Pd clusters supported on 75–150 μm diameter SiO_2 particles within a 765 μm inner diameter PBR system used for direct synthesis rate measurements.[189] The small diameters of the reactor and the catalyst particles and the range of gas and liquid flow rates used (0.035–0.07 $m\,s^{-1}$ combined 9.1% H_2 in air and 1 wt% H_2SO_4 and 10 ppm NaBr in H_2O) resulted in Taylor flow, as illustrated in Fig. 6. Under such conditions, H_2 and O_2 readily diffuse through a thin liquid film on the outer surface of catalyst particles and do not present inter-particle (*i.e.*, external) mass transfer limitations, as shown by H_2O_2 formation rates that do not depend on the gas and liquid flow rates.[189] Notably, these methods cannot probe

for intra-particle mass transfer limitations, which are best assessed *via* the Madon–Boudart criteria,[203] as discussed later. Despite the complications presented by the flow regime, PBRs are effective for studying direct synthesis, because they can achieve steady-state and minimize the extent of H_2O_2 hydrogenation.

Less traditional reactors used to study direct synthesis include microfluidic devices[157–159] and membrane reactors.[160–163] Microfluidic reactors are much smaller versions of PBRs with diameters less than 400 μm and are often fabricated from glass. The small diameters of these reactors are less than that of the flame quenching distance for H_2 (640 μm), which helps to prevent H_2 combustion and allows direct synthesis to be studied with flammable reactant mixtures (>5 vol.% H_2).[37,164,196] Additionally, the high surface to volume ratios of these reactors dissipate heat well, which provides excellent temperature control.[204] However, microfluidic reactors suffer from high pressure drop and poor mixing from primarily laminar flow,[204] both of which introduce mass-transfer artifacts during kinetic measurements. Membrane reactors are made by the electroless deposition of catalytic material (*e.g.*, Pd) onto a porous tubular support such as α-alumina.[161–163] During the reaction, gaseous H_2 flowing across the exterior of the tubular membrane diffuses through the porous membrane to react with O_2 dissolved in a solvent flowing inside the tubular membrane. Consequently, H_2 and O_2 only contact at very low concentrations, which eliminates the potential for explosions. Like microfluidic devices, membrane reactors are useful for performing direct synthesis within the flammable region although the obvious mass transport limitations make them poorly suited for fundamental studies.

Regardless of the type of reactor used, intra-pellet mass transport restrictions (*i.e.*, small Thiele modulus, or an effectiveness factor of one) must be avoided to acquire mechanistically interpretable rate measurements. The Madon–Boudart criteria (*e.g.*, turnover rates must not depend on catalyst loading or the diameter of the support particle for a given metal dispersion or cluster size)[203] should be satisfied to demonstrate directly the lack of diffusional restrictions within catalyst particles.[148] If this condition is satisfied, and if inter-pellet concentration gradients are negligible, then reliable rate measurements may be collected in several of the reactors discussed. Clearly, each reactor has its own advantages and disadvantages, therefore, it is important for the researcher to assess which reactor would be the most applicable for each study on a case by case basis.

3.3 Mechanistic investigations of H_2O_2 and H_2O formation

The detailed mechanisms by which H_2O_2 ($H_2 + O_2 \rightarrow H_2O_2$) and H_2O ($2H_2 + O_2 \rightarrow 2H_2O$) form during direct synthesis are yet to be resolved and are the subject of numerous studies over the past two decades. In addition, the mechanism and intermediates for the decomposition ($2H_2O_2 \rightarrow 2H_2O + O_2$) and hydrogenation ($H_2O_2 + H_2 \rightarrow 2H_2O$) of H_2O_2 on transition metal catalysts has received significant attention.

Historically, the most commonly suggested mechanisms for H_2O_2 and primary H_2O formation during direct synthesis involve Langmuir–Hinshelwood type elementary steps between chemically adsorbed surface

$$H_2 + 2* \rightleftharpoons 2H* \quad (1)$$

$$O_2 + * \rightleftharpoons O_2* \quad (2)$$

$$O_2* + H* \rightleftharpoons OOH* + * \quad (3)$$

$$OOH* + H* \rightleftharpoons H_2O_2* + * \quad (4)$$

$$H_2O_2* \rightleftharpoons H_2O_2 + * \quad (5)$$

$$O_2* + * \rightleftharpoons 2O* \quad (6)$$

$$OOH* + * \rightleftharpoons OH* + O* \quad (7)$$

$$O* + H* \rightleftharpoons OH* + * \quad (8)$$

$$OH* + H* \rightleftharpoons H_2O* + * \quad (9)$$

$$H_2O* \rightleftharpoons H_2O + * \quad (10)$$

$$H_2O_2* + * \rightleftharpoons 2OH* \quad (11)$$

Scheme 4 Proposed elementary steps for a Langmuir–Hinshelwood mechanism for H_2O_2 and H_2O formation. Here, * denotes an empty site, X* represents an adsorbate bound to a single surface atom. Recreated from N. M. Wilson and D. W. Flaherty, Mechanisms for the Direct Synthesis of H2O2 on Pd Clusters: Heterolytic Reaction Pathways at the Liquid–Solid Interface, *J. Am. Chem. Soc.*, 2016, **138**, 574. Copyright 2015 American Chemical Society.

intermediates,[149,155,167,183,189,193,194,205–207] such as that depicted in Scheme 4. Here, H_2 dissociatively chemisorbs forming H* (where * denotes a chemisorbed surface species) while O_2 chemisorbs molecularly. Chemisorbed molecular oxygen (O_2*) reacts with an adjacent H* forming hydroperoxy (OOH*) and then with a second H* forming the H_2O_2*, which desorbs. Lunsford *et al.* demonstrated that O–O bond rupture occurs irreversibly during direct synthesis of H_2O_2 and inevitably leads to the formation of H_2O.[172] These conclusions were reached by performing direct synthesis using mixtures of $^{16}O_2$ and $^{18}O_2$ along with H_2. Figure 7 shows Raman spectra of the product mixture, which contains $H_2{}^{16}O_2$ and $H_2{}^{18}O_2$ but no detectable quantities of $H_2{}^{16}O^{18}O$. These results demonstrate O–O bond scission in O_2*, OOH*, and H_2O_2* must produce O* and OH* intermediates, which can only undergo subsequent hydrogenation and form H_2O*.

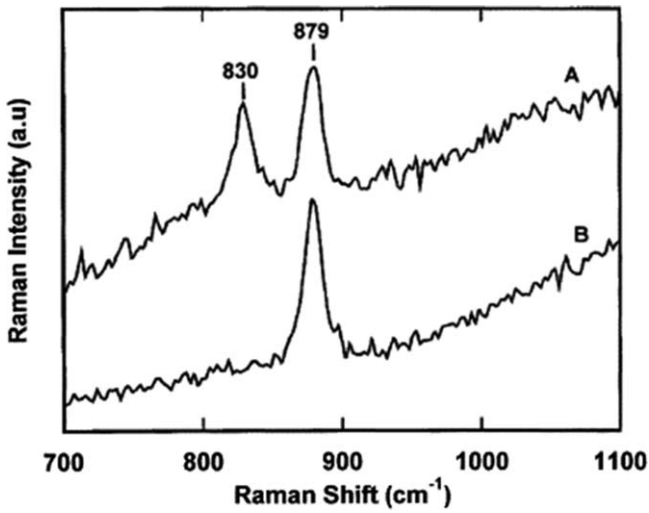

Fig. 7 Raman spectra of products from the direct synthesis of H_2O_2 in (a) the presence of $^{16}O_2$ and $^{18}O_2$ and (b) in the presence of $^{16}O_2$ only. Shifts at 879 and 830 cm^{-1} correspond to $H_2{}^{18}O_2$ and $H_2{}^{16}O_2$ respectively. Reproduced from D. P. Dissanayake and J. H. Lunsford, The direct formation of H2O2 from H2 and O2 over colloidal palladium, *J. Catal.*, **214**, 113. Copyright 2003 with permissions from Elsevier.

Several groups have proposed that direct synthesis occurs by Langmuir–Hinshelwood mechanisms, similar to those steps shown in Scheme 4, and have supported this claim by mathematical comparisons between measured rates and microkinetic models. Lawal *et al.* published a series of studies that probed the mechanism for direct synthesis on supported Pd catalysts by comparisons of rates measured in a PBR to proposed rate expressions.[156,189,208] In the first study, the dependence of H_2O_2 formation rates were measured as a function of the partial pressure of O_2 (82–414 kPa) and H_2 (28–207 kPa) and compared to rate expressions derived from four previously proposed sets of assumptions concerning the kinetic relevance of individual elementary steps.[189] Eremin *et al.* proposed three potential kinetically relevant steps for H_2O_2 formation ($H^* + OOH^* \rightarrow H_2O_2 + 2^*$, $O_2^* + H^{**}H \rightarrow H_2O_2^{**} + ^*$, and $O_2^{**} + H^{**}H \rightarrow H_2O_2^{**} + ^{**}$)[209] and Zhou and Lee proposed a similar step ($O_2^* + H_2^* \rightarrow H_2O_2^{**}$).[205] Measured H_2O_2 formation rates were reported to have a sub-linear dependence on both the O_2 and the H_2 pressures, however, the precise power law dependencies were not reported. The rate law proposed by Zhou and Lee (*i.e.*, kinetically relevant direct reaction of molecular H_2 with O_2)[205] best described the rate dependence data collected by Lawal *et al.*,[189] which is surprising considering the propensity for Pd to readily dissociate H_2.[120] Gemo and coworkers also measured rates for H_2O_2 formation in batch, semi-batch, and continuous flow reactors in order to determine the mechanism of formation.[149] This study combined simple rate expressions derived from Langmuir–Hinshelwood kinetics for primary (H_2O_2 and H_2O formation) and secondary (H_2O_2 decomposition and hydrogenation) rates with mass balances for the gas and liquid phase in each type of reactor to generate a series of differential and algebraic equations for comparison to

Table 3 Activation energies (E_a) and pre-exponential factors (A) for direct H_2O_2 formation (ds), direct H_2O formation (wf), H_2O_2 decomposition (d), and H_2O_2 hydrogenation (h), regressed from batch, semi-batch, and trickle bed reactor (TBR) experiments.[a]

	Batch		Semibatch		TBR	
	E_a (kJ mol^{-1})	A	E_a (kJ mol^{-1})	A	E_a (kJ mol^{-1})	A
ds	42.6	1.47×10^{9}	67.0	8.90×10^{21}	6.9	3.18×10^{17}
wf	92.3	4.38×10^{23}	133.8	1.15×10^{14}	8.0	5.52×10^{15}
d	30.1	1.47×10^{9}	58.9	1.09×10^{20}	5.1	4.66×10^{3}
h	53.2	1.38×10^{19}	29.8	7.07×10^{2}	7.3	3.87×10^{15}

[a] Reproduced from N. Gemo, T. Salmi and P. Biasi, *React. Chem. Eng.* 2016, **1**, 300; with permission from the Royal Society of Chemistry.

the experimental results. Table 3 shows rate constants and activation energies derived from fits to kinetic data, which suggest that the flow reactor gave the lowest activation energies for all primary and secondary reactions by a significant margin (4–17 fold).[149] These differences were attributed to differences between the average oxidation state of Pd in each of the reactors, specifically that the continuous flow reactor contained the smallest fraction of Pd^{2+} on the surface of Pd clusters because the concentration of H_2O_2 and the contact time were much less than in the batch-type reactors. This hypothesis may be consistent with earlier studies that have demonstrated that Pd^{2+} gives lower H_2O_2 formation rates by direct synthesis than those on Pd^0.[210,211] The differences in apparent activation energies may also reflect a significant change in the identity of the predominant surface intermediates. Whether or not the different ratios of Pd^{2+} to Pd^0 on the surface of clusters are responsible for the differences between apparent activation energies measured in different reactors, it is clear that the choice of experimental setup and reaction conditions impact the results of kinetic and mechanistic studies of direct synthesis, even among careful measurements within a single group. Consequently, such differences may be responsible, in part, for the seemingly disparate results reported by different groups studying direct synthesis of H_2O_2.[37]

Computational chemistry (*e.g.*, density functional theory (DFT)) has been used to calculate reaction and activation energies for sets of Langmuirian elementary steps that are commonly invoked to describe H_2O_2, as well as secondary decomposition of H_2O_2, on metal surfaces.[193,194,207,212–214] Notably, these theoretical investigations typically study periodic slabs at low coverages in contact with a vacuum, which differs from the liquid environment in which direct synthesis occurs. Mavrikakis *et al.* have predicted the geometry of the transition states and intrinsic activation energies for elementary steps for H_2O_2 formation and H_2O_2 decomposition and hydrogenation on the (111) facets of Pt, Pd, Cu, Ag, and Au.[193] The binding energy of atomic oxygen (BE_O) is an important parameter in direct synthesis, because BE_O correlates to O–O bond dissociation activity of each surface,[212] as such, the values of BE_O were compared with the calculated intrinsic activation energies, which showed that potential catalysts for direct synthesis can be grouped in three distinct classes.[193] These three classes consist of metals that bind O*

strongly ($BE_O < -4$ eV) and consequently dissociate O–O but kinetically hinder O* hydrogenation (*e.g.*, Cu), metals that weakly bind O* ($BE_O > -3.5$ eV) and therefore do not dissociate O–O and favor H_2O_2 formation (*e.g.*, Au, Ag), or metals with an intermediate BE_O ($-4 < BE_O < -3.5$ eV) that readily dissociate O–O and favor complete reduction of O* to H_2O (*e.g.*, Pd, Pt). It is important to note that while Au and Ag have higher energy barriers for O–O dissociation than the other metals, their low BE_O values would suggest low availability of O_2 on the surface and therefore the rates of both H_2O_2 and H_2O formation are quite slow. As such, Pd remains the catalyst of choice for direct synthesis research, because Pd has higher barriers for O–O bond scission than Cu and BE_O values that allow for reasonable rates of H_2O_2 formation.

Modification of the Pd by alloying with Au is also an effective strategy for increasing H_2O_2 selectivity. Lim *et al.* predicted that monomers of Pd within a 4×4 Au atomic slab with 15 Au atoms and one Pd atom, give barriers for O–O bond scission within O_2*, OOH*, and H_2O_2* that are 1.04, 0.5, and 0.3 eV, respectively, greater than those on Pd(111).[213] Todorovic and Meyer examined the effects of alloying metals on the activation energies for a mechanism involving hydrogenation of O_2* and OOH* by H* to form H_2O_2 in tandem with dissociation of O–O bonds and subsequent hydrogenation of O* and OH* by H* to form H_2O.[194] They found that the kinetically relevant steps that formed H_2O were O_2* dissociation on Pd(111), OOH* dissociation into O* and OH* on Pt(111), and H_2O_2* dissociation into 2OH* on a AuPd(221) surface with a stoichiometry of Au_9Pd_1. Other investigators found also that dissociation of the O–O bond in H_2O_2* occurred more readily than that of O_2* and OOH* on 12-atom Au clusters[212] and on Pd monomers in a 4×4 Au atomic slab with 15 Au atoms and one Pd atom.[213] The investigation by Todorovic and Meyer also addressed direct synthesis on a 0.4 ML H-covered Pd hydride (PdH(211)) surface, which may form at the H_2 and O_2 pressures and temperatures used for direct synthesis.[215] Activation energies for O_2* dissociation are greater on the PdH(211) (0.77 eV) than on the Pd(111) (0.59 eV), while the activation energies for the dissociation of OOH* to O* and OH* and for the hydrogenation of OOH* to H_2O_2* are both lower on PdH(211) (0.12 and 0.73 eV) than on Pd(111) (0.35 and 1.13 eV). Thus, the decrease in activation energies for steps that lead to H_2O_2 formation and the concomitant increase in barriers for steps preceding H_2O formation suggest that Pd hydrides may be more selective for direct synthesis of H_2O_2 than Pd. In general, DFT studies largely agree that the binding energy of O* is an important factor for determining activity towards direct synthesis and that catalysts that preferentially cleave O–O bonds within H_2O_2* over O_2* and OOH* are more selective. These studies suggest that greater H_2O_2 selectivities may be achieved on modified surfaces (*e.g.*, bimetallics), which primarily form H_2O through H_2O_2 dissociation (as discussed below in Section 3.4).[32,213,216] While DFT studies provide invaluable guidance that helps researchers to understand direct synthesis at the catalyst surface, experimental studies of technical catalysts remain critical for revealing the predominant mechanism for H_2O_2 and H_2O formation during direct synthesis.

Langmuir–Hinshelwood mechanisms involving homolytic dissociation of H_2 are the most commonly proposed mechanisms by far, however, alternative mechanisms have been proposed. The alternative to the homolytic surface reactions described above involve elementary steps between highly charged intermediates in both the solvent and at the catalyst surface, namely proton–electron transfer processes. Lunsford *et al.* showed that Pd catalysts can form trace amounts of H_2O_2 corresponding to an average of 0.5 turnovers per Pd (*i.e.*, 2.7×10^{-5} mol H_2O_2 with 4.7×10^{-5} mol Pd) in a batch reactor containing an acidic aqueous solution (0.1 M HCl) saturated with O_2 at atmospheric pressure.[154] Lunsford proposed that Cl^- from HCl and dissolved O_2 combine to form Cl_2PdO_2 complexes, which react with H^+ and Cl^- in solution to form $PdCl_4^{2-}$ and H_2O_2, inspired by the work by Stahl *et al.* on the oxygenation of nitrogen-coordinated Pd^0.[217] Subsequently, $PdCl_4^{2-}$ could be reduced to Pd^0 and HCl by reaction with dissolved H_2 (Scheme 5).[154] Notably, this mechanism involves homogenous intermediates that form from supported Pd clusters, which would then leach from continuous flow reactors at high rates. Moreover, this mechanism would not explain H_2O_2 formation in the absence of acids or strongly coordinating anionic species, such as CL^-. In their 2005 patent, Zhou and Lee[205] suggested that H_2O_2 formed by a Langmuir–Hinshelwood mechanism involving electron transfer from H_2 to O_2 prior to the reaction between H_2^{2+} and O_2^{2-} surface species, however, the patent did not contain data that supports this mechanism. Centi *et al.* proposed that H_2O_2 forms by protonation of O_2* to OOH^{*+} by protons (H^+) in solution, followed by reaction between OOH^{*+} and non-chemisorbed H_2 to form H_2O_2* and a H^+.[161] The authors claimed that the mechanism was supported by the observation that Pd membrane catalysts that had been soaked in concentrated H_2O_2 longer (*i.e.*, higher O_2* coverage) had a higher propensity

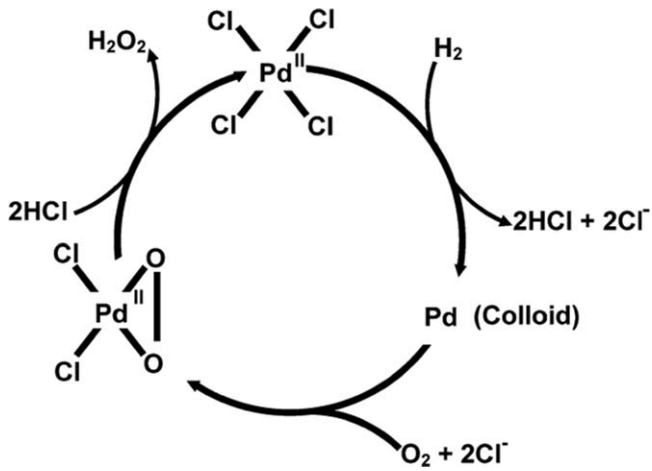

Scheme 5 Mechanism proposed by Lunsford *et al.* for HCl-facilitated direct synthesis on Pd clusters. Reprinted from S. Chinta and J. H. Lunsford, A mechanistic study of H2O2 and H2O formation from H2 and O2 catalyzed by palladium in an aqueous medium, *J. Catal.*, 2004, **225**, 249. Copyright 2004 with permissions from Elsevier.

to form H_2O_2, although this pretreatment procedure may also have affected the oxidation state of the Pd clusters. Our group has performed a mechanistic study for direct synthesis on SiO_2-supported Pd clusters by measuring formation rates of H_2O_2 and H_2O (in the absence of secondary decomposition) over a wide range of H_2 (5–400 kPa) and O_2 (25–400 kPa) pressures.[148] Rate data were inconsistent with previously proposed Langmuirian mechanisms but instead fit an Eley–Rideal mechanism involving proton–electron transfer to O_2** and OOH** (where ** denotes adjacent surface sites) following heterolytic dissociation of H* (to H^+ and e^-), as shown in Scheme 6. The importance of proton–electron transfer pathways was further supported by experiments showing that H_2O_2 formation rates are undetectable in aprotic solvents. This mechanism involving proton–electron transfer is similar to the two electron oxygen reduction reaction (ORR),[218,219] however, this chemistry occurs in the absence of an applied voltage. Instead, H_2 provides a chemical potential needed to drive the reaction, depicted in Scheme 7. This finding provides a useful link between the direct synthesis of H_2O_2 to the well-studied field of ORR chemistry and catalyst design.

$$H_2 + 2* \rightleftharpoons 2H* \quad (1)$$

$$H* \rightleftharpoons H^+ + e^- + * \quad (2)$$

$$O_2 + ** \rightleftharpoons O_2** \quad (3)$$

$$O_2** + H^+ + e^- \rightleftharpoons OOH** \quad (4)$$

$$OOH** + H^+ + e^- \longrightarrow H_2O_2** \quad (5)$$

$$H_2O_2** \rightleftharpoons H_2O_2 + ** \quad (6)$$

$$O_2** \longrightarrow 2O* \quad (7)$$

$$OOH** \longrightarrow OH* + O* \quad (8)$$

$$O* + H* \longrightarrow OH* + * \quad (9)$$

$$OH* + H* \longrightarrow H_2O* + * \quad (10)$$

$$H_2O* \rightleftharpoons H_2O + * \quad (11)$$

$$H_2O_2** \longrightarrow 2OH* \quad (12)$$

Scheme 6 Proposed elementary steps for mechanism for H_2O_2 formation by proton–electron transfer and H_2O formation by hydrogenation. Here, * denotes an empty site, X* represents an adsorbate bound to a single Pd atom, and $\rightleftharpoons$ indicates that an elementary step is quasi-equilibrated. Adapted from N. M. Wilson and D. W. Flaherty, Mechanism for the Direct Synthesis of H2O2 on Pd Clusters: Heterolytic Reaction Pathways at the Liquid–Solid Interface, *J. Am. Chem. Soc.*, 2016, **138**, 574; © 2015 American Chemical Society.

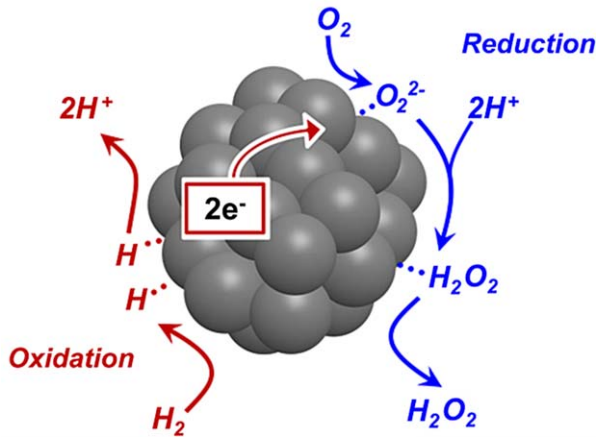

Scheme 7 Pd clusters catalyze both heterolytic H_2 oxidation and O_2 reduction steps in order to form H_2O_2 at steady-state while conserving charge. Adapted from N. M. Wilson and D. W. Flaherty, *J. Am. Chem. Soc.*, 2016, **138**, 574; © 2016 American Chemical Society.

In practice, H_2O_2 yields depend not only on the primary rates of H_2O_2 and H_2O formation but reflect also loss of H_2O_2 by secondary decomposition ($2H_2O_2 \rightarrow 2H_2O + O_2$) and hydrogenation ($H_2O_2 + H_2 \rightarrow 2H_2O$) reactions on the surface of the catalyst.[25] Dumesic *et al.* directly compared hydrogenation and decomposition rates on SiO_2 supported Pd and AuPd clusters in a batch reactor.[186] Rates of hydrogenation on Pd (0.61 (mol H_2O_2)(mol Pd_s s)$^{-1}$ where Pd_s denotes surface Pd atoms) and AuPd (2.35 (mol H_2O_2)(mol Pd_s s)$^{-1}$) clusters were much higher than rates for decomposition (0.029 and 0.067 (mol H_2O_2)(mol Pd_s s)$^{-1}$, respectively).[186] Surprisingly, AuPd decomposed H_2O_2 more quickly than Pd by both pathways, thereby resulting in a lower selectivity than Pd. It was suggested that the AuPd clusters used in this study had poor H_2O_2 selectivities because groups of contiguous Pd atoms existed on the surface even at 0.69 ML Au,[186] however, it is not discussed why the hydrogenation and decomposition rates were higher on AuPd than on Pd. Choudhary *et al.* also found that rates of H_2O_2 hydrogenation (42 h^{-1}) were much higher than those for H_2O_2 decomposition (0.5 h^{-1}) on Al_2O_3 supported Pd in a batch reactor in aqueous solution of 0.3 M H_3PO_4.[220] Unlike the findings of Dumesic *et al.*,[186] modification of the surface of the Pd catalyst led to a decrease in hydrogenation rates (8 fold). Mavrikakis *et al.* recently reported a thorough investigation of the mechanisms by which H_2O_2 decomposes on Pd that combined experimental and DFT results.[191] The conclusions of this study agree with previous work[172] that suggested H_2O_2 decomposes predominantly through dissociation of the O–O bond in OOH*. Hydrogenation then occurs *via* thermodynamically driven H-transfer steps from H_2O_2*, H_2O*, or OOH* to form OH* from O* (H_2O_2* + O* → OOH* + OH*; H_2O* + O* → 2OH*; OOH* + O* → O_2* + OH*) or H_2O* from OH* (H_2O_2* + OH* → OOH* + H_2O*; OOH* + OH* → O_2* + H_2O*). Table 4 shows the full proposed mechanism including calculated energy barriers and reaction energies for each step. H-transfer from H_2O_2* and OOH* to O* and OH* is more thermodynamically favored

Table 4 Proposed list of elementary steps for H_2O_2 decomposition and their calculated energy barriers (E_a) and forward reaction energies (ΔE) on Pd(111) and Pd(100) surfaces.[a,b]

		Pd(111)[c]		Pd(100)	
Number	Elementary step	E_a (eV)	$\triangle E$ (eV)	E_a (eV)	$\triangle E$ (eV)
1	$H_2O_2 + * \leftrightarrow H_2O_2*$	—	−0.32	—	−0.36
2	$H_2O* \leftrightarrow H_2O + *$	—	0.22	—	0.30
3	$O_2* \leftrightarrow O_2 + *$	—	0.50	—	1.27
4	$H* + H \leftrightarrow H_2 + 2*$	—	1.11	—	1.19
5	$H_2O_2* + * \leftrightarrow OH* + OH*$	0.18	−1.53	0.05	−2.29
6	$OOH* + * \leftrightarrow O* + OH*$	0.08	−1.50	0.02	−1.83
7	$O_2* + * \leftrightarrow O* + O*$	0.85	−1.23	0.30	−0.98
8	$OH* + * \leftrightarrow O* + H*$	1.02	0.07	1.03	0.17
9	$H_2O* + * \leftrightarrow OH* + H*$	1.10	9.37	0.67	0.00
10	$OOH* + * \leftrightarrow O_2* + H*$	0.59	−0.20	0.52	−0.67
11	$H_2O_2* + * \leftrightarrow OOH* + H*$	0.62	0.05	0.44	−0.29
12	$H_2O* + O* \leftrightarrow OH* + OH*$	0.33	0.33	0.00	−0.51
13	$H_2O_2* + O* \leftrightarrow OOH* + OH*$	0.04[d]	−0.44	0.14[d]	−0.87
14	$H_2O_2* + OH* \leftrightarrow OOH* + H_2O*$	0.00	−0.16	0.00	−0.17
15	$OOH* + O* \leftrightarrow O_2* + OH*$	0.00	−0.27	0.02	−0.81
16	$OOH* + OH* \leftrightarrow O_2* + H_2O*$	0.00	−0.38	0.00	−0.13
17	$H_2O_2* + O_2* \leftrightarrow OOH* + OOH*$	0.20	−0.02	0.00	0.00

[a] Replicated from A. Plauck, E. E. Strangland, J. A. Dumesic and M. Mavrikakis, Active sites and mechanisms for H2O2 decomposition over Pd catalysts, *Proc. Natl. Acad. Sci.*, 2016, **113**(14), E1973; with permission from Proceedings of the National Academy of Sciences.
[b] Energetics are reported with respect to either reactants/products at infinite separation (steps 1–11) or coadsorbed for H-transfer reactions (steps 12–17) because of these reactants/products are generally stabilized through hydrogen bonding. Elementary steps are classified as follows: adsorption/desorption (steps 1–4); O–O scission (steps 5–7); dehydrogenation (steps 8–11); and H transfer (steps 12–17). E_a and $\triangle E$ represent the calculated activation energy and reaction energy in the forward direction. No activation barriers are calculated for adsorption/desorption steps.
[c] Data for steps 1–12 on Pd(111) are based on ref. 193.
[d] Activation energy corresponds to breaking Pd–O bonds to lift O* from its preferred site (fcc or fourfold hollow).

over hydrogenation by H* in the presence of H_2O_2, but rates of hydrogenation might be higher than those for H-transfer when H_2 is present and creates an abundance of H*. Lawal *et al.* studied the hydrogenation of H_2O_2 and found that increasing H_2 partial pressure increased the rate of H_2O_2 hydrogenation between 28 and 140 kPa, above which hydrogenation rates no longer depended on H_2 pressure.[156] Increasing the concentration of H_2O_2 also increased the hydrogenation rate but there was a maxima at ~0.6 M H_2O_2 followed by a slight decrease in hydrogenation rate with further increases in H_2O_2 concentration. Comparisons between the quality of fit between rate expressions derived from several proposed mechanisms and the kinetic data suggested that O–O bonds primarily ruptured by unimolecular dissociation of H_2O_2 (*i.e.*, $H_2O_2* + * \rightarrow 2OH*$) rather than direct hydrogenation of H_2O_2* by H* (*i.e.*, $H_2O_2* + 2H* \rightarrow 2H_2O* + *$). However, the difference in the quality of fit between these two models do not appear to be statistically significant (*e.g.*, reported R^2 values of 0.9360 and 0.9362 respectively), such that it seems difficult to state definitively whether one pathway for O–O rupture dominates. Work by Hutchings *et al.* found that the hydrogenation of H_2O_2 in a batch reactor can be suppressed

significantly on carbon supported AuPd by pretreating the support with acid (*e.g.*, HNO_3, CH_3COOH)[168] or by using a specific oxidation/reduction pretreatment on TiO_2 supported PdSn.[169] Both of these findings are discussed in more detail below (Section 3.4).

Despite the significant research into the mechanisms responsible for the formation and decomposition reactions that occur during direct synthesis, it is clear that there is no consensus on the mechanism. Individual reports of kinetic measurements acquired in batch and packed bed reactors provide evidence for both Langmuir–Hinshelwood and Eley–Rideal mechanisms and for homolytic and heterolytic dissociation of H_2. Computational studies agree that the binding energy of atomic oxygen is an important factor for gauging the catalytic activity of direct synthesis. Both experimental and computational studies found that rates of H_2O_2 hydrogenation were more significant than those for H_2O_2 decomposition. Future work should emphasize collecting additional evidence for the mechanisms of H_2O_2 formation using computational or experimental methods. Computational studies will need to consider the presence of the solvent, which is ubiquitous during H_2O_2 formation, and which may participate directly (as a source of H^+) and indirectly (*via* solvation, hydrogen-bonding interactions, H^+ shuttling, *etc.*). Experimental investigations must take the appropriate precautions to ensure that mass transport restrictions do not introduce artifacts to rate measurements, the hydrodynamics of the reactors used are well-understood, and that secondary decomposition of H_2O_2 is either suppressed or accounted for correctly.

3.4 Strategies for improving H_2O_2 selectivity during direct synthesis

3.4.1 Use of acidic solvents and halide modifiers. The success of direct synthesis as a viable alternative to AO relies on achieving high H_2O_2 selectivities, and consequently, a number of different catalyst design (*e.g.*, addition of halides, alloying metals, modified supports) and reaction engineering (*e.g.*, addition of acids to solution, changing solvent identity) approaches have been investigated for their potential to improve H_2O_2 selectivities. One of the earliest and most effective strategies for increasing H_2O_2 selectivity during direct synthesis is the addition of mineral acids (*e.g.*, HCl,[195,221] HBr,[151,153,154] H_2SO_4,[151,153,154] H_3PO_4,[153,222] HNO_3,[222] H_2CO_3 from dissolved CO_2[168,223]) to the reaction solution. However, the mechanism by which adding acids or halides to the reaction medium increases selectivity is currently unclear. Work by Liu and Lunsford has shown that increasing the concentration of H_2SO_4 (in the presence of HCl) in ethanol increases overall rates of H_2O_2 formation by up to 2-fold on SiO_2 supported Pd clusters.[195] The addition of NaCl (*i.e.*, as a source of Cl^-), however, had shown no selectivity towards H_2O_2, which suggests that mainly the changes in the acidity of the solution increases H_2O_2 formation rates and that the presence of SO_4^{2-} or Cl^- anions is less significant.[195] The same group also found that 0.12 M H_2SO_4 solutions give somewhat higher H_2O_2 selectivities (40%) and H_2O_2 yields (1.5 wt% H_2O_2 in 5 hours) than 0.17 M HCl (35% selectivity, 1.2 wt% H_2O_2) on the same Pd catalyst.[198] Unfortunately, the reasons for

these differences are difficult to understand as pH values were not reported and the concentrations of the acids were different. Thus, it is unclear if the differences in rates and selectivity result from different concentrations of H^+ in solution or the difference in the identity of the counterion. Recently, our group examined the effects of proton concentration on H_2O_2 and H_2O formation and found a slight increase in H_2O_2 formation rates (10 fold) over a very wide range of proton concentration (10^7 fold).[148] This trend was consistent for four different acids (HCl, H_2SO_4, H_3PO_4, H_2CO_3), and the rates and selectivities for H_2O_2 formation did not depend on the identity of the acid at a given pH value. The slight increase in H_2O_2 formation rate was attributed to modification of the ionic strength of the solution surrounding the catalyst surface, which can help to stabilize highly charged transition states as described by Debye–Huckel theory. While acidic solutions clearly help to increase rates and selectivities for H_2O_2 formation,[189,224,225] the reasons for these differences remain speculative.

In addition to acids, the presence of halide-containing compounds (*e.g.*, NaBr,[222,226] KBr,[153] KCl[153]) in solution have been found to improve H_2O_2 selectivity.[153] Halides may increase H_2O_2 selectivities by adsorbing strongly and blocking sites that readily dissociate O–O bonds, as suggested in studies of Cl and Br on $PtPd/SiO_2$,[40] Cl and Br on Pd/SiO_2,[195,198] and Br on AuPd/C and AuPd/MgO.[222] Alternatively, the halides may also affect the electronic structure of the catalyst surface, shifting electrons lower in energy than the Fermi level, decreasing the extent of electron back donation to $2\pi^*$ orbitals of O_2^* (and OOH* and $H_2O_2^*$), and thus making O–O bond dissociation more difficult.[153,227–231] Notably, halides and acids may work cooperatively. Specifically, acidic solutions can lower the solution pH beneath the isoelectric point of the catalyst surface (*i.e.*, protonate the surface) such that negatively charged halides adsorb and influence surface chemistry.[232] While the exact mechanism by which the presence of acids and halides in solution improve H_2O_2 selectivity is not clear, it is generally accepted that they do so *via* a direct interaction with the catalyst surface. Choudary and Samanta found that the post-synthetic addition of Br^- to a Al_2O_3 supported 5 wt% Pd catalyst resulted in high H_2O_2 selectivity (increase from 1 to 61%) in a semi-batch reactor.[153,233] This improvement was attributed to charge transfer from the halides to O_2^*, which could facilitate the reaction of O_2^* with H^+ in solution. The involvement of H^+ in the proposed mechanism is supported by experiments, which showed that the addition of Br^- in the absence of acid (*i.e.*, a low concentration of H^+ in solution) did not improve catalyst performance.[153,195,232] In contrast to Br^-, I^- significantly decreased H_2 conversion (perhaps due to the strong coordinating ability of I with Pd which indiscriminately blocks all active sites) while F^- resulted in a decrease in H_2O_2 selectivity which was attributed to the high electronegativity of F, which makes it more difficult to transfer e^- to O_2^*. Overall, the addition of halides and acids to the reaction mixture is an undesirable solution to the selectivity problem because direct synthesis plants would need to purify the H_2O_2 formed and dispose of acidic waste in practice. Therefore, other surface modification strategies may be able

to alter the surface chemistry in a similar way, but without the use of harmful solutions.

3.4.2 Effects of metal cluster size. The caustic nature of acid and halide additives and the detrimental effects on the stability of direct synthesis catalysts has motivated research to find non-hazardous means of increasing H_2O_2 selectivity during direct synthesis. One simple approach has been to investigate the effects of cluster size on H_2O_2 selectivity. Several studies found that increasing the average particle diameter of Pd clusters over a range of 0.7–7 nm,[148] 4–5 nm,[234] and 3.4–4.2 nm[235] lead to a 4, 1.5, and 1.3 fold increases in H_2O_2 selectivity, respectively. Increasing cluster size is known to alter the electronic landscape of the catalyst surface by decreasing the ratio of under-coordinated (corners and edges) to coordinated (terraces) surface atoms.[236] Under-coordinated surface atoms have decreased d-orbital overlap, resulting in an increase in the density of states at energies near the Fermi level and higher than the lowest unoccupied molecular orbitals (LUMO) of O_2.[228] Therefore, Pd surfaces with more under-coordinated surface atoms (*i.e.*, small clusters) will have a greater extent of electron back donation into the π^* orbital of O_2*, increasing rates of O–O bond dissociation. These findings are in agreement with measurements of the activation enthalpy for H_2O formation, which showed an increase of 14 kJ mol^{-1} when the Pd cluster size was increased from 0.7 to 7 nm.[148] However, increasing the size of Pd clusters alone does not achieve sufficiently high H_2O_2 selectivities and is doubly ineffective because a significant portion of the (expensive) Pd cannot interact with the reagents. Thus, despite the benefits of increasing cluster size, an alternative means for changing the electronic structure of Pd surfaces has been pursued through alloying with various metals.

3.4.3 Alloys and bimetallic catalysts. Alloying Au with Pd can significantly increase both H_2O_2 selectivities and formation rates in comparison with monometallic Pd.[19,54,63,81,194] One of the most well-known examples of this phenomenon are the high H_2O_2 selectivities on AuPd bimetallic clusters supported on Al_2O_3 reported by Hutchings and coworkers.[151] In their initial study, a 1 : 1 Pd to Au catalyst had markedly improved rates (4.5×10^6 (mol H_2O_2) (kg catalyst h)$^{-1}$) and selectivities (14%) over monometallic Pd (3.7×10^5 (mol H_2O_2) (kg catalyst h)$^{-1}$and 1%, respectively). These results have since inspired multiple studies on AuPd,[165–167] which have achieved reasonably high H_2O_2 selectivities (40–80%). These studies span a range of supports (*e.g.*, Al_2O_3, TiO_2, C, CeS, ZS) and solvents (*e.g.*, water, ethanol, methanol), yet H_2O_2 selectivity increases upon the addition of Au to Pd in all cases. The mechanistic or energetic reasons for these improvements are still the subject of active research.

DFT work by Lim compared activation energies for O–O bond scission in O_2*, OOH*, and H_2O_2* between Pd monomers, dimers, and trimers on a AuPd surface with those on Pd(111) and found that barriers for O–O bond rupture uniformly decrease with the increasing number of Pd–Pd

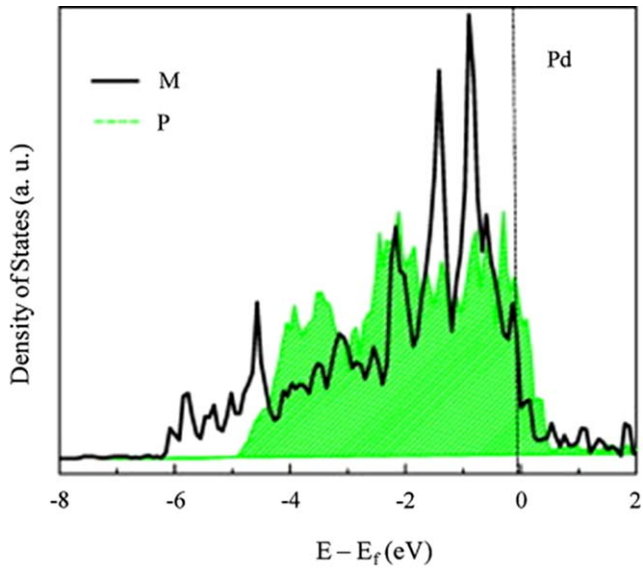

Fig. 8 Projected density of states for Pd in a monometallic slab (P) and as a monomer surrounded by Au atoms (M). Reproduced from H. C. Ham, J. A. Stephens, G. S. Hwang, J. Han, S. W. Nam and T. H. Lim, Pd ensemble effects on oxygen hydrogenation in AuPd alloys: A combined density functional theory and Monte Carlo study, *Catal. Today*, 2011, **165**(**1**), 138–144. Copyright 2011 with permissions from Elsevier.

nearest neighbors.[213,216] These findings were explained as the result of Pd having a greater propensity to back donate electrons to π* orbitals of O_2* in comparison to Au. Thus, these results suggest that the highest H_2O_2 selectivities will be given by AuPd surfaces that contain primarily Pd monomers rather than ensembles of two or more Pd atoms. Figure 8 shows that the calculated density of states of Pd monomers in the Au surface are broader and shifted lower in energy relative to the Fermi level than on Pd atoms within the pure Pd(111) surface clusters.[213,216] The broadening of the density of states suggests that Au not only rehybridizes orbitals within the surface but also withdraws electrons from Pd atoms, which can further reduce electron back donation. There is a significant amount of experimental evidence from X-ray photoelectron spectroscopy (XPS) measurements showing that there is a decrease in the binding energy of the Pd 3d (0.4–1.4 eV) and Au 4f (0.3–1.4 eV) orbitals relative to bulk Pd and Au respectively.[237–242] Many of these reports state that these changes in binding energy result from charge transfer from the Pd to adjacent Au, reducing the electron density on Pd.[237,240–242] Collectively, these computational and experimental findings suggest that the greater H_2O_2 selectivities on AuPd result from electronic changes. There is, however, evidence that indicates that the improved H_2O_2 selectivities on AuPd simply occur due to differences in the number of sites that form H_2O_2 over those that form H_2O (*i.e.*, changes result from ensemble effects). Jirkovský *et al.* suggested that Pd monomers in Au cannot easily dissociate O–O bonds but readily form H_2O based on comparisons of H_2O_2 and H_2O selectivities among AuPd clusters during electrocatalytic

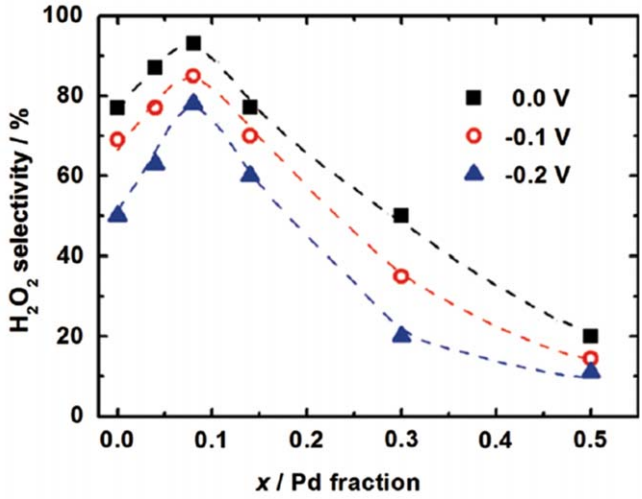

Fig. 9 H_2O_2 selectivity as a function of the molar fraction of Pd in AuPd catalysts (x), at potentials of 0, −0.1, and −0.2 V. The dashed lines are intended to guide the eye. Reproduced with permissions from J. S. Jirkovský, I. Panas, E. Ahlberg, M. Halasa, S. Romani and D. J. Schiffrin, Switching on the Electrocatalytic Ethene Epoxidation on Nanocrystalline RuO2, *J. Am. Chem. Soc.*, 2011, **133**, 19432. Copyright 2011 American Chemical Society.

ORR conducted with a rotating ring-disc electrode.[32] Figure 9 shows that the H_2O_2 selectivities increase initially with Pd content and reach a maximum at 10% Pd, where Pd dimers are thought to begin to form on the clusters used in the study. DFT calculated energy barriers show that Pd monomers have higher activation energy barriers for H_2O formation than dimers and Pd surfaces,[32] which agrees with the calculations reported by Lim and coworkers.[213,216] The combined evidence for ensemble and electronic effects indicates that the improved H_2O_2 selectivities after alloying Pd with Au likely arise from a combination of these two effects, which are intrinsically linked. Regardless of the specific manner by which AuPd promotes H_2O_2 formation over O–O bond rupture, isolated surface Pd atoms are preferred over contiguous Pd ensembles for direct synthesis catalysts. Consequently, other Pd-based bimetallic and intermetallic compounds may also show greater H_2O_2 selectivities than Pd.

The success of alloying Au and Pd has inspired investigations into alternative alloys in order to find other selective catalysts. For example, Lunsford *et al.* examined SiO_2 supported PtPd alloy clusters in a semi-batch reactor in ethanol acidified with H_2SO_4 and found that mono-metallic Pd (~70%) had significantly higher H_2O_2 selectivity than Pt (~10%). However, the addition of an extremely small amount of Pt to Pd (1% Pt, 99% Pd) resulted in a two fold increase in H_2O_2 formation rate with no loss in selectivity (60–70%).[40] The increase in H_2O_2 formation rate was attributed to electronic modification of the Pd by the Pt (and not a direct interaction between Pt and adsorbates), because Pt would most likely be located within the bulk of the cluster due to its preference to alloy with Pd.[40,243] Zecca *et al.* reported that PtPd (5% Pt, 95% Pd) clusters

gave a greater H_2O_2 selectivity (43%) than did monometallic Pd clusters (37%) when both were supported on Lewatit K2621 resin and studied in a batch reactor, however, the H_2O_2 formation rate decreased almost two fold upon addition of Pt.[188] The difference between the report of Zecca *et al.* and that of Lunsford *et al.* could be attributed to differences in the systems used (Lunsford *et al.* used a semi-batch reactor at atmospheric pressure and Zecca *et al.* implemented a batch reactor at pressures exceeding 2.4 MPa), yet in both cases there was an improvement in the overall performance of the catalyst through the addition of small amounts of Pt to the Pd. Recent studies of bimetallic ORR catalysts have revealed that PtHg,[29,30] AgHg,[29] Pt_3Y,[244] Pt_5Y,[244] and Pt_5La[244] are all highly selective catalysts for the two electron ORR that produces H_2O_2. While many of these metals are still expensive, the similarities between the mechanism of direct synthesis and ORR (Section 3.3) may suggest that these alloys would be new and fruitful search directions for new catalysts for thermal H_2O_2 formation.

Hutchings *et al.* have shown recently that PdSn alloy catalysts (synthesized by incipient wetness and treated with a specific heating protocol) can give H_2O_2 selectivities greater than 95% in the absence of corrosive and toxic additives.[169] Results from STEM-EELS mapping of the PdSn catalysts suggested that the initial oxidation step in air (773 K for three hours) forms a secondary SnO_x support (Scheme 8a) which, when reduced in H_2 (473 K for two hours) in a second step, encases small Pd clusters that actively dissociate H_2O_2 by a strong metal-support interaction (Scheme 8b). The larger PdSn alloy clusters will also dissociate H_2O_2 when reduced, so a second oxidation step (673 K for four hours) is used to decrease the propensity for these clusters to dissociate H_2O_2 (Scheme 8c). This system may be generalized to metals other than Sn provided that they do not readily decompose H_2O_2 in their oxide form,

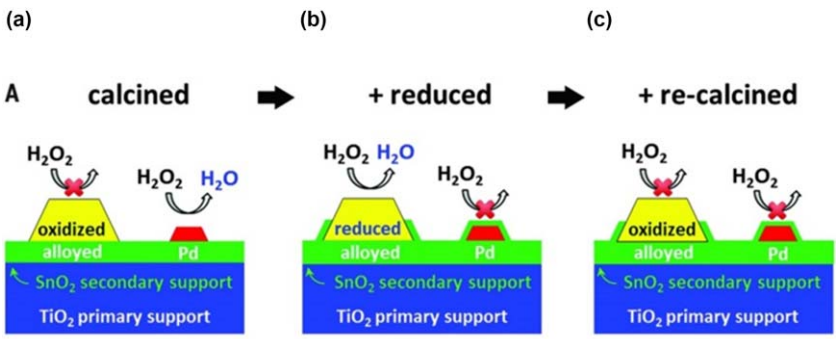

Scheme 8 Selective PdSn catalysts are created by (a) oxidation (calcined), forming a SnO_2 secondary support, then (b) reduction to cover the small Pd clusters with the SnO_2 so they cannot undergo secondary decomposition of H_2O_2, and (c) a final oxidation step which suppresses the PdSn alloy from decomposing/hydrogenating H_2O_2. Reproduced with permissions from S. J. Freakley, Q. He, J. H. Harrhy, L. Lu, D. A. Crole, D. J. Morgan, E. N. Ntainjua, J. K. Edwards, A. F. Carley, A. Y. Borisevich, C. J. Kiely and G. J. Hutchings, palladium-tin catalysts for the direct synthesis of H2O2 with high selectivity, *Science*, 2016, **351**, 965. Copyright 2016 American Associated for the Advancement of Science (AAAS).

form exothermic alloys or intermetallics with Pd, and can cover the small Pd clusters formed.[169] Additional metals were tested in this study (*e.g.*, Ni, Zn, Ga, In, Co) and found to also form highly selective catalysts when alloyed with Pd and subjected to the pretreatment procedure described above. Studies on alternatives to AuPd are an important advancement in direct synthesis research, because these findings help to provide new concepts for the design of selective catalysts, perhaps from more abundant and less costly metals.

Despite the significant improvements seen by alloying different metals with Pd, it would be desirable to find alternative and less expensive metals that can selectively catalyze the direct synthesis reaction. Towards this goal, Rankin and Greeley generated a two-dimensional Sabatier volcano plot of H_2O_2 formation rates and selectivities (calculated from a microkinetic model) for a number of transition metals (*e.g.*, Pt, Pd, Ag, Au, Cu, Ir, Rh, Ni, Os, Co, Ru, Fe) as a function of the binding energies of O* and H* on those surfaces (Fig. 10).[207] Metals that lie within the red area at the center of the volcano plot (*i.e.*, $\Delta G_O = 1.5$ eV and $\Delta G_H = -0.4$ eV) oxidize H_2 at the greatest rates, however, these metals bind O-atoms (and O_2) strongly, and preferentially dissociate O–O bonds, which is consistent with previous reports on Pt and Pd and their location within the red region.[40,172] Metals that fall within the shaded black region at the far right of the volcano plot (*i.e.*, $\Delta GO > 2$ eV) have more negative free energy changes for steps in the selective pathway (*i.e.*, O_2* and OOH* hydrogenation and H_2O_2 desorption) than those in the unselective pathway

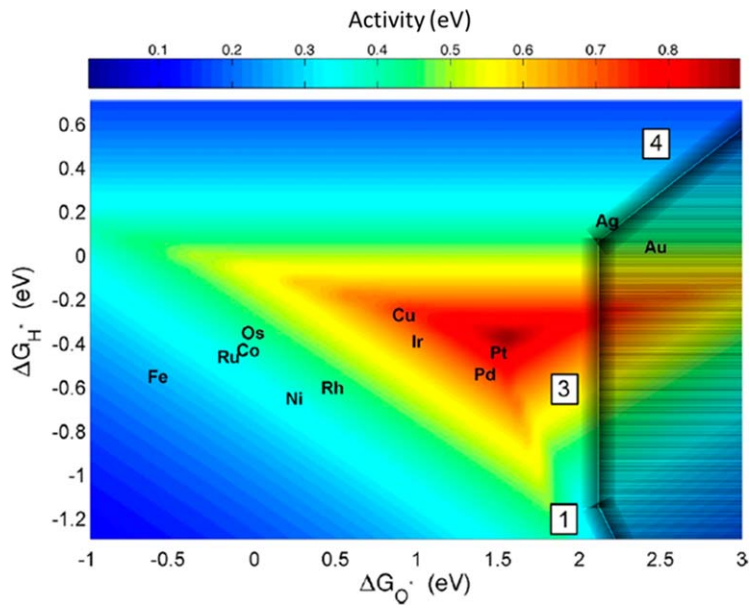

Fig. 10 Sabatier volcano depicting the binding energies of H* and O* on different metals. The shaded black region represents an area of high selectivity represented by inequalities 1, 3, and 4 in the original published work (not reproduced here). Reproduced with permissions from R. B. Rankin and J. Greeley, Trends in Selective Hydrogen Peroxide Production on Transition Metal Surfaces from First Principles, *ACS Catal.*, 2012, **2**, 2664. Copyright 2012 American Society of Chemistry.

(*i.e.*, O–O bond dissociation). These metals are predicted to give greater selectivities to H_2O_2, which is consistent with Au falling into this category.[151] A simple interpolation between the points representing Pd and Au suggests that alloys of the two metals could fall within both the red and shaded black portions of the volcano and thus be both active and selective, although such interpolations are a grossly simplified representation of the reactivity of bimetallics (but may provide guidance for new search directions). This interpolation approach implies also that the ratio of Au to Pd surface atoms would have a significant effect on H_2O_2 selectivity, which is consistent with other studies.[32,213,216] Importantly, similar interpolations suggest that other alloys containing both an active (red region) and selective (shaded black region) metal could be effective for direct synthesis, such as CuAg, CuAu, or PdAg.

Mavrikakis *et al.* studied H_2O_2 formation on the PdAg(110) surface and determined that PdAg alloys would most likely not be selective for H_2O_2 formation.[190] Specifically, alloying Pd with Ag shifts the d-band center of both Pd and Ag terrace atoms to values that are 0.14 eV and 0.49 eV, respectively, closer to the Fermi level than those of Pd(111) and Ag(111). Such changes are expected to increase the reactivity of the catalyst and its propensity to cleave O–O bonds and form H_2O in comparison to Pd(111). The authors state that Pd_1Ag_1 alloys would likely be ineffective for direct synthesis.[190] Greater Ag to Pd ratios, however, might be more effective, especially considering that AuPd catalysts with high Au to Pd ratios appear to be among the most productive and selective catalysts for direct synthesis.[32,213,216] Grabow and coworkers examined the (211) surface of other Au alloys (*e.g.*, AuPt, AuAg, AuCu, AuCd) using DFT in order to find alternative catalysts with potential to be highly selective towards H_2O_2.[212] This study demonstrated that the selectivity towards H_2O_2 depends strongly on the position of the atoms within the clusters. All surfaces with step-sites fully occupied with Au atoms were predicted to give H_2O_2 selectivities greater than 98%. Similarly high selectivities are given when Pd or Ag are present at step-sites, however, H_2O_2 selectivities are expected to drop to 6% or less in the presence of Cu, Cd, or Pt at those edges. These results also show that the interactions between Au and Pd are somewhat unique and different from other transition metals.

The studies described above assume a Langmuirian mechanism for H_2O_2 formation, which is not consistent with experimental findings suggesting proton–electron transfer pathways.[148,154,161] However, it seems likely that the predicted differences between barriers for O–O bond rupture and the hydrogenation of the resulting surface intermediates will be accurate, and consequently, these investigations can help to identify bimetallics that may be useful as next generation direct synthesis catalysts.

3.4.4 Effects of the catalyst support. H_2O_2 selectivities and formation rates can differ significantly among metal (*e.g.*, Pd) clusters, which are nominally identical but contact different carbon or metal oxide supports. For example, Hutchings *et al.* showed that the identity of the support can dramatically affect rates of H_2O_2 formation, hydrogenation, and decomposition on Pd, Au, and AuPd clusters supported on Al_2O_3,

TiO_2, MgO, or C.[183] AuPd and Pd on C gave the highest H_2O_2 formation rates and selectivities, while AuPd and Pd on MgO provided the highest rates of H_2O_2 hydrogenation and decomposition. Reaction rates of metal clusters on TiO_2 and Al_2O_3 had values between those on MgO and C. Figure 11 shows that the H_2O_2 formation rates on AuPd clusters supported on these materials correlate roughly to the isoelectric points of the supports; specifically, supports with isoelectric points at lower pH values gave the highest rates of H_2O_2 formation and the lowest rates of H_2O_2 decomposition and hydrogenation. These reactions were conducted presumably at moderate pH (aqueous methanol with 33 MPa CO_2), which suggests that more negatively charged surfaces of supports favor H_2O_2 formation. These findings differ from trends observed in systems containing catalytically consequential anions originating from acid or halides added to the solvent,[232] where it was suggested that positively charged surfaces were important to bind these negatively charged surface modifiers. However, the data for Fig. 11 was acquired in the absence of strongly binding anions (only H_2CO_3 in solution), and so some other phenomena provides the relationship between H_2O_2 selectivity and the isoelectric point of the support. Ouyang and coworkers studied direct synthesis on AuPd clusters supported on TiO_2 and claimed that the interface between the Au and the TiO_2 support provided unique sites favorable for H_2O_2 formation.[199]

Supports may also influence H_2O_2 *via* strong metal-support interactions (SMSI), especially in cases where metal clusters are supported on reducible metal oxides such as SnO_2 or TiO_2, where the metal atoms from the support can migrate onto the metal clusters, subsequently re-oxidize, and block sites.[245] The SMSI phenomenon appears prominently in the investigation of PdSn catalysts for H_2O_2 formation, in which selectivities

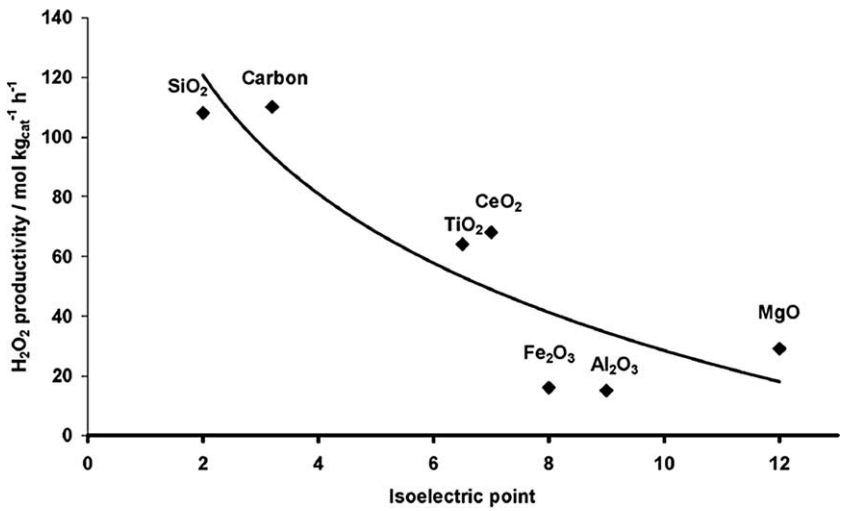

Fig. 11 H_2O_2 productivity as a function of the support isoelectric point over AuPd catalysts. Adapted from E. Ntainjua, J. K. Edwards, A. F. Carley, J. A. Lopez-Sanchez, J. A. Moulijn, A. A. Herzing, C. J. Kiely and G. J. Hutchings, *Green Chem.*, 2008, **10**, 1162 with permission from the Royal Society of Chemistry.

increase after a SnO_x layer forms on PdSn alloys and completely encapsulates small Pd clusters following sequential oxidative and reductive treatments.[169] Moreover, differences between the strength of the interactions between the support and each of the two metals in a bimetallic cluster can affect the distribution of each element within the cluster. For example, the surfaces of RuAu clusters are enriched with Ru when supported on MgO in comparison to those same clusters supported on SiO_2.[246] This same phenomenon likely affects the distribution of metal atoms with AuPd catalysts for direct synthesis, which are frequently supported on materials expected to interact strongly with metal atoms (*e.g.*, MgO,[183] TiO_2[155,167]).

Acids are not just beneficial as an additive to the reaction solution, treatment of the catalyst support with the acid prior to the addition of the catalyst can also yield high selectivities towards H_2O_2. Hutchings *et al.* found that treating a carbon support with a non-halide containing acid (*e.g.*, HNO_3 or CH_3COOH) prior to the deposition of AuPd clusters increased H_2O_2 selectivities from 80 to >98%.[168] The increase in selectivity was attributed to an increase in the ratio of Au to Pd surface atoms, however, it is possible that the acid treatment also removed small metal impurities (capable of H_2O_2 hydrogenation) from the carbon support. In summary, there are a number of mechanisms by which the metal oxide and carbon supports used in these studies can affect the formation of H_2O_2 significantly. Therefore, these topics certainly deserve further study.

3.4.5 Effects of the solvent. The solvent itself may assist in the formation of H_2O_2 directly (*e.g.*, by acting as a co-reactant or catalyst) or indirectly (*e.g.*, by influencing H_2 transport or solvating intermediates). Rates of H_2O_2 formation are more than three orders of magnitude lower in aprotic solutions (*e.g.*, acetonitrile, propylene carbonate, dimethyl sulfoxide) than in protic solutions (*e.g.*, H_2O, CH_3OH).[148] This indicates that H^+ in solution are directly involved in direct synthesis of H_2O_2, likely by a proton–electron transfer mechanism[148,154,161] as described in Section 3.3. Burch and Ellis examined the effects of individually combining 16 different organic co-solvents to a standard mixture of 1.6 M H_3PO_4 and 6×10^{-4} M NaBr over Pd catalysts in water.[247] The greatest H_2O_2 selectivity (64%) was achieved when acetonitrile was combined with the aqueous solvent (33 vol.% acetonitrile in water). In comparison, 2-propanol and toluene gave H_2O_2 selectivities of 31 and 3%, respectively. The authors attributed the greater H_2O_2 selectivities achieved with acetonitrile to more effective H_2 transport to the Pd surface, as a result of an increase in solubility of H_2 in the solution as well as the complete miscibility of acetonitrile with the aqueous mixture. Notably, H_2O_2 was formed in this acetonitrile mixture likely because the water present in the system provided a catalytic amount of H^+. Paunovic *et al.* performed a similar study of the effects of co-solvents using AuPd catalysts that showed also that aqueous acetonitrile solutions gave greater H_2O_2 selectivities than just water (95 and 50% respectively) and confirmed the finding by Burch and Ellis on pure Pd.[248] Therefore, organic co-solvents such as aqueous acetonitrile or methanol (more

commonly used) are frequently used in studies of direct synthesis to overcome the limited solubility of H_2 into H_2O while also providing a source of H^+.[155,195,221,247]

It would be desirable to use solvents that are both non-toxic and more easily separated from the product H_2O_2/H_2O solution than methanol. One seemingly elegant solution to this problem is the use of supercritical CO_2 as a solvent as first reported by Hutchings *et al.*[151,182] The CO_2/H_2O solution is slightly acidic, non-toxic, and readily separated by lowering the pressure, however, the use of supercritical CO_2 requires significant energy for compression and suppresses catalytic activity towards direct synthesis.[249] Finally, solvents may influence the formation rates of H_2O_2 (and H_2O) by preferentially stabilizing certain reaction intermediates present on the catalyst surface. As one example, hydrogen-bonding interactions are likely to be important, although this idea is not discussed much in the literature on direct synthesis. Computational work on electrochemical ORR by Janik *et al.* shows that hydrogen bonding in liquid water stabilizes charge transfer from the Pt(111) into the π^* orbitals of O–O bonds, which facilitates O–O bond cleavage.[250] Based off of this interaction and other DFT calculations, which demonstrate that H_2O stabilizes charge separation of the polar hydroxyl species within the transition state for CO oxidation on Pt(111),[251] it is safe to assume that hydrogen bonding similarly stabilizes specific transition states within the network of reactions that form H_2O_2 by direct synthesis.

3.5 Outlook of direct synthesis

There have been many published methods for improving H_2O_2 selectivities for direct synthesis such as using additives,[153,222] alloying metals,[151,169] or implementing specific solvents[148] or supports.[183] However, many of these methods are impractical for the industrial scale due to environmental or economic constraints. In general, it is beneficial to reduce the number of contiguous sites on the catalyst surface by using strongly binding anions or by alloying with a less reactive metal. It is essential to use protonated solvents, otherwise the reaction cannot occur.[148] In order to avoid secondary reactions that form H_2O from H_2O_2, the reaction should be carried out near or below room temperature and in flow reactors with low residence times (*e.g.*, trickle bed reactors).[37] If the residence time is low, then high H_2 to O_2 ratios increase selectivity towards H_2O_2 formation rather than hydrogenation.[148] Acidic solutions and halide additives can dramatically increase selectivity, however, their role is not entirely clear. Future work investigating the mechanism by which these species increase the selectivity of direct synthesis would be valuable. CO_2 can seemingly perform the same function (in the form of H_2CO_3) as other acids and still achieve high selectivities,[148,168,223] therefore, CO_2 is an excellent non-corrosive alternative to strong mineral acids. Bimetallic clusters have been shown to give the highest reported H_2O_2 selectivities (*e.g.*, AuPd[151] and PdSn[169]), likely because these catalysts expose well dispersed monomers and small ensembles of the active metal (*e.g.*, Pd).[213] These catalysts still rely on precious metals (*e.g.*, Pd, Au), therefore, directed searches for catalysts comprised of more abundant metals

could reduce the costs of the industrial scale direct synthesis of H_2O_2. In addition, direct synthesis will be more economically viable if it can be conducted at higher temperatures (*e.g.*, >300 K) and at lower pressures (*e.g.*, <200 kPa), therefore, future work should focus on achieving high H_2O_2 selectivities at these conditions since many studies are conducted at conditions inherent to high selectivity (low temperature and high pressure).[37] The implication of proton–electron transfer during direct synthesis (Scheme 7) suggests that future work could combine the chemical driving force of the H_2 with an applied electrical field during the reaction in order to stabilize critical reaction intermediates and increase selectivity towards H_2O_2. Continued research will likely lead to a more complete understanding of direct synthesis chemistry and, potentially, to the replacement of the anthraquinone auto-oxidation process by on-site direct synthesis production plants.

4 General oxidation reactions for commodity chemicals

H_2O_2 is an environmentally benign oxidant with the potential to replace halogenated and noxious oxidants currently used in industry such as halogenated organics,[48,80,252,253] nitric acid,[91] nitrous oxide,[91,254] and permanganates,[47] which generally require organic solvents (discussed in Section 1).[77,255] Epoxidations are a closely related class of reactions, which have received a great deal of attention and are discussed in Section 5. Here we provide a brief overview of a few classes of oxidation reactions in which H_2O_2 has been demonstrated to be an effective replacement for the harmful oxidants currently used.

4.1 Alkane and alkene oxidation

The oxidation of lower alkanes (*e.g.*, methane and ethane) to produce oxygenates is an important industrial reaction,[58,71,76] because the products formed (*i.e.*, methanol and ethanol) can be further utilized and upgraded to produce fuels and commodity chemicals.[256,257] Currently, these small-molecule oxygenates are synthesized from alkanes *via* indirect reaction pathways, such as the steam reformation of natural gas to syngas and subsequent conversion to methanol at high temperature[258] or the dehydrogenation of ethane followed by hydroxylation.[256] These processes require high energy input, which has motivated the study of direct oxidation pathways of small alkanes to more synthetically and commercially useful oxygenates. Several strategies are being investigated to directly oxidize the alkanes to oxygenates, such as high temperature and pressure O_2 activation with supported Cu,[71,259–261] C–H activation by cationic Au in strongly acidic media,[262] and activation of N_2O/O_2 using transition metal catalysts (*e.g.*, Fe,[263] Co,[60] Mo[264]). Unfortunately, many of these strategies to directly oxidize lower alkanes suffer from low rates or selectivities,[263,265,266] pose safety and environmental risks,[267] or use greenhouse gases (*e.g.*, NO_x) for oxidation.[268]

Hutchings and coworkers studied the oxidation of methane and ethane with H_2O_2 over Cu and Fe oligomers supported within an MFI-type zeolite, ZSM-5 ($SiO_2/Al_2O_3 = 30$).[51,52,59,73,269] Fe-containing ZSM-5 (Fe/ZSM-5)

catalysts, prepared by hydrothermal synthesis, activate H_2O_2 and oxidize methane at mild temperatures (*i.e.*, <373 K).[269] The reaction of methane with H_2O_2 over Fe/ZSM-5 gives high selectivity (71%) towards formic acid production. X-ray diffraction (XRD), X-ray absorption near edge spectra (XANES), Fourier transform infrared spectroscopy (FTIR), and UV-vis spectroscopy suggest that the Fe centers exist in ZSM-5 as extra-framework FeO_x clusters in both isolated and oligomeric forms, the latter of which is thought to be an active site for alkane oxidation.[53,73] Increasing the Fe content from 0.5% to 2.5% resulted in increased methane conversion (0.3 to 0.8%) at constant residence time and increased selectivity towards CO_2 (4 to 12%) using 0.5 M H_2O_2 at 323 K.[73] Diffuse reflectance UV-vis (DRUV) spectroscopy and high angle annular dark field (HAADF)-scanning tunneling electron microscopy (STEM) imaging show that high Fe loadings formed bulk (mean diameters 20–50 nm)[270] Fe_2O_3 clusters located on the external surface of the zeolite crystals, which non-selectively oxidize methane.[53] Consequently, a small amount of the Fe forms the oligomeric FeO_x clusters responsible for the formation of methanol. Interestingly, addition of Cu to Fe/ZSM-5 (Fe-Cu/ZSM-5) increased the selectivity for methanol from 15 to 92% at 0.5% conversion (323 K, 0.123 M H_2O_2).[269] The addition of Cu to Fe/ZSM-5 has little effect on the conversion of methane. High resolution transmission electron microscopy (HR-TEM) shows the presence of copper oxide species on the external zeolite surface. These CuO_x species may limit the formation of hydroxyl radicals, which are generated by Fenton chemistry and can drive the non-selective oxidation of methane.[53]

Hutchings *et al.* have also investigated the oxidation of ethane with H_2O_2 over Fe/ZSM-5 catalysts prepared by chemical vapor impregnation.[52] Reaction of ethane with H_2O_2 over Fe/ZSM-5 catalysts gave high selectivity towards acetic acid (73%), whereas Fe-Cu/ZSM-5 primarily produces ethylene (38%) by oxidative dehydrogenation.[51,59] Similar to their previous findings, both catalysts consume methane at similar rates when normalized on a per-kg catalyst basis. Increasing the Cu weight loading from 0 to 2.5 wt% on 1.25% Fe/ZSM-5 decreased the selectivity towards acetic acid from 65 to 43% and increased the ethylene selectivity sharply from ~0 to 38%, while all other oxygenates (*i.e.*, methanol, ethanol, carbon dioxide) accounted for the remaining 19%. From 1 : 1 to 1 : 6 ratio of Fe : Cu (at 0.4 wt% Fe), the selectivities to acetic acid and ethylene remained fairly constant at 43% and 38% respectively.[59] Increasing Fe content (0.4 to 2.5 wt%) decreases the ethane conversion from 8% to 4%, which is attributed to the decomposition of H_2O_2 on bulk Fe_2O_3 clusters (mean diameter 20–50 nm)[270] on the external surface.[51,59] As the reactor pressure was increased from 1 bar to 30 bar (10% C_2H_6/Ar) at 0.123 M H_2O_2, the selectivity to liquid products including acetic acid (40 to 75%), ethanol (0 to 5%), and formic acid (5 to 15%) increased,[59] which the authors attributed to greater interaction between the substrate, oxidant and catalyst at higher ethane concentrations (*i.e.*, at high pressures).[51,59] The authors noted that Fe/ZSM-5 gave different product distributions when subjected to different high-temperature oxidative or reductive treatments. For example, oxidative treatments (823 K, 3 h, air)

result in higher selectivities to formic and acetic acid from methane and ethane, respectively,[52] whereas reductive treatments (823 K, 3 h, 5 kPa H_2) give high selectivity towards methanol and ethanol. For instance, a 1.1 wt% Fe/ZSM-5 subjected to oxidative treatments exhibited a methanol selectivity of 12% whereas the same catalyst, when subjected to a reductive treatment, gave relatively high selectivity (36%) in methanol. These differences may arise from an increase in the fraction of isolated and oligomeric Fe species,[52] which, most likely, prevents the decomposition of H_2O_2 and activates the methane. Román-Leshkov and coworkers have investigated the catalytic oxidation of methane to methanol using zeolite-based Cu catalysts with oxygen at low reaction temperatures (483–498 K) to determine the structure of the Cu species which lead to the direct formation of methanol from methane.[260] Cu-Na-ZSM-5 (Cu/Al = 0.37, Na/Al = 0.26) gave a methanol selectivity of ~71% (483 K, 2.5 Pa O_2) with CO_2 as the only other product. Using UV-vis spectroscopy and GC measurements over Cu-Na-ZSM-5, the authors have implicated mono-(μ-oxo) dicupric cores[271,272] for methane oxidation. These electrophilic metal-oxygen species are highly reactive and readily cleave the C–H bond of methane to generate surface-bound methoxy groups. Similar structures may form upon exposing Cu-oligomers to H_2O_2 at lower temperatures. Other studies have also implicated $[Cu_3O_3]^{2+}$ trimeric sites as being responsible for the C–H activation of methane and subsequent oxidation.[273,274] Despite the widespread interest in small alkane upgrading, the mechanism behind direct oxidation of ethane[51,59] and methane[53,73] to alcohols and acids by H_2O_2 is not well understood on these materials. Fundamental insight into the roles that the catalyst and reaction conditions play in preventing H_2O_2 decomposition and secondary oxidation reactions will allow for the design of increasingly selective catalysts for alkane oxidation with H_2O_2.

The oxidation of cyclohexene can form adipic acid, which is an important monomer used in nylon.[54,275] Currently, adipic acid is produced on industrial scales by the oxidation of cyclohexanol or cyclohexanol/cyclohexanone mixtures with HNO_3.[91] This reaction produces NO_x gases as a byproduct, which are harmful to human and environmental health,[45] and results in a highly corrosive reaction mixture with subsequent quenching and purification steps.[42] To produce adipic acid with a greener oxidant, Sato *et al.* have used aqueous 30% H_2O_2 to oxidize cyclohexene to adipic acid using Na_2WO_4–$2H_2O$ catalyst with $[CH_3(n\text{-}C_8H_{17})_3N]HSO_4$ as a phase-transfer catalyst (PTC) between the organic-aqueous phase to obtain a 93% yield of adipic acid at 348–363 K.[42,54] Scheme 9 depicts the proposed mechanism for adipic acid formation from cyclohexene, which was supported by direct detection of the intermediates, cyclohexene oxide and 2-hydroxycyclohexanone by GC analysis of the reaction mixture. The mechanism involves three types of oxidation reactions: olefin epoxidation, secondary-alcohol oxidation, and the Baeyer Villager oxidation, followed by hydrolysis. The reaction requires 4.4 M H_2O_2 and the aqueous solvent containing the PTC and unreacted H_2O_2 can be reused. This process is also applicable to the oxidation of substituted cyclohexenes, and notably, the reaction uses

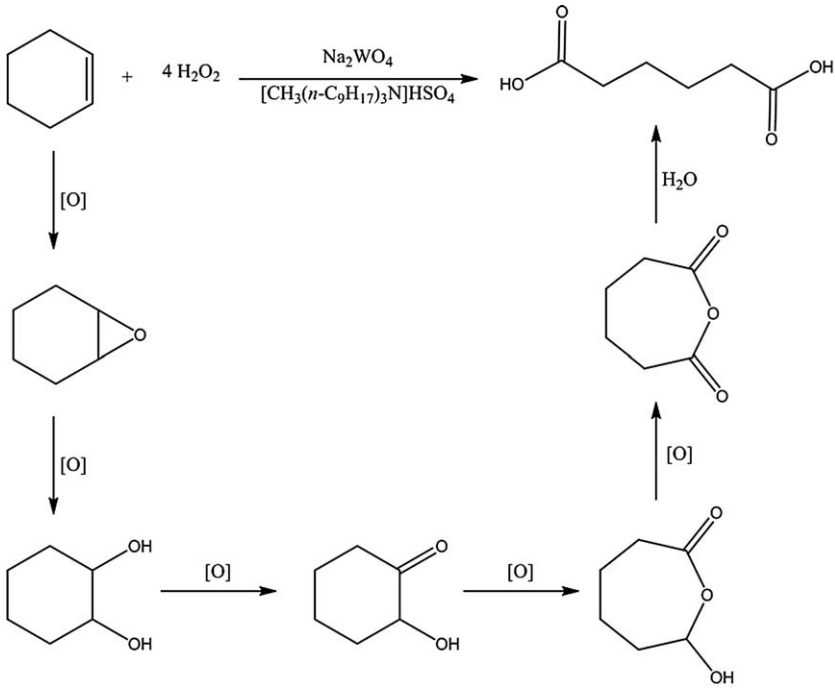

Scheme 9 Reaction pathway for oxidation of cyclohexene to adipic acid by H_2O_2. Reprinted from R. Noyori, M. Aoki and K. Sato, *Chem. Commun.* 2003, 1977 with permission from the Royal Society of Chemistry.

much milder conditions than cyclohexene oxidation by HNO_3.[42] Apart from Na_2WO_4, many tungsten based catalysts have been studied for cyclohexene oxidation using H_2O_2 (*e.g.*, tungsten-containing SBA-15,[276] peroxo tungstanates,[277] H_2WO_4 on acidic resins,[278] and $[BMIm]_2WO_4$ supported on silica sulphamic acid[279]) because tungsten is able to efficiently activate H_2O_2 to form a bisperoxytungstanate intermediate which is the believed to be the active intermediate of this reaction (see Section 5.2). Additionally, activated W-peroxy intermediates exhibit high stability and reactivity under acidic conditions, which is necessary for the hydrolysis of the intermittent anhydride to form adipic acid.[43,278–280]

4.2 Oxidation of alcohols

The oxidation of alcohols is an industrially important type of reaction that is used in the production of pharmaceuticals, polymer precursors, fertilizers, and various other commodity chemicals.[57,68,75,78,280] Alcohol oxidations are one of the most studied reactions in organic chemistry and, as such, numerous methods have been developed for the selective oxidation of alcohols to aldehydes, ketones, and carboxylic acids.[42,75,255,281] However, many homogeneous and heterogeneous oxidation reactions that utilize organic and corrosive oxidants with harsh reaction conditions produce organic and corrosive waste, which requires subsequent separation and waste-treatment units, preventing many of these methods from becoming easily adopted by industry.[42,47,74,75,255,282] Researchers

have made extensive efforts to activate O_2 or H_2O_2 to replace various reaction systems containing organic solvents (*e.g.* DMSO with *N,N′*-dicyclohexylcarbodiimide (DCC))[255] and corrosive oxidants (*e.g.*, TEMPO, pyridinium chlorochromate (PCC)).[77] Unfortunately, many oxidations with activated O_2 tend to have low rates of reaction (*e.g.*, oxidation dehydrogenation of alcohols to aldehydes) and are certainly not viable for the selective oxidations of air-sensitive pharmaceutical precursors.[281]

Jacobson and co-workers in 1979, were among the first to demonstrate the oxidation of secondary alcohols (*e.g.*, 2-octanol and cyclohexanol) to the corresponding ketones over W- or Mo-based catalysts using 90 wt% H_2O_2 in methanol.[283] Oxidation rates of secondary alcohols show a first-order dependence on catalyst concentration and a first-order dependence on the concentration of the alcohol implying that the rate determining step involved the interaction of the catalyst-peroxo complex with the alcohol.[283] Since then, significant effort has been made to increase the safety and economic viability of such processes. In the late 1990s, Noyori and co-workers demonstrated the oxidation of several long-chain primary (*e.g.*, 1-octanol) and secondary (*e.g.*, 2-octanol) alcohols by 3–30% wt H_2O_2 using an inexpensive sodium tungstanate (Na_2WO_4) catalyst.[68,280] This reaction proceeds in a biphasic system consisting of an organic phase consisting of the hydrophobic alcohol and an aqueous phase containing Na_2WO_4 and H_2O_2. To prevent the use of any additional organic solvents, a phase-transfer catalyst (PTC) was used to facilitate the migration of the H_2O_2 and activated Na_2WO_4 from the aqueous to the organic phase. The acidity of the PTC was found to drastically affect the yield of the reaction. For example, $[CH_3(n\text{-}C_8H_{17})_3N]HSO_4$ gave 97% yield of ketones whereas $[CH_3(n\text{-}C_8H_{17})_3N]Cl$ gave much lower ketone yields (*i.e.*, 11%),[68,280] because of the higher pH value in the aqueous phase when $[CH_3(n\text{-}C_8H_{17})_3N]Cl$ was used.[56,68] Scheme 10 shows the bisperoxotungstanate ions formed by activation of H_2O_2 with Na_2WO_4, which has been proposed to be the active intermediate(s) in these oxidations.[284–286] However, these intermediates have yet to be shown to be directly involved in the oxidation of alcohols (*i.e.*, they are proposed intermediates). Additionally, the three structures in Scheme 10, are believed to be

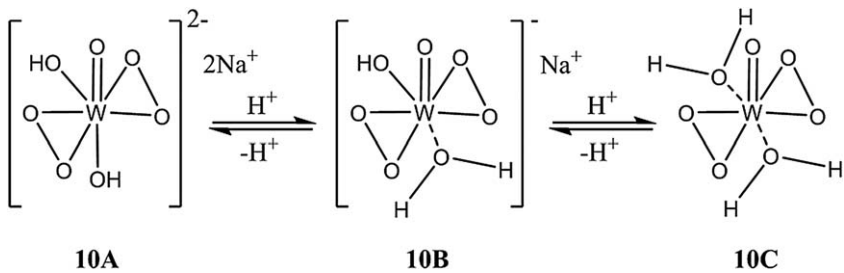

Scheme 10 Structures of biperoxotungstanate ions which are believed to be the active species for alcohol oxidation upon activation of H_2O_2. Additionally, the three structures are believed to be in rapid equilibrium with each other. Recreated from K. Sato, M. Aoki, J. Takagi, K. Zimmermann and R. Noyori, *Bull. Chem. Soc. Jpn.*, 1999, **72**, 2287. Copyright The Chemical Society of Japan.

in rapid equilibrium with one another. The academic consensus is that compound 10a is not very active for alcohol oxidation, and that compound 10c is unable to shuttle to the organic phase of the reaction (*i.e.*, does not move with the PTC to react).[280] This is because compound 10b can undergo ion exchange between Na^+/PTC to shuttle to the organic phase and react. As such, Scheme 10b is believed to be the active intermediate for oxidation reactions, and exhibits high stability in acidic media (*i.e.*, pH between 0.3–4), which supports the use of PTCs with a hydrogen sulfate counterion.[68] Biphasic oxidations such as this one have been extensively used for olefin oxidation and with intermediates similar to the center intermediate observed.[86,87] Noyori and co-workers found that the rate for oxidizing secondary alcohols to ketones was greater than that for oxidizing primary alcohols to aldehydes.[280] Secondary alcohols that possess a C=C bond provide an opportunity to study the chemoselective preference to form a ketone in comparison to an epoxide. The biphasic system promotes olefin epoxidation in the presence of a promoter (*e.g.*, (aminomethyl)phosphoric acid),[55] which may either act as a protecting group for the alcohol or occupy W centers on the catalyst and activate the olefin epoxidation pathway. Without the promoter, the selectivity towards alcohol oxidation to form the unsaturated aldehyde increases primarily due to the decrease in the rate of olefin epoxidation.[55,68,280]

Scheme 11 shows the oxidation pathways of primary alcohols to aldehydes, esters, and carboxylic acids, which is more complex than the oxidation of secondary alcohols.[77,255] The over oxidation of aldehydes to

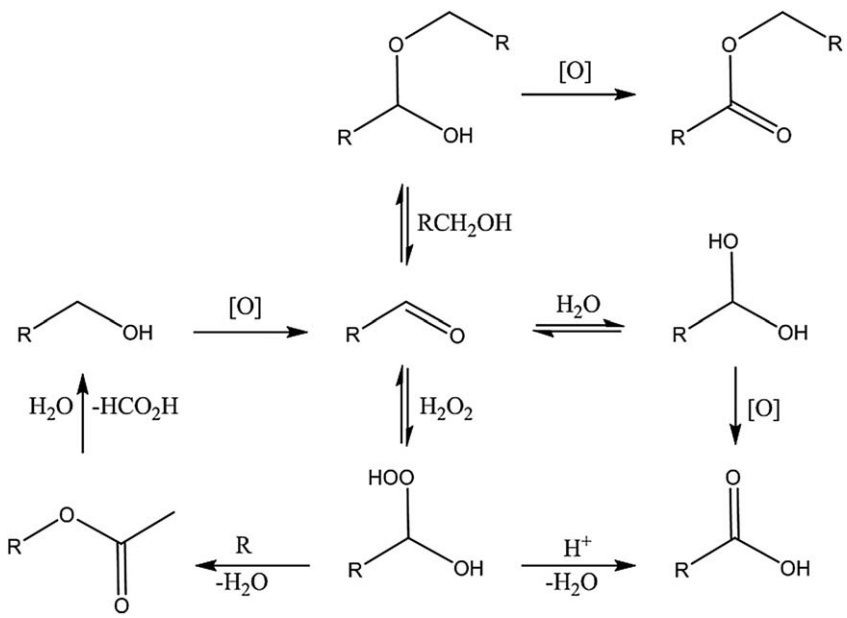

Scheme 11 Possible reaction pathways for the oxidation of primary alcohols by H_2O_2. Recreated from K. E. Pfitzner and J. G. Moffatt, A New and Selective Oxidation of Alcohols, *J. Am. Chem. Soc.*, 1963, **85**, 3028. Copyright 1963 American Chemical Society.

form esters or carboxylic acids makes selective formation of specific functional groups challenging, as water, alcohols, and other nucleophiles present in the system may react with aldehydes to give a number of secondary products. For example, upon formation of aldehydes, further oxidation produces hemiacetals, geminal alcohols, or 1,1-peroxy alcohols that can further react to produce esters or carboxylic acids.[68] Additionally, oxidation rates of primary alcohols (*e.g.*, 1-octanol) were less (37% lower) than those for the corresponding secondary alcohols (*i.e.*, 2-octanol).[68] Further, primary alcohol oxidation with H_2O_2 tends to form the corresponding carboxylic acid as the primary product (*e.g.*, 87% yield for octanoic acid from 1-octanol oxidation). Noyori and co-workers demonstrated that Na_2WO_4 selectively oxidizes benzyl alcohol to either benzaldehyde or benzoic acid and that the product selectivity depends sensitively on the concentration of H_2O_2.[57,280] For example, at 2.5 equivalents of H_2O_2 (with respect to benzyl alcohol), benzoic acid is the major product (81% yield) because benzaldehyde readily undergoes successive oxidation with the remaining H_2O_2 to form benzoic acid in the presence of a PTC at 363 K (Scheme 11). The electronic properties of the active intermediates in these reactions were probed by developing Hammett relations based on comparisons of the relative rates of reaction (v_x/v_H) of parasubstituted benzyl alcohols (*e.g.*, *p*-methoxybenzyl alcohol, *p*-chlorobenzyl alcohol) over Na_2WO_4 catalysts in 5 wt% H_2O_2 with a PTC (363 K).[280] Figure 12 shows that the Hammett constant (ρ) is −0.31, which suggests that a slight positive charge accumulates in the transition state for benzyl alcohol oxidation and that electron rich alcohols oxidize at higher rates.[280]

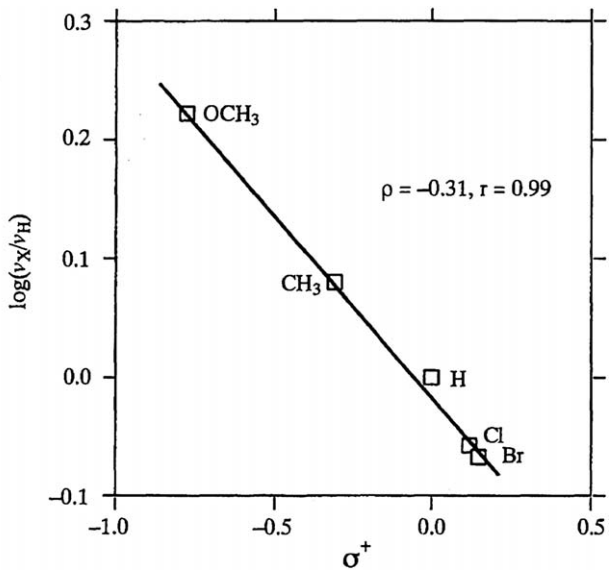

Fig. 12 Hammett plot for the oxidation of *p*-substituted benzyl alcohols. Reproduced from K. Sato, M. Aoki, J. Takagi, K. Zimmermann and R. Noyori, *Bull. Chem. Soc. Jpn.*, 1999, **72**, 2287; with permission from the Chemical Society of Japan.

Despite a significant amount of research on the topic of the oxidation of alcohols with H_2O_2, these reactions have still not been incorporated into medium scale industries, due in part to the high cost of H_2O_2. These oxidations are clean, simple, and as demonstrated in the cases above, can give reasonable product yields.

4.3 Other oxidation reactions with H_2O_2

Sulfides (R_2S) and sulfones (R_2SO_2) are common chemical moieties in various commodity chemicals and pharmaceuticals.[79,81,287] Typically, sulfones are prepared by the stepwise oxidation of sulfides to sulfoxides (R_2SO) then to sulfones.[43] NaClO,[80] $NaBO_3$,[288] RuO_4,[282] HNO_3,[254] and $KMnO_4$[47] are commonly used to produce sulfones, however these species are non-catalytic and are used in stoichiometric amounts.[80,254,282,288] Moreover, these oxidants are generally corrosive and pose an environmental risk.[43,46,288] As such, researchers have attempted to develop processes that use greener oxidants (*e.g.*, H_2O_2 and O_2) as alternatives. Oxidations of organosulfur compounds (*e.g.*, thiophenes, benzothiophenes, bis(2-chloroethyl) sulfide) are relevant for the production of clean burning fuels (by oxidative desulfurization processes) and the destruction of chemical warfare agents (CWA, by hydroperoxidolysis and oxidative hydrolysis)[289,290] by converting sulfides into less harmful and easily extracted sulfoxides and sulfones. Current methods (*e.g.*, hydrodesulfurization (HDS), hydrolysis) for removing sulfur from crude oil and destroying CWAs suffer from low rates and require energy-intensive process conditions (*i.e.*, high temperatures and pressures).[84]

The oxidation of a dialkyl sulfide to the corresponding sulfone proceeds *via* the sulfoxide intermediate. The sulfoxide can be obtained as a product by reacting an equimolar mixture of the sulfide and 30% wt H_2O_2 at 308 K in the absence of a catalyst.[43] The absence of the catalyst slows down the oxidation to sulfone drastically and the sulfoxide can be isolated. Noyori *et al.* used Na_2WO_4 and H_2WO_4 catalysts to oxidize diphenyl sulfide to the corresponding sulfone with 30 wt% H_2O_2 (2.5 equiv.), $[CH_3(n\text{-}C_8H_{17})_3N]HSO_4$ (*i.e.*, a PTC), and $C_6H_5PO_3H_2$ (*i.e.*, a typical additive), as shown in Scheme 12.[43] At 298 K and using Na_2WO_4 catalyst, the reaction yield was 72% after 2 hours. H_2WO_4 gave comparable sulfone yield (~66%) under similar reaction conditions suggesting that the counter ion (*i.e.*, H^+ or Na^+) does not affect the reaction and the tungstanate activates H_2O_2 for sulfide oxidation. The yield decreased when $[CH_3(n\text{-}C_8H_{17})_3N]Cl$ was used as a PTC,[68] likely because of an increase in pH of the aqueous medium akin to alcohol oxidation. The reason for this pH dependence can be that the bis η^2 W-(O_2), which is considered to be the active species of the reaction, is most stable at low pH value (0.3–4). Interestingly, the authors suggest that the HSO_4^- anion of the PTC assists in the formation of the bis η^2 W-(O_2) active intermediate (see Section 5.2), while the ammonium counter-ion shuttles the active oxidant (Scheme 12) to the organic phase for reaction with the sulfide.[280] The phenyl phosphonic acid additive ligates to the W-atom and increases the rate of sulfide oxidation, perhaps by donating electron density and thus increasing the reactivity of the η^2 W-(O_2) (Scheme 12). These catalysts

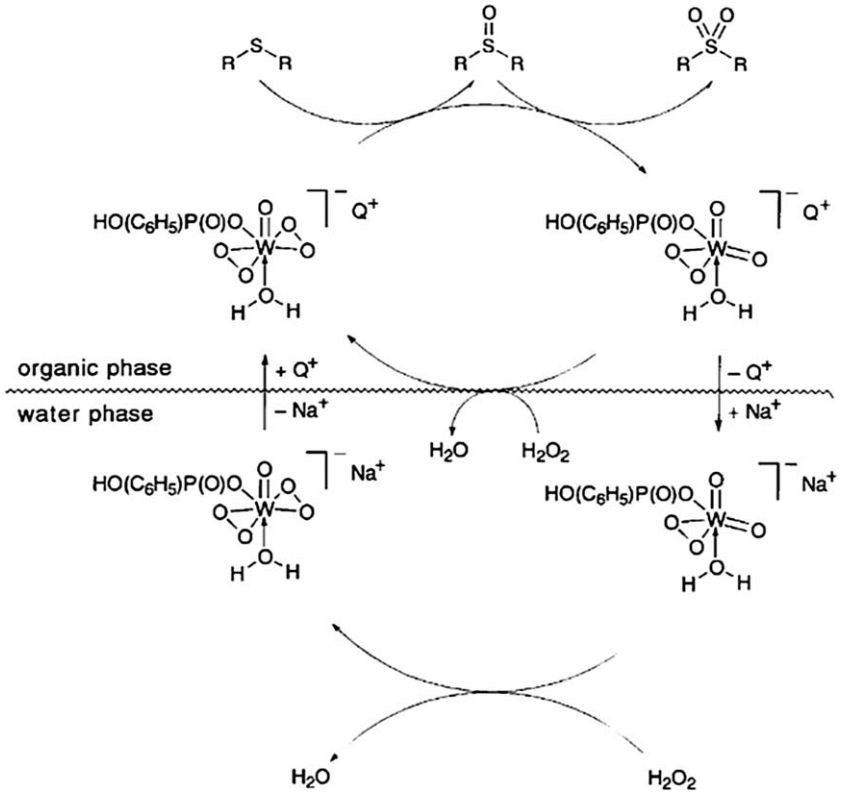

Scheme 12 Catalytic cycle showing the oxidation of sulfides to sulfoxides and sulfones by H_2O_2. Reproduced from K. Sato, M. Hyodo, M. Aoki, X.-Q. Zheng and R. Noyori, Oxidation of sulfides to sulfoxides and sulfones with 30% hydrogen peroxide under organic solvent- and halogen-free conditions, *Tetrahedron*, 2001, **57**, 2469. Copyright 2001 with permission from Elsevier.

effectively oxidizes both aliphatic and aromatic sulfides, although oxidation rates of aromatic sulfides are greater.[43] High yields (>90%) were obtained for all substrates (diphenyl sulfide, di(*p*-nitrophenyl) sulfide, 2-hydroxyethyl phenyl sulfide, *etc.*) with 30 wt% H_2O_2, Na_2WO4, $C_6H_5PO_3H_2$ and $[CH_3(n\text{-}C_8H_{17})_3N]HSO_4$, which suggested that the presence of electron withdrawing groups like $–NO_2$ or even bulky tertiary alkyl groups on the phenyl ring did not affect yields significantly.[43]

Current research is directed toward oxidative desulfurization by H_2O_2 using transition metal based catalysts (*e.g.*, Mo-,[291] Nb-,[291–293] Ti-,[293] and W-[84,294]) that are known to readily oxidize thiophenes and sulfides. Hutchings and co-workers studied the oxidation of sulfides to sulfones using H_2O_2 over Ti-incorporated zeolite catalysts (*e.g.*, TS-1 and Ti-β) in methanol.[70] The authors studied the relationship between substrate oxidation reactivity and shape-selectivity by probing the oxidation of four isomerical butyl-methyl thioethers using 30 wt% H_2O_2. TS-1 catalyzed reaction gave high yields of sulfone (>90%) and almost 100% selectivity for all isomers except the *tert*-butyl methyl isothioether (8% yield after 96 h), because the *tert*-butyl group is sterically too large to fit into the

pores of TS-1 (5 Å diameter).[70] Ti-β possess larger pores (7 Å diameter)[70] and accommodates the *tert*-butyl substituted sulfides. Consequently, Ti-β rapidly oxidized all isomeric sulfides to the corresponding sulfones. Additionally, allyl methyl thioethers were used to study the competitive reactions between sulfide oxidation and olefin epoxidation. The authors found that the sulfide was predominantly oxidized with the allylic double bond intact. This result has been attributed to the greater nucleophilicity of the lone pair of electrons on S as compared to the π electrons of the carbon–carbon double bond which coordinate strongly to the Lewis acidic Ti active sites,[295] leading to preferential sulfur oxidation.[70] Titanate nanotubes (TiNTs) have been shown to catalyze the oxidation of sulfides using H_2O_2[293] and also to be useful supports for tungsten oxide catalysts that can catalytically oxidize sulfides to corresponding sulfones.[294] H-TiNT (synthesized by hydrothermal method) gave complete conversion of dibenzothiophene (DBT) to the sulfone (*e.g.*, 0.1 mol DBT per gram of H-TiNT) using 0.1 M H_2O_2 after 60 min at 298 K.[293] The high surface area of the mesoporous TiNTs leads to the formation of high concentrations of superoxide radicals (O_2•$^-$) on the surface, which was detected by electronic paramagnetic resonance (EPR) spectroscopy.[293] Cortes-Jácome *et al.* also used DBT to test the catalytic properties of WO_x supported on TiNTs with 30 wt% H_2O_2 at 333 K.[294] The authors proposed the formation of Na_2WO_4 nanoparticles (residual atoms from the alkaline precursor) with W atoms coordinated in a tetrahedral geometry, which exposed the sites that gave the greatest rates for DBT oxidation to the corresponding sulfone. Carniato *et al.* synthesized a bifunctional catalyst with strong oxidizing and Brønsted acid properties by incorporating Nb(v) into a saponite clay (SAP) framework using a hydrothermal synthesis process.[292] In the presence of 30 wt% H_2O_2 at 298 K, pure SAP (without Nb) oxidized 20% of the 2-chloroethyl ethyl sulfide (CEES) substrate, which demonstrated that Brønsted acid sites in the support were active for oxidation. However, Nb/SAP gave high conversion of the CEES to the sulfoxide and sulfone at identical conditions (298 K, 14 mM CEES, 20 mg catalyst) showing that the NbO*x* species formed were active. The most desired product of CEES oxidation is the sulfoxide, because it is less hazardous than the corresponding sulfone. The selectivity to the sulfoxide (CEESO) was 73% at a CEES conversion of 98% after 8 h, and the selectivity to the sulfone ($CEESO_2$) increased after the complete consumption of the sulfide as the reaction time was increased beyond 8 h.[292] Another transition metal based material, molybdate catalyst was used with 50 wt% H_2O_2 at 243 K to study the oxidation of bis(2-chloronethyl)sulfide.[291] It was seen that in a microemulsion of water and oil, bis(2-chloronethyl)sulfide oxidizes rapidly to the sulfoxide (half-life less than 30 s). Molybdate is thought to activate peroxide and produce singlet oxygen species, which diffuse through the solvent and homogeneously oxidize the substrate.[296] Despite the recent interest in these new catalytic systems, the literature could benefit from detailed fundamental studies behind sulfide oxidation, which will help guide the rational design of novel catalytic systems.

The oxidation of alkyl and aromatic sulfides with H_2O_2 is a relevant set of chemistry for oxidative desulfurization and organosulfur deactivation,

among other uses. Although the literature contains several examples of successful catalysts for this chemistry, there are relatively few published studies that address fundamental questions regarding the mechanism or structure–function relationships for these reactions. This is a major roadblock in the rational design of catalysts for sulfur oxidation reactions and effort needs to be directed towards understanding the nature of active sites, the role of support morphology, and the cooperative effects of the support and active sites in influencing the efficiency of the oxidation process.

5 Olefin epoxidation catalysts

5.1 Zeolites

Although a number of different transition metal substituted zeolites have been used for epoxidations, titania silicalite (TS-1) has received the most attention since the report by Clerici *et al.* in 1991.[66] This seminal work demonstrated that TS-1 catalyzed the epoxidation of propylene with H_2O_2 in both water or aqueous methanol solutions with the epoxide selectivity exceeding 90%.[66] Clerici *et al.* showed later that epoxidation rates of α-olefins decrease with increasing chain length (*e.g.*, 1-pentene > 1-hexene > 1-octene; Table 5)[102] and that epoxidation rates of cyclic alkenes (*e.g.*, cyclohexene) are an order of magnitude less than those for 1-pentene.[297] These lower epoxidation rates for cyclohexene result from the difficulty of larger molecules to diffuse through the relatively small pores (~5 Å diameter)[298,299] such that epoxidation occurs primarily on the external surface of TS-1 crystals. Comparisons in Table 5 show that epoxidation rates of allylic alcohols, allylic chloride, and α-olefins increase with the electron-richness of the C=C bond of the olefins, which suggests that H_2O_2 activates on TS-1 to form an electrophilic intermediate. Scheme 13 shows the penta-coordinated metallacycle, proposed by Clerici, gains its electrophilic character from the polarization of the –OOH appendage by interaction with a neighboring silanol defect or solvent molecule.[300]

Table 5 H_2O_2 conversion and selectivities for linear, cyclic, and electron-rich olefin epoxidation over TS-1 (recreated from Clerici *et al.*).[a,b]

Olefin	$t_{1/2}$[c] (min)	t[d] (min)	H_2O_2 (conv. %)	Selectivity (% on H_2O_2)
1-Pentene	5	60	94	91
1-Hexene	8	70	88	90
1-Octene	5	45	81	91
Cyclohexene	—[e]	90	9	—[e]
Allyl chloride	7	30	98	92
Allyl alcohol	16	35	81	72

[a] Recreated from M. Clerici and P. Ingallina, Expoxidation of Lower Olefins with Hydrogen Peroxide and Titanium Silicalite, *J. Catal.*, 1993, **140**, 71–83, Copyright 1993, with permission from Elsevier.
[b] 0.90 M Olefin, 0.18 M H_2O_2, 6.2 g L^{-1} TS-1, Methanol solvent.
[c] $t_{1/2}$ is the time required for 50% H_2O_2 conversion, monitored by iodometric titration.
[d] t is the reaction time.
[e] Not determined.

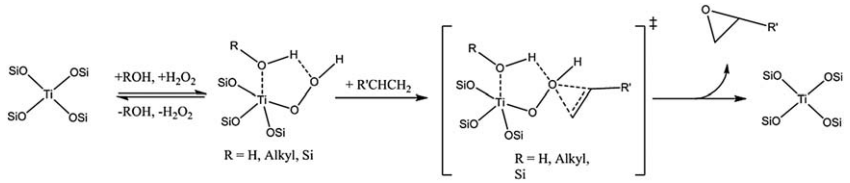

Scheme 13 Proposed mechanism for olefin epoxidation with H_2O_2 utilizing a hypothesized penta-coordinate metallocycle. Adapted from B. Notari, Titanium Silicalites, *Catal. Today*, 1993, **18**, 163. Copyright 1993 Published by Elsevier, with permission from Elsevier.

The initial success of TS-1 as an epoxidation catalyst sparked interest in developing new schemes to maximize selectivity to epoxide products, especially by minimizing the secondary reaction of epoxides with solvent molecules. During the epoxidation of propylene over TS-1 in a batch reactor, investigators noted that the pH of the solution decreased after 90 minutes at 333 K, which was attributed to leaching of trace amounts of aluminum atoms from the MFI framework resulting in acidic silanol defects within the zeolite.[301] Epoxides are known to ring open in acidic media, which results in lower yield by the conversion of epoxides *via* solvolysis.[302] These reactions can be suppressed by washing TS-1 with a dilute sodium acetate (NaOAc) solution, which is thought to neutralize the silanol defects by ion exchange. This treatment increases propylene oxide (PO) selectivities from 70% to upwards of 90% PO by decreasing the degree of PO solvolysis to form propane-diol and propylene glycol methyl ether.[66] Subsequently, Wang *et al.* showed that the addition of Na_2CO_3 to a pure methanol solution increased the PO selectivity of TS-1 from 5.1% to 94%.[301] Both NaOAc and Na_2CO_3 are believed to act as basic pH buffers, which neutralize acid sites and consequently increase PO selectivities. These observations,[301,302] together with those of Clerici *et al.*,[66] suggest that epoxide yields are sensitive to the presence of even small numbers of acid sites in TS-1 (or related catalysts) and that pH buffers (or basic-site titrants) are needed to avoid the activation and ring opening of epoxides.

Several groups have used a range of spectroscopic methods to probe the structure of the active intermediate(s) that forms by the reaction between H_2O_2 and Ti-atoms within TS-1. In the early 2000s, Frei *et al.* exposed TS-1 to H_2O_2/H_2O mixtures and acquired infrared (IR) spectra of the resulting intermediates *in vacuo*.[303] Reaction between TS-1 and $H_2{}^{16}O_2$ generated an absorbance peak at 837 cm^{-1}; however, the same experiment performed with $H_2{}^{18}O_2$ gave a peak at 793 cm^{-1}, which suggests that the feature corresponds to a O–O stretching mode within a η^1 titanium–hydroperoxy (Ti–OOH) or a η^2 peroxide ($Ti–O_2^-$) intermediate.[303] Consequently, the authors assigned these peaks to the ν_s(O–O) mode of the η^1 Ti–OOH moiety (Fig. 13), as this was the most stable intermediate proposed from *ab initio* and DFT calculations.[303] Alternatively, Zecchina *et al.* proposed that a ''side on'' η^2 Ti–OOH complex forms by activation with H_2O_2 on TS-1 based on a combination of UV-vis and resonant Raman spectra.[304,306] In these studies, Raman spectra show a strong peak that emerges at 618 cm^{-1}, which was attributed to the

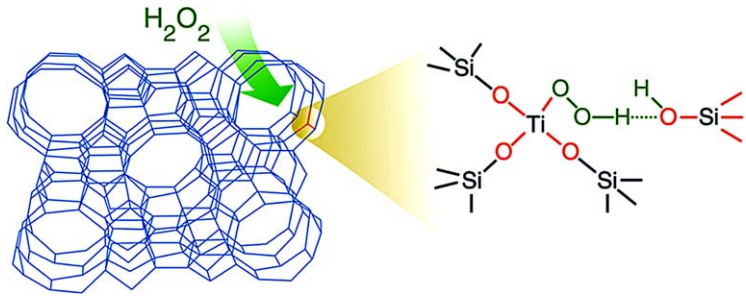

Fig. 13 Proposed η^1 Ti–OOH intermediate after reaction of TS-1 with H_2O_2. Reproduced with permissions from W. Lin and H. Frei, Photochemical and FT-IR Probing of the Active Site of Hydrogen Peroxide in Ti Silicalite Sieve, *J. Am. Chem. Soc.*, 2002, **124**, 9292. Copyright 2002 American Chemical Society.

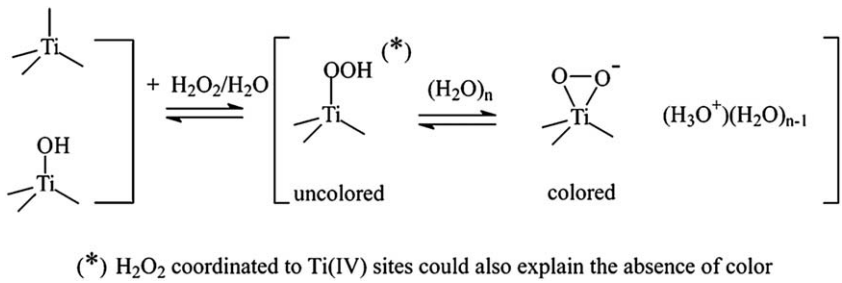

Fig. 14 Proposed intermediates corresponding to 220 nm (uncolored) and 385 nm (colored) intermediates observed *via* diffuse reflectance UV-vis spectroscopy. Reproduced from F. Bonino, A. Damin, G. Ricchiardi, M. Ricci, G. Spano, R. D'Aloisio, A. Zecchina, C. Lamberti, C. Prestipino and S. Bordiga, Ti-Peroxo Species in the TS-1/H2O2/H2O System, *J. Phys. Chem. B*, 2004, **108**, 3573. Copyright 2004 American Chemical Society.

symmetric breathing mode of a Ti–O_2^- ring.[304,306] The feature at 618 cm^{-1} was assigned based on similarities to the vibrational structure of a solid-crystalline standard ($[NH_4^+]_3[TiF_5O_2]^{3-}$), which is known to possess an analogous Ti–O_2 metallacycle based on crystallographic data. UV-vis spectra show that charge-transfer features form at 220 and 385 nm after dosing TS-1 with H_2O_2 solutions, and concomitantly, the TS-1 develops a yellow color.[307] Figure 14 suggests that the Ti–OOH and Ti–O_2^- complexes that were assigned to the 220 and 385 nm features, respectively. The identity of the species that is responsible for epoxidations is still debated because these intermediates rapidly interconvert, making it difficult to definitively link one to the selective formation of PO or other epoxides. Consequently, Ti–OOH intermediates are generally invoked as the active species for olefin epoxidations over TS-1 (and M–OOH intermediates on similar metal oxide catalysts), because Ti–OOH more closely resembles the electrophilic intermediate posited by Clerici[102] than does the electron-rich Ti–O_2^- species.

Despite the apparent success of TS-1 as a catalyst for propylene epoxidation, it has been integrated into few processes with the exception of the HPPO process because the small pores (~5 Å in diameter)[299] of the MFI framework accommodate only small substrates. Consequently, a

number of researchers have attempted to translate the active site structure of TS-1, and the associated high selectivities and rates, to the epoxidation of larger olefins by using other zeolite frameworks with larger pore diameters.[78,97,98,308–312] The zeolite *BEA polymorph is an appealing candidate, because *BEA has larger pores (~7 Å in diameter)[299] and a relatively low framework density, which together allow bulkier olefins access to active sites for epoxidation. For example, cyclooctene (a reactant which is not epoxidized over TS-1), was epoxidized with 100% selectivity to the epoxide with H_2O_2 in a titanium-substituted *BEA (Ti-BEA) catalyst.[98] Corma *et al.* show that Ti-BEA catalyzes the epoxidation of various olefins (*e.g.*, 1-hexene, 1-octene, cyclohexene, 1-methyl-1-cyclohexene, *etc.*) in methanol with higher rates of reaction for the substituted and cyclic olefins in comparison to TS-1, but with increased rates of solvolysis resulting in diol and glycoether formation.[313] Interestingly, they demonstrated that increases in the small amount of framework aluminum present in the Ti-BEA gave lower selectivities towards epoxides, apparently by facilitating the nucleophilic attack of the epoxide by water or methanol to form diols or glycoethers, respectively.[97] Notably, the link between epoxide selectivity and aluminum content in Ti-BEA is similar to the previously mentioned findings on TS-1,[66,301] which confirms that acid sites related to framework aluminum atoms catalyze the solvolysis of epoxides. As seen for TS-1, epoxide selectivities greater than 90% can be achieved by eliminating the acid sites in Ti-BEA. For example, aluminum-free Ti-BEA synthesized through a hydrothermal precipitation method epoxidizes linear olefins (*e.g.*, 1-hexene, 1-octene, 4-octene, 1-decene, *etc.*) with turnover rates greater than 127 $mol_{epoxide}\ mol_{Ti}^{-1}\ h^{-1}$ with greater than 90% selectivity to the epoxides.[96] Van der Waal *et al.* compared the rates and selectivities for the epoxidation of larger alkenes (*e.g.*, norbornene and limonene) between TS-1 and Ti-BEA to probe the effects of different pore sizes on these reactions.[96] Ti-BEA catalyzes the epoxidations of norbornene with H_2O_2 and achieves 8% conversion with 89% selectivity after one hour (acetonitrile, 343 K); however, TS-1 did not produce measurable quantities of the epoxide under the same conditions. Yet, Ti-BEA gave little regioselectivity towards specific C=C bonds in reactants presenting multiple C=C bonds such as limonene, which was epoxidized to form both endocyclic and terminal epoxides with comparable selectivities of 45% and 55%, respectively (Scheme 14).

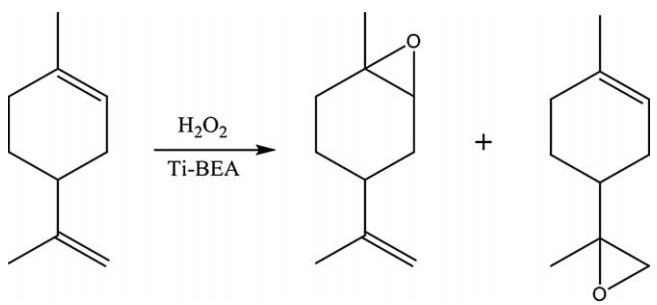

Scheme 14 Epoxidation products of racemic Limonene with H_2O_2 over a Ti-BEA catalyst.

Titanium has also been incorporated into the MWW zeolites, which contain a range of pore diameters (5–10 Å)[299] and possess reaction rates for cyclohexene epoxidation that are comparable to Ti-BEA.[314] Ti-MWW was shown to have high thermal stabilities and recyclability (5 sequential uses with no detectable drop in reactivity) after post-reaction calcination. However, the authors found that residual B-atoms in the framework (where B is present from the synthesis of the framework) form Brønsted acid sites, which reduce the selectivity for epoxides and favor the formation of diols and glycoethers. The authors synthesized a series of Ti-MWW with increasing loadings of Ti (0.1–0.7 $mmol_{Ti}$ g^{-1}) and found that the reaction rate of 1-hexene epoxidation to form 1-hexene oxide initially increases with the Ti content of the zeolite (due to greater numbers of Lewis acid active sites). Rates eventually decrease due to the presence of non-selective and diffusion hindering TiO_x oligomers within the pores (~5.7 Å in diameter).[314] When the loading of Ti in Ti-MWW catalysts is low, the Ti atoms are dispersed fairly evenly throughout the framework. As the amount of Ti is increased, TiO_x oligomers form in the pores and channels of the zeolite, which sterically hinder the diffusion of reactant molecules. As such, the synthesis procedure and metal loading for the incorporation of Ti-atoms into other zeolite frameworks affects olefin epoxidation, and therefore, molecular control of the Ti-atom density within the framework must be considered to fine-tune the reactivity and selectivity of these catalysts.

A number of transition-metals (*e.g.*, Ti,[309] Nb,[315] V,[316] Sn,[317–319] Zr,[320,321] Hf,[322] Cu,[323] and Fe[324]) have been substituted into zeolite frameworks using synthetic and post-synthetic methods to produce epoxidation catalysts. Figure 15 depicts one convenient method for post synthetic modification of Al-containing zeolites, described by Hunger and coworkers.[309] This approach utilizes dealumination of commercial Al-containing zeolites either by steam hydrolysis,[325] microwave irradiation in acidic media,[326] or acid treatment in hot HNO_3,[317] all of which remove Al-atoms to trace levels and yield silanol pockets in the zeolite framework. Subsequently, cationic metal complexes are ion exchanged into these pockets by either solid-state ion exchange (*i.e.*, the metal

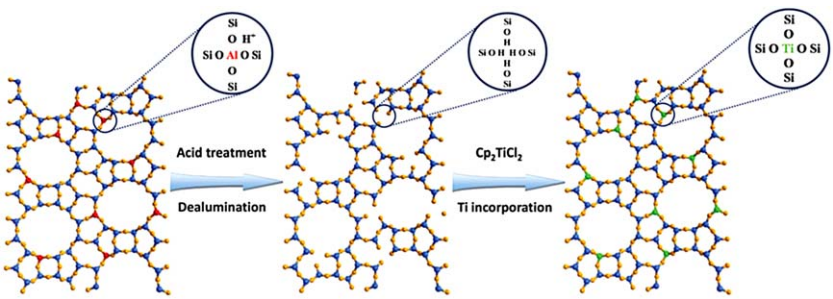

Fig. 15 The post-synthetic modification of zeolite *BEA. First, acid treatment results in a dealuminated sample, followed by ion exchange, and oxidative heat treatment to produce the substituted zeolite. Reproduced from B. Tang, W. Dai, X. Sun, N. Guan, L. Li and M. Hunger, *Green Chem.*, 2014, **16**, 2281; with permissions from the Royal Society of Chemistry.

precursor and the dealuminated zeolite are intimately combined by mechanical grinding)[317] or liquid-phase ion exchange (*i.e.*, the dealuminated zeolite is mixed with a solution containing the cationic precursor).[315,316]

Wang and coworkers developed an Fe-substituted MCM zeolite (Fe-MCM) that epoxidizes styrene with H_2O_2 with reasonable reaction rates (8.9 $(mol_{Styrene})(mol_{Fe}\ h)^{-1}$) and with moderate epoxide selectivity (42%) with respect to benzaldehyde formation (37%).[327] The reaction rate was found to increase in proportion with the Fe loading, which results from the increased density of active sites on the catalyst, but eventually decreases (above 1.1 wt% Fe) due to the decomposition of H_2O_2 over FeO_x clusters that begin to form at these high metal loadings from extra-framework Fe. When H_2O_2 was added dropwise (*i.e.*, the concentration was kept low throughout the reaction), the selectivity for epoxide formation increased from 7.8% (when H_2O_2 was added all at once) to 17% over two hours at 346 K. The decomposition of H_2O_2 occurs through the bimolecular reaction with the M–OOH intermediate over metal–oxide catalysts. Therefore, epoxides form selectively following the formation of Fe–OOH if the concentration of styrene is much higher than that of H_2O_2.[328] Our group synthesized a Nb-incorporated *BEA zeolite (Nb-BEA) to study the mechanism of cyclohexene epoxidation with H_2O_2.[329] Cyclohexene epoxidation reacts *via* an Eley–Rideal mechanism where H_2O_2 reversibly adsorbs to a Nb active site, followed by irreversible formation of both Nb–$(O_2)^-$ superoxide and Nb–OOH intermediates. Nb–$(O_2)^-$ was found to epoxidize cyclohexene, while Nb–OOH appears to interconvert to form Nb–$(O_2)^-$. Interestingly, both the rate and selectivity of cyclohexene oxide formation depends heavily on the ratio of cyclohexene concentration to that of H_2O_2 ($[C_6H_{10}]:[H_2O_2]$). The highest rates (13 $mol_{epoxide}\ mol_{Nb}^{-1}\ h^{-1}$) and selectivities (97%) are observed at high $[C_6H_{10}]:[H_2O_2]$, because Nb–$(O_2)^-$ reacts with cyclohexene or H_2O_2 at rates proportional to their liquid-phase concentrations.[329] Additionally, comparisons of activation enthalpies ($\Delta H^{\ddagger}$) and entropies ($\Delta S^{\ddagger}$) for epoxidation ($\Delta H^{\ddagger} = 72 \pm 7$ kJ mol^{-1}, $\Delta S^{\ddagger} = -35 \pm 21$ kJ mol^{-1} K^{-1}) and H_2O_2 decomposition ($\Delta H^{\ddagger} = 45 \pm 5$ kJ mol^{-1}, $\Delta S^{\ddagger} = -91 \pm 30$ kJ mol^{-1} K^{-1}) show that H_2O_2 decomposition is enthalpically favored and H_2O_2 selectivity towards epoxidation increases with increasing temperatures. Thus, epoxidation reactions will give maximum selectivities at both high ratios of $[C_6H_{10}]$ to $[H_2O_2]$ and high temperatures.[329]

Transition metal substituted zeolites have been a well-studied class of catalysts since the introduction of TS-1 in the early 1990s. The narrow substrate scope of TS-1 has led to the incorporation of Ti (and other transition metals) into larger zeolite frameworks (*e.g.*, *BEA, MCM, MWW) to catalyze the epoxidation of bulkier alkene substrates. A number of studies have demonstrated that high epoxide selectivities rely on eliminating or neutralizing Brønsted acid sites within the zeolite, because such sites catalyze solvolysis reactions that ring open epoxides and reduce yields. Yet, despite the interest in developing novel and increasingly selective epoxidation catalysts, a number of questions remain regarding the mechanism and active intermediates for olefin epoxidation as well as

correlations between catalyst reactivity and selectivity to the elemental identity of the metal atom. As such, there is significant potential for developing useful epoxidation catalysts using other transition metal substituted zeolites.

5.2 Polyoxometallates

Polyoxometallates (POMs) are an important class of homogeneous and heterogeneous catalysts with complex metal oxide structures generally consisting of catalytically active anions with a variety of cations that balance charge. POMs have garnered attention over the past decades for their use in a number of reactions involving epoxidations. While peroxotungstates (W-POMs) and peroxomolybdates (Mo-POMs) were the first POMs reported as catalysts for epoxidations, a number of other transition-metal substituted POMs have been developed for this chemistry in recent years.

Early studies of POM-catalyzed olefin epoxidations primarily focused on homogeneous W-POMs with less emphasis on their Mo counterparts,[86,87] because the Mo-POMs gave higher non-selective H_2O_2 decomposition rates and thus lower epoxidation selectivities.[87,330,331] In addition, Mo-POMs were more frequently used in stoichiometric amounts, making the process non-catalytic.[86,87] Ishii and coworkers discovered that the $H_3[PW_{12}O_{40}]$ POM efficiently epoxidizes linear (*e.g.*, 1-octene) and cyclic (*e.g.*, cyclooctene, 3-vinyl cyclohexene) alkenes with H_2O_2 in the presence of a PTC, such as cetyl pyridinium chloride.[332] PTCs transfer the active oxidant from the aqueous to the organic phase in biphasic systems, and consequently provides greater selectivities for epoxides by minimizing hydrolysis of the oxirane rings and the formation of diols.

Typically, W-POMs are synthesized *in situ* by reactions between tungstic acid (H_2WO_4), a phosphate, and an ammonium or phosphonium counter ion.[87] The identity of both the POM and its counter ion affect the catalytic rate and selectivity for olefin epoxidation.[87] Efforts to determine the optimal combinations of counter ions *a priori* have been unsuccessful,[86,333] therefore, the optimization process remains largely empirical. For instance, Noyori *et al.* demonstrated that W-POM catalysts deactivate when used with PTCs that incorporate either chloride or hydroxyl anions, whereas those consisting of hydrogen sulfate gave higher yields (Table 6).[56]

Clear and accurate descriptions of the structure of the active metal centers of POM catalysts are difficult to acquire, because most POMs form *in situ*. However, in 1985, Venturello *et al.* synthesized a novel W-POM ($[[(C_6H_{13})_4N^+]_3[PO_4[W(O)(O_2)_2]_4]^{3-}$) and characterized the structure using X-ray crystallography.[112] Scheme 15 shows the structure of this W-POM, which consists of a PO_4^{3-} group and four $[W(O)(O_2)_2]$ species, each of which contain two η^2-O_2 metallacycles that are believed to be active for olefin epoxidation.[112] Importantly, this crystal structure helped in identifying the active oxygen species (η^2 W-O_2) in the W-POM ($H_3[PW_{12}O_{40}]$) developed by Ishii *et al.*[332] Aubry *et al.*[334] combined UV-vis, IR, Raman, and NMR characterization to independently confirm that the active species for epoxidation is in fact the $[PO_4[W(O)(O_2)_2]_4]^{3-}$ ion

Table 6 Effects of phase-transfer catalyst on the epoxidation of 1-octene.[a,b]

Phase-transfer catalyst	Yield[c] (%)	
	Without solvent[d]	In toluene[e]
None	0	0.1
$[(n\text{-}C_{10}H_{21})_4N]HSO_4$	69	83
$[CH_3(n\text{-}C_8H_{17})_3N]HSO_4$	86	94
$[R_3(CH_3)N]HSO_4$[f]	71	91
$[(n\text{-}C_6H_{13})_4N]HSO_4$	4	36
$[(n\text{-}C_4H_9)_4N]HSO_4$	0	0.5
$[CH_3(n\text{-}C_8H_{17})_3N]_2SO_4$[g]	29	24
$[CH_3(n\text{-}C_8H_{17})_3N]Cl$	22	18
$[CH_3(n\text{-}C_8H_{17})_3N]Cl$[h]	7	3
$(n\text{-}C_{16}H_{33}NC_5H_5)Cl$[i]	11	7
$[(n\text{-}C_4H_9)_4N]Cl$	0	0.1
$[(n\text{-}C_{10}H_{21})_4N]OH$	2	4
$[(n\text{-}C_8H_{17})_4N]OH$	2	4
$[(n\text{-}C_4H_9)_4N]OH$	0	0
$[C_6H_5CH_2(C_2H_5)_3N]OH$	0	0

[a] Recreated from K. Sato, M. Aoki, M. Ogawa, T. Hashimoto, D. Panyella and R. Noyori, *Bull. Chem. Soc. Jpn.*, 1997, **70**, 905; with permission from the Chemical Society of Japan.
[b] 30% H_2O_2, 1-octene, $Na_2WO_4 \cdot 2H_2O$, $NH_2CH_2PO_3H_2$, and PTC in 150 : 100 : 2 : 1 : 1 molar ratio at 363 K and 1000 rpm stirring.
[c] Determined by GC Analysis, based on initial 1-octene concentration.
[d] Reaction run for 2 h.
[e] Reaction run for 4 h with 4 mL of toluene.
[f] R is a mixture of C_6 to C_{10} alkyl chains.
[g] 30% H_2O_2, 1-octene, $Na_2WO_4 \cdot 2H_2O$, $NH_2CH_2PO_3H_2$, and PTC in 150 : 100 : 2 : 1 : 0.5 molar ratio.
[h] H_3PO_4 was used instead of $NH_2CH_2PO_3H_2$.
[i] *N*-Hexadecylpyridinium chloride.

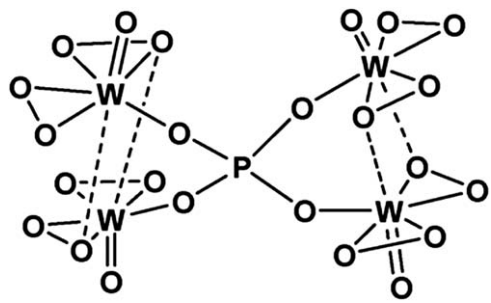

Scheme 15 Molecular structure of $[PO_4[W(O)(O_2)_2]_4]^{3-}$, determined *via* X-ray crystallography. Adapted from C. Venturello, R. D'Aloisio, J. Bart, and M. Ricci, A New peroxotungsten heteropoly anion with special oxidizing properties: synthesis and structure of tetrahexylammonium tetra(diperoxotungsto)phosphate(3-), *J. Mol. Catal.*, 1985, **32**, 107. Copyright 1985 with permisison from Elsevier.

proposed by Venturello (Scheme 15).[112] Contact of $H_3[PW_{12}O_{40}]$ with aqueous H_2O_2 decreased the intensity of a UV-vis absorbance feature at 252 nm,[334] which is evidence for the formation of a reactive intermediate, while ^{31}P NMR spectra showed peaks at −12.4 and −11.8 ppm, which are

attributed to η^2-O_2. Additionally, Aubry and coworkers showed that when H_2O_2 is added to a solution of $H_3[PW_{12}O_{40}]$, the Raman spectra gives rise to three significant bands at 962 cm^{-1}, 556 cm^{-1}, and 619 cm^{-1} which are assigned to ν(W=O), ν_s(W–O_2), and ν_{as}(W–O_2), respectively. These three characterization methods (*i.e.*, UV-vis, NMR, and Raman) all suggest that the active intermediate for epoxidation over $H_3[PW_{12}O_{40}]$ is the same η^2-O_2 intermediate proposed by Venturello *et al.*[112] While POMs are active for epoxidation, their homogeneous nature makes catalyst recovery difficult, thereby presenting a clear need to create catalytic systems that are easily recovered and separated from the product stream.

Significant effort has been spent to immobilize POMs onto insoluble solid supports[113,335,336] and to create homogeneous systems from which the inactive catalyst precipitates.[114] Villa de P *et al.* showed that the Venturello anion (*i.e.*, $[PO_4[W(O)(O_2)_2]_4]^{3-}$) can be ion exchanged onto PW-amberlite (a cationic resin) to create a heterogeneous catalyst (W-POM-Amb) that epoxidizes terpenes with high turnover numbers (>160 turnovers for limonene).[335,336] Mechanistic interpretation of epoxidation rates, measured as a function of reactant concentrations, suggested that epoxidation occurs through a Langmuir–Hinshelwood type mechanism. Interestingly, the addition of limonene epoxide reduced epoxidation rates over the W-POM-Amb catalyst (likely due to strong adsorption of the epoxide to the active site), but reactivity was completely recovered after washing with acetone.[336] In 2001, Zuwei and coworkers developed a W-POM ($[\pi$-$C_5H_5NC_{16}H_{33}]_3[PO_4(WO_3)_4]$), which activates H_2O_2 to form a soluble peroxo species that is active for epoxidation of propylene but which spontaneously precipitates after complete H_2O_2 consumption (Scheme 16).[114] This W-POM gave 94% selectivity to PO at high propylene conversions (91%). Importantly, this catalyst could also be coupled with the 2-ethylanthraquinone (EAH) auto-oxidation process (Section 2), which generates H_2O_2 *in situ* (from H_2 and O_2) to be activated for propylene epoxidation. EAH was first reduced by reaction with H_2 over a Pd catalyst and O_2 was subsequently added to regenerate EAH and form H_2O_2 as a reagent for epoxidation.[114] The authors did not add EAH, Pd, H_2, and O_2 to the reaction mixture containing propylene and the W-POM, likely because this would result in the hydrogenation of propylene to propane over the Pd catalyst. When these two processes are coupled, the system gave yields of PO as high as 85% with greater than 90% catalyst recovery. IR spectra taken *ex situ* of the W-POM before reaction recovery revealed a clear absorption peak at 890 cm^{-1} which is assigned to the ν_{as}(W–O–W) mode, while IR spectra of H_2O_2-activated W-POM lacked the 890 cm^{-1} feature, but possessed a distinct peak at 840 cm^{-1}, which is assigned to ν(O–O).[114]

Many other metals (*e.g.* Cr,[337] Mn,[109,338] Ti,[339] Bi,[340] Fe,[341,342] Nb,[343] Ni,[344,345] Ag[346]) have been incorporated into POM and POM-based catalytic systems that can be used for epoxidation. Amanchi *et al.* developed a Bi-substituted sandwich-type POM ($[Sn_2Bi_2(ZnW_9O_{34})_2]^{14-}$) that activates H_2O_2 to form a nucleophilic intermediate that is active for the epoxidation of cyclooctene.[340] Notably, these nucleophilic active species oxidize allylic alcohols to form aldehydes or ketones *via* C–H activation at greater

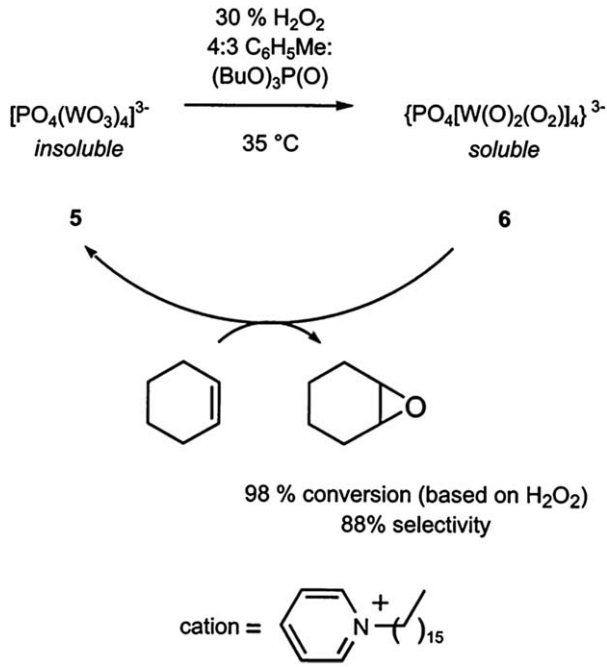

Scheme 16 A recoverable tungsten-based catalytic system where the activated catalyst is soluble and precipitates out as an insoluble salt when no H_2O_2 is present. Reproduced from X. Zuwei, Z. Ning and L. Kunlan, *Science*, 2001, **292**, 1139.

rates than for the epoxidation of the C=C double bond, which are targeted by the electrophilic intermediates formed on zeolite catalysts and many W-based POMS. The authors proposed the reactive intermediate to be a nucleophilic Bi-peroxo ($Bi–O_2^-$) moiety, similar to the $W–O_2$ intermediates proposed for W-POMs, in order to explain the unexpected inversion of substrate oxidation rates and selectivities in comparison to W-POMs.

Metal substituted POMs are an interesting class of catalysts with a great deal of flexibility that allows the materials and solvents used to be finely tuned in order to increase rates, selectivities, and the success of catalyst recovery. Since the introduction of W-POMs in the late 1980s, POMs have been adapted for the catalytic epoxidation of various cyclic (*e.g.*, substituted cyclohexenes) and bulky (*e.g.*, terpenes) olefins. Despite the research efforts that POMs have garnered, the *ab initio* prediction of novel transition metal substituted POMs for epoxidations has been largely unsuccessful and new POMs are created through an Edisonian approach.[340] The development of increasingly selective POMs, where reactivity can be estimated *a priori*, for the activation of H_2O_2 and epoxidation of various olefins remains a challenge and a potentially rewarding area of study for collaborative efforts between computational and experimental researchers in catalysis.

5.3 Metal oxides

Heterogeneous metal oxide catalysts are desirable for use in industrial epoxidation, because they are highly stable and can be easily recovered

from reactant streams and reused. A variety of supported metal oxides containing (*e.g.*, Ti,[103,328,347–349] V,[103,350] Nb,[103,351–353] Mo,[354] Ta,[103,328,355–357] and W[358]) and mixed-metal oxide (*e.g.*, Al_2O_3–ZrO_2, Al_2O_3–TiO_2, ZrO_2–TiO_2)[359] catalysts have been prepared and studied for olefin epoxidations with H_2O_2. Notestein *et al.* developed a calixarene-assisted synthesis method, which involves the formation of bulky calixarene–metal complexes that are grafted onto to the surface of SiO_2 followed by high-temperature oxidative treatment (723–823 K in flowing dry air) to create supported metal oxide catalysts with isolated metal centers at a range of metal loadings (0.1–3 wt%).[103,108] This method has been used recently by Notestein *et al.* to investigate periodic trends among group IV (*i.e.*, Ti, Zr, Hf) and V (*i.e.*, V, Nb, Ta) metals for the epoxidation of cyclohexene and styrene.[103] Initial turnover rates correlate linearly with increasing Pauling electronegativity of the transition metal used in epoxidation. Interestingly, site isolated Nb–SiO_2 catalysts prepared by the calixarene grafting method give particularly high cyclohexene epoxidation rates (~2.4 $mol_{epoxide}$ mol_{Nb}^{-1} min^{-1}) and outperformed Ti–SiO_2, which was long thought to be the optimal metal for epoxidation reactions based on the success of TS-1 in the HPPO process.[103]

Supported Ta catalysts have been used for epoxidations and in recent years, mechanistic interpretation of rate measurements and spectroscopic data have provided evidence for specific active intermediates. Morlanes *et al.* used a calixarene-assisted grafting method to make a site-isolated Ta catalyst (Ta–SiO_2), on which they determined the kinetics and mechanism for cyclooctene epoxidation with H_2O_2 by measuring initial rates in a batch reactor as a function of reactant concentrations (*i.e.*, H_2O_2 and cyclooctene).[328] They determined that the epoxidation of cyclooctene occurs through an Eley–Rideal mechanism, in which H_2O_2 reversibly adsorbs to a Ta active site and forms a complex proposed to be quasi-equilibrated with the formation of the reactive intermediate (Ta–OOH*). Subsequently, Ta–OOH* reacts with cyclooctene in solution to form cyclooctene oxide.[328] H_2O_2 decomposition was proposed to occur by reaction of a free H_2O_2 molecule with Ta–OOH*, and notably, a calixarene ''capping'' agent was bound to the Ta active site to partially block the open coordination site and decrease H_2O_2 decomposition by 50%.[328] This likely succeeds because the calixarene capping agent is bulky and non-polar, which creates an environment that preferentially solvates and stabilizes cyclooctene, rather than H_2O_2, in the immediate vicinity of Ta–OOH*. Tilley and coworkers independently developed a synthesis procedure that uses siloxane-assisted grafting of Ta atoms onto SBA-15 (Ta-SBA-15) to produce a catalyst with similar function.[356] UV-vis spectra show that the reaction of H_2O_2 with Ta-SBA-15 forms an absorbance feature at 260 nm, which is attributed to the ligand-to-metal charge transfer (LMCT) of an –OOH appendage to the Ta metal center.[356] It should be noted that this UV-vis absorbance feature is similar to the feature observed by Zecchina,[307] for H_2O_2 activation over TS-1.

Supported Nb oxide catalysts have also attracted attention recently for use as epoxidation catalysts. Kholdeeva and coworkers used an evaporation-induced self-assembly (EISA) method to prepare hydrothermally stable

mesoporous niobium–silicates (Nb–SiO_2), which epoxidize bulky cyclic olefins (*e.g.*, cyclooctene, styrene, limonene) with moderate-to-high selectivities (50–99%).[352] Interestingly, Nb–SiO_2 epoxidizes electron deficient substrates (*e.g.*, substituted quinones) with high selectivities (>68%). This is in contrast to TS-1, which was observed to have increased epoxidation rates for electron-rich alkenes, due to the electrophilicity of the Ti–OOH* reactive intermediate.[102] Additionally, the identity of the Nb precursor used in the EISA method has a significant effect on the dispersion of Nb in the final catalyst. The authors found that the catalyst yielded mostly site-isolated Nb species, as determined by diffuse reflectance UV-vis when using ammonium niobate oxalate as the precursor.[352] When niobium(v) ethoxide was used, the catalyst consisted primarily of dimers and small oligomers of Nb-oxide domains. Site-isolated Nb catalysts are more effective for the formation of epoxides sensitive to secondary decomposition (*e.g.*, cyclooctene and cyclohexene), likely because oligomeric Nb oxide provides Lewis acid sites in the immediate post-epoxidation vicinity for the activation of the oxirane ring for secondary reactions (*e.g.*, hydrolysis to form a diol). However, no appreciable differences in reaction rates or epoxide selectivities were seen between site-isolated and oligomeric Nb catalysts for the formation of stable epoxides (*e.g.*, limonene epoxide).[352] Somma *et al.* developed a niobia–silica aerogel mixed oxide catalyst that is active for the epoxidation of unsubstituted olefins (*e.g.*, cyclooctene) and substituted allylic alcohols (*e.g.*, geraniol and *trans*-2-pentene-1-ol) by co-precipitation of a niobium alkoxide precursor (NbO^iPr_5) with tetramethyl orthosilicate.[104,353] The authors found that increasing the loading of Nb (1 to 6 wt%) decreased the selectivity of epoxide formation (*i.e.*, cyclooctene oxide selectivity from 100 to ~10%) due to increased rates of epoxide solvolysis to produce 1,2-cyclooctadiol. This is similar to the observations made by Kholdeeva,[352] where oligomeric Nb-oxide sites would give increased rates of diol formation post epoxidation. Flaherty *et al.* have synthesized a Nb-incorporated *BEA zeolite (Nb-BEA) to study cyclohexene epoxidation with spectroscopic evidence for the formation of the reactive intermediate Nb-$(O_2)^-$.[329] Upon contact with H_2O_2, a broad absorbance feature at 335 nm is deconvoluted to reveal two overlapping bands at 330 and 370 nm, which are assigned to the LMCT of an $-O_2^-$ and –OOH moieties to a Nb metal center. Reaction of H_2O_2-activated Nb-BEA with ethylene attenuates the broad absorbance feature, and time resolution of the two components combined with kinetic parameter optimization reveals that the Nb-superoxide species (*i.e.*, Nb-$(O_2)^-$) is responsible for olefin epoxidation and is potentially the reactive intermediate on related Nb-oxide catalysts.

Metal oxide catalysts are ubiquitous and desirable catalysts with high hydrothermal stability and low costs that can be easily adopted by industry for large-scale epoxidation reactions with H_2O_2. A large number of transition metal oxide catalysts have been investigated for the epoxidation of various olefins, however, the synthesis procedure has a significant effect on the selective use of H_2O_2 and the prevention of secondary reactions from occurring (resulting in lower epoxide yields).

As such, there is still much work to be done to understand the structure–function relationships between catalysts synthesis and morphology and how these physical properties translate to the efficacy of an epoxidation catalyst.

5.4 Homogeneous coordination compounds

A large body of literature describes olefin epoxidations using homogeneous transition metal catalysts and H_2O_2 as an oxidant. Several excellent reviews discuss different aspects of this field of work in great detail,[85,86,92,360] therefore, we introduce a broad perspective on the historical developments and recent advances of three commercially available classes of homogeneous epoxidation catalysts: methyltrioxorhenium, metalloporphyrins, and Schiff-base complexes.

5.4.1 Methyltrioxorhenium. Methyltrioxorhenium (MTO) has garnered much attention due to its high catalytic activity for epoxidation reactions even at low temperatures (263–343 K). Herrmann *et al.* were among the first to report MTO as an effective epoxidation catalyst for the epoxidation of substituted olefins (*e.g.*, *cis*-2,3-pentene, β-pinene, allyl alcohol, and propene) with fairly good yields (90%, 50%, 90%, and 50%, respectively).[361,362] ^{17}O NMR performed by these authors suggest that two H_2O_2 molecules are needed to initially form the reactive species from MTO (Scheme 17). Infrared spectra of the complex formed by reaction of H_2O_2 with MTO show an absorption peak at 872 cm^{-1}, which is attributed to an η^2 Re-O_2 intermediate that is thought to be active for olefin epoxidation. After activation of H_2O_2, Herrmann was

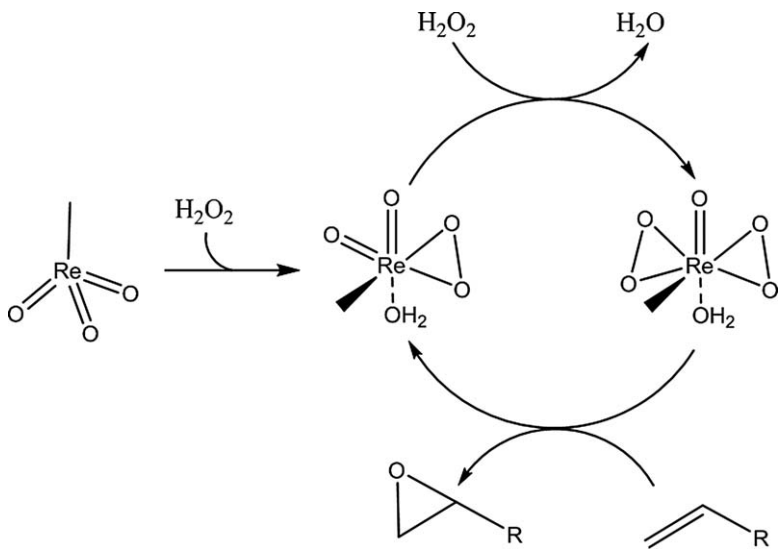

Scheme 17 Proposed catalytic cycle for the activation of H_2O_2 over MTO and subsequent epoxidation of a generic olefin. Adapted from B. R. Goldsmith, T. Hwang, S. Seritan, B. Peters and S. L. Scott, Rate-Enhancing Roles of Water Molecules in Methyltrioxorhenium-Catalyzed Olefin Epoxidation by Hydrogen Peroxide, *J. Am. Chem. Soc.*, 2015, **137**, 9604. Copyright 2015 American Chemical Society.

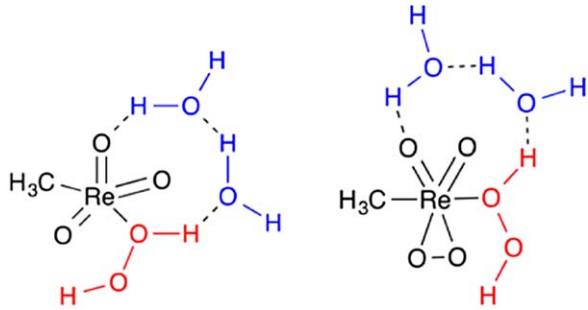

Scheme 18 Proposed cyclic transition state for H_2O-assisted the activation of H_2O_2 over MTO. Reproduced from B. R. Goldsmith, T. Hwang, S. Seritan, B. Peters and S. L. Scott, Rate-Enhancing Roles of Water Molecules in Methyltrioxorhenium-Catalyzed Olefin Epoxidation by Hydrogen Peroxide, *J. Am. Chem. Soc.*, 2015, **137**, 9604. Copyright 2015 American Chemical Society.

able to chelate the intermediate with diglyme and isolate crystals, which were then used to show the existence of two η^2 Re-O_2 moieties on the activated material.[362] This $Re(O_2)_2$ intermediate is relatively stable and does not decompose spontaneously near 300 K, however, upon heating it becomes explosive.[361] In 2015, Goldsmith *et al.* combined computational and experimental evidence to show that an H_2O-mediated hydrogen bonding network accelerates the reaction between H_2O_2 and MTO to form the active $Re(O_2)_2$ complex (Scheme 18).[363] The authors conclude that small amounts of H_2O accelerate the formation of $Re(O_2)_2$, which also increases the rate of epoxidation. However, increasingly high H_2O concentrations induce significant rates for hydration of the epoxides to form diols.

Although MTO gives high rates and selectivities for the epoxidation of various olefins, H_2O coordinated to MTO tends to be a moderately strong Brønsted acid ($pK_a \sim 3.6$), which can activate and hydrate epoxides (*i.e.*, form diols) and reduce product yields.[361] Consequently, researchers have invested considerable efforts to develop catalytic systems involving MTO that are not acidic. For example, Rudolph and Sharpless developed a pyridine-assisted MTO catalytic system that selectively epoxidizes a number of linear (*e.g.*, 1-decene, *cis*- and *trans*-4-octene), cyclic (*e.g.*, cyclohexene, norbornene, cyclooctene), and conjugated (*e.g.*, 1-phenylcyclohexene, indene, 1,2-dihydronaphthalene) alkenes with selectivities and yields greater than 98% and 92%, respectively.[364] Addition of the pyridine is believed to have two benefits. First, the coordination of pyridine to MTO aids in the reaction between H_2O_2 and MTO to form the active intermediate (similar to the conclusions from Goldsmith *et al.*[363]). Second, pyridine acts as a H^+ scavenger and prevents H^+ donors from activating the epoxide to form diol byproducts, and thus increases reaction rates and yields. Since the discovery of the synergistic role that pyridine plays in olefin epoxidations with MTO, many other catalytic systems have been devised that utilize 3-cyano pyridine,[365] 3-methyl pyrazole,[366] and urea–H_2O_2 adducts[367,368] to accelerate the activation of H_2O_2 over MTO and neutralize the solution pH to increase epoxide yields. However, harsh, undesirable organic solvents (*e.g.*, dichloromethane and chloroform)[366,368]

are needed to solubilize both MTO and these additives for improved catalytic performance. As a result, MTO has not been adopted on industrial scales, but remains a focus of fundamental studies for epoxidation reactions.

5.4.2 Metalloporphyrins. Groves *et al.* were among the first to demonstrate the epoxidation of an olefin (in this case, norbornene) using a high-valent Fe(IV) porphyrin (Fe(IV)–POR) complex, which was inspired by biology's cytochrome P-450 and peroxidase.[369] ^{1}H NMR, ^{57}Fe Mössbauer, and EPR spectroscopies were used to identify the active intermediate that formed upon reaction of Fe(IV)–POR with *m*-chloroperoxybenzoic acid (*m*-CPBA), a Fe(IV)-oxo cation (*i.e.*, Fe=O^{+}).[369] This intermediate structurally resembles the Fe(IV)-oxo intermediate of P-450, which contains a heme (*i.e.* porphyrin) complex that is active for hydrocarbon oxidation and which forms by a series of e^{-} transfer steps to an O_2 molecule that initially binds to form a η^1 Fe(IV)–OO complex.[370] Groves soon demonstrated that the presence of pro-chiral addendums (*e.g.*, anilide, Scheme 19) on the porphyrin ring allows the Fe(IV)–POR complex to perform the enantioselective oxidation of styrene.[371] The aniline functional groups are rotationally hindered, such that olefins prefer specific binding configurations. Anilide groups also create identical active sites on both sides of the Fe(IV)–POR, which give high purities of product with enhanced enantioselectivities. Research groups further developed this theme by creating "basket handled" aniline-modified Fe(IV)–POR *via* the connection of two anilide appendages by an aromatic tether.[372] Mansuy *et al.* found that a dual "basket handled" Fe(IV)–POR reversed the enantioselectivity (15%

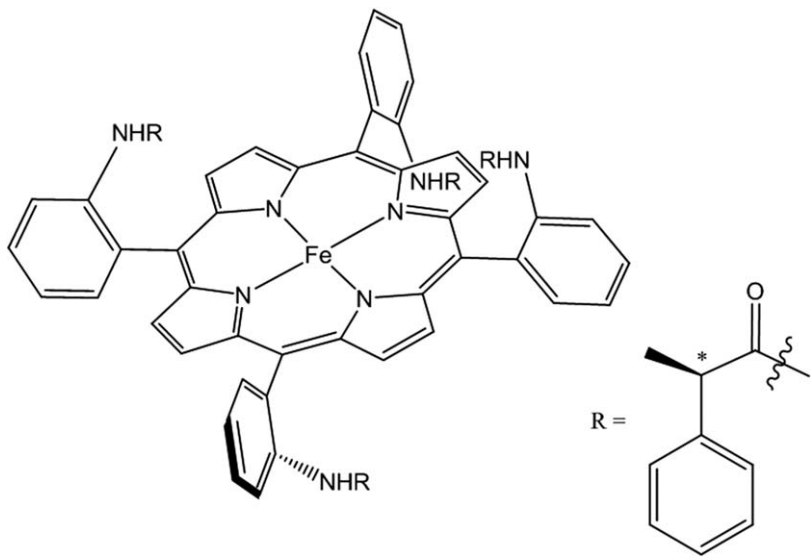

Scheme 19 Rotationally hindered anilide substituted Fe–POR catalyst resulting in an enantioselective active site for olefin epoxidation. Adapted from J. T. Groves and R. S. Myer, Catalytic asymmetric epoxidations with chiral iron porphyrins, *J. Am. Chem. Soc.*, 1983, **105**, 5791. Copyright 1983 American Chemical Society.

enantiomeric excess (ee) for (S) enantiomer) observed with Groves' chiral Fe(IV)–POR[371] to instead give selectivity for the opposite enantiomer (*i.e.*, (R)-*p*-chlorostyrene oxide with 50% ee from *p*-chlorostyrene).[372] These early Fe(IV)–POR catalysts[369,371,372] required organic oxidants (*e.g.*, *m*CPBA and iodosylbenzene) and solvents (*e.g.*, DCM, toluene), and researchers did not report the use of H_2O_2, perhaps because the low solubility of H_2O_2 in these solvents would limit its efficacy.

In 1993, Traylor and coworkers developed a new Fe(III) porphyrin (Fe(III)–POR) that catalyzes the epoxidation of cyclic olefins (*e.g.*, cyclohexene, cyclooctene, and norbornene) with H_2O_2 with fairly high yields (*i.e.*, 83%, 100%, 64%, respectively).[99] Importantly, Traylor determined that this chemistry involves the heterolytic cleavage of an Fe–OOH* intermediate to form an active Fe–oxene (Fe^{+}=O), as opposed to a homolytic O–O bond rupture that forms hydroxyl radicals and additional Fenton-reaction byproducts (Scheme 20).[99] *Cis*-stilbene was used as a molecular probe of the relative contributions of the heterolytic and homolytic activation pathways, because the ratio of *cis*- and *trans*-epoxide products reports directly on the relative rates of Fe^{+}=O and radical mediated epoxidation reactions, respectively.[99] The authors showed that only *cis*-stilbene oxide formed and that Fe^{+}=O was the predominant active species.[99] If epoxidation were to occur through a radical-based mechanism, *trans*-stilbene oxide would be the predominant product because radical-mediated epoxidations occur through a transition state with free rotation about the C–C bond, which would eliminate the eclipsing interactions between the two phenyl groups that is observed for *cis*-stilbene oxide.[302] Additionally, the presence of electron-donating substituted (*i.e.*, perfluorinated phenyl groups) on the porphyrin increased epoxidation rates of cyclooctene more than 50-fold at 298 K. These results suggest that Fe^{+}=O likely forms as a result of the

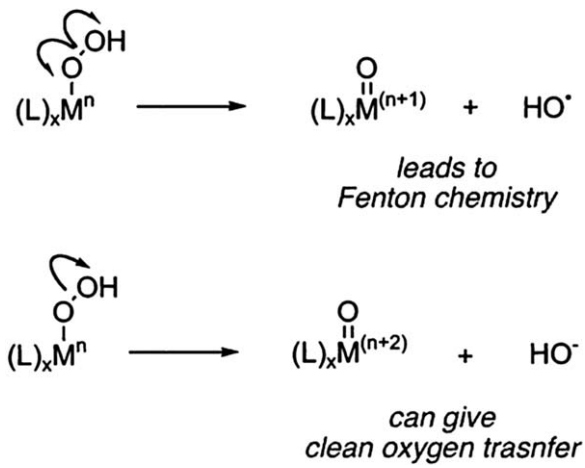

Scheme 20 Homolytic (top) and heterolytic (bottom) cleavage of the O–O bond in M–OOH. Reproduced from B. S. Lane and K. Burgess, Metal-Catalyzed Epoxidations of Alkenes with Hydrogen Peroxide, *Chem. Rev.*, 2003, **103**, 2457. Copyright 2003 American Chemical Society.

significant charge transfer from the electron-rich porphyrin rings (when tetra-substituted with perfluorinated phenyl rings) to the π^* of the O_2 and helps to cleave the O–O bond in the Fe–OOH species formed upon H_2O_2 activation.[99,373–375] Notably, this situation differs from that for TS-1 and related heterogeneous materials, where Ti-atoms apparently lack sufficient charge density to cleave the O–O bond of Ti–OOH*. Similarly, many heterogeneous catalysts are believed to utilize peroxo (M–O_2*) and hydroperoxo (M–OOH*) intermediates for the epoxidation of olefins.[303,307] In the subsequent decades, multiple modifications have increased the epoxidation rates and selectivities of Fe–POR catalysts. For example, Vinhado *et al.* immobilized pentafluorophenyl Fe(III)–POR complexes onto bis-functionalized silica using covalently bonded imidazolium and sulfonyl tethers.[376] These Fe(III)–POR complexes gave greater cyclooctene epoxidation yields (*i.e.*, up to 50%) than the homogeneous catalyst with no additives (up to 38%), likely due to the promotion of heterolytic cleavage of the O–O bond in Fe–OOH to form Fe=O.

Other approaches include the substitution of a tridentate or tetradentate carbazole ligand for the porphyrin core over Fe-based catalysts (Scheme 21).[116,377] Niwa *et al.* developed a carbazole-substituted Fe(III) complex (Fe(III)–CAR) that epoxidizes various pro-chiral (*e.g.*, substituted stilbenes) and electron-poor (*e.g.*, unsaturated esters) olefins with PhIO as the oxidant.[377] Fe(III)–CAR is isoelectronic to the Fe(III)–POR, and epoxidizes conjugated planar *trans*-olefins to selectively form the (*S*,*S*) epoxide with up to 97% ee. Recently, Dai *et al.* have created a tetradentate diamino oxazoline ligand that when bound to Fe(III), epoxidizes α,β-unsaturated ketones with high yields (up to 94%) and high enantioselectivities (up to 99% ee) with *m*-CPBA.[116] This Fe(III) catalyst was shown to epoxidize more than 23 electron-poor olefins with greater than 80% ee and typical yields of ~80%. It should be noted, that the reported selectivity trends run counter to those for Fe(III)–PORs, which prefer to epoxidize electron-rich olefins, due to the electron-poor nature of the Fe^{+}=O intermediate.[99] An explanation of why these carbazole–Fe(III) catalysts are active towards electron-poor olefin epoxidation is not immediately apparent or explained by the authors.[377] We speculate that these trends are caused by the lack of aromaticity (*i.e.*, the porphyrin core

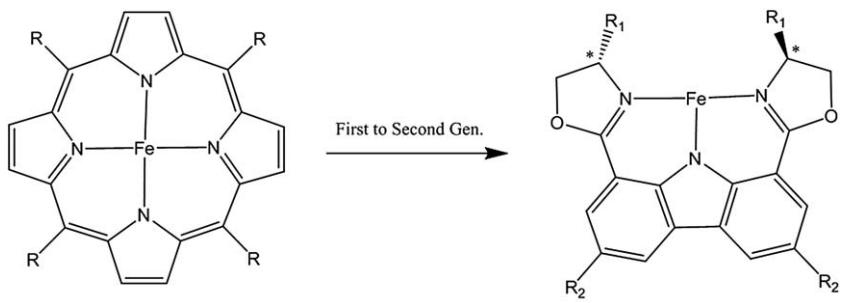

Scheme 21 Fe–POR catalysts and the Fe–POR-inspired carbazole derivatives.

is withdrawing electron density from the Fe atom) and substitution of the oxazoline (*i.e.*, electron-rich) ligand shifts electron density onto the Fe center, which makes the active intermediate formed more electron rich and increases selectively towards the epoxidation of electron-poor olefins. Despite the recent research efforts put into carbazole-derived Fe catalysts and their rather unique selectivity patterns, these catalysts have yet to be adapted in ways that would allow them to use H_2O_2 for epoxidation reactions, which would be an important next step for carbazole-based catalysts.

Mn-based porphyrin (Mn–POR) catalysts activate H_2O_2 for the epoxidation of various olefins (*e.g.*, cyclooctene, cyclohexene, and 1-nonene) with complete conversion (~100%) and high selectivities for epoxide formation (greater than 90%) when combined with imidazole additives.[378,379] Imidazole coordinates and donates electron-density to the Mn metal center, which accelerates the activation of H_2O_2 for epoxidations. For example, imidazole is clearly needed to facilitate the epoxidation of styrene because under identical reaction conditions and times in the absence of imidazole, only trace amounts of styrene oxide form (less than 2.5% yield).[378] Quici and coworkers developed a Mn–POR catalyst, which contains a carboxylic acid and an imidazole tether, that epoxidizes cyclooctene with turnover rates greater than 500 min^{-1}.[380] The imidazole tether coordinates and donates electron density to the Mn metal center and increases the rate of H_2O_2 activation, while the carboxylic acid is believed to coordinate to the opposite face of the complex and assist in the activation of H_2O_2 through a Mn–OOH intermediate.[380] Arasingham studied olefin epoxidations over Mn–POR catalysts with H_2O_2 and correlated the rate constants with the oxidation potentials of the various olefin reactants, which suggests that H_2O_2 activates through a transition state involving a Mn(v)=O intermediate with little charge separation.[381] EPR spectroscopy shows that the reaction of Mn–POR with *m*-CPBA forms a broad resonance feature at *g* 4.5, which is consistent with the formation of Mn(v)=O species and also similar to the intermediates proposed for Fe–POR catalysts.[382] Dai *et al.* have developed a Mn–POR-inspired diamino oxazoline-ligated Mn complex (MnL_n) that epoxidizes a variety of conjugated and cyclic olefins (*e.g.*, indene, 1-phenylpropene, stilbene, *etc.*) with a wide range of yields (17–94%) and fairly good enantioselectivites (51–99% ee).[383] The addition of carboxylic acids (*e.g.*, propanoic acid, carboxycyclohexane, heptanoic acid) increases the rate and the enantioselectivity of the reaction, because the diamino oxazoline ligand synergistically binds with the carboxylic acid and promotes the activation of H_2O_2 and epoxidation of an olefin (Scheme 22). Unfortunately, there are few publications that give mechanistic interpretation or spectroscopic evidence for the bond structure or identity of specific reactive intermediate over MnL_n catalysts, which hinders the rational development of novel ligands to improve rates and selectivities.

Mn–PORs have been immobilized onto solid supports to create hybrid heterogeneous catalysts that are easily removed from the product stream for catalyst recovery. Rebelo *et al.* synthesized a Mn–POR that is covalently tethered to an amine-functionalized silica gel that retained much

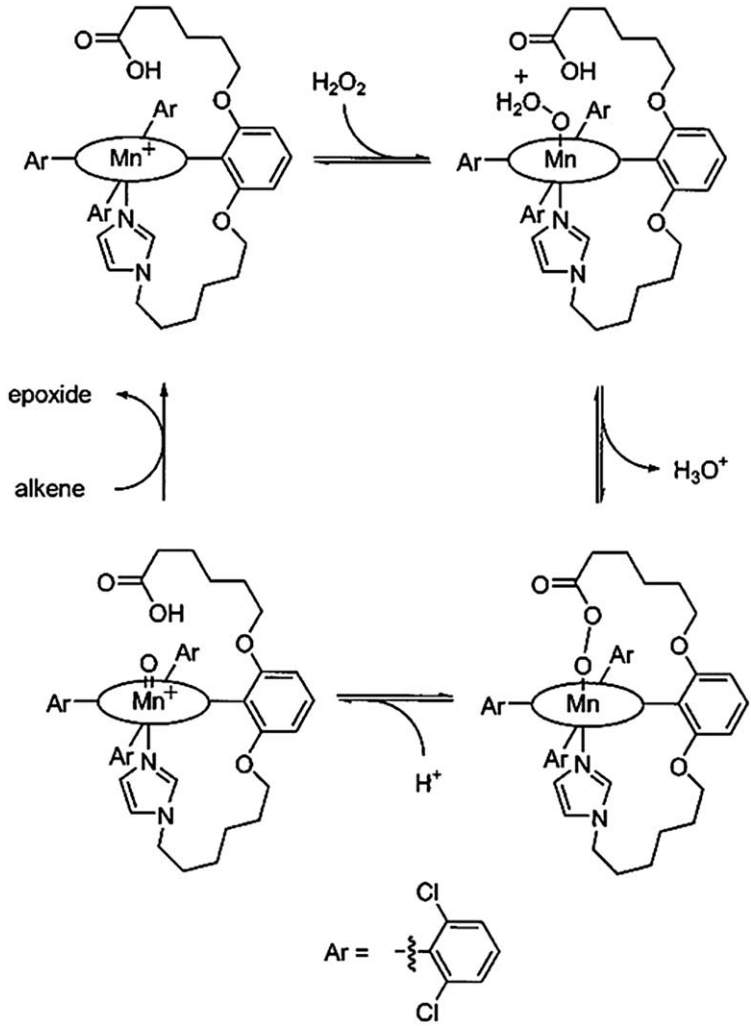

Scheme 22 Doubly-tailed (with imidazole and carboxylic acid end groups) Mn–POR catalyst synthesized by Banfi. Reproduced from B. S. Lane and K. Burgess, Metal-Catalyzed Epoxidations of Alkenes with Hydrogen Peroxide, *Chem. Rev.*, 2003, **103**, 2457. Copyright 2003 American Chemical Society.

of its reactivity towards cyclooctene epoxidation (*i.e.*, 97% for untethered catalyst, 88% for immobilized).[384] Unfortunately, the conversion of cyclooctene epoxidation decreased to 51% in identical reaction conditions upon recovery and reuse, which is likely due to leaching of the catalyst by oxidative cleavage of the amine tethers by H_2O_2. De Paula and coworkers immobilized Mn–POR catalysts on both silica gel (Mn–POR–SG) and modified resins (Mn–POR–MR) to investigate the differences in stability and reactivity that the identity of the support has on olefin epoxidation with H_2O_2.[385] For both solid supports, high yields were obtained for the epoxidation of cyclooctene (greater than 99%). However, upon catalyst recovery, the conversion of cyclooctene over Mn–POR–SG dropped to 4.9%, while the reactivity for Mn–POR–MR was maintained over 4 reuse cycles

(97.4% yield). The authors attributed the greater stability of Mn–POR–MR, in comparison to Mn–POR–SG, to orbital stabilization and increased electron exchange between the resin support to the Mn–POR complex (*i.e.*, electron donation from the modified resin into the antibonding orbitals of Mn-POR, similar to electron back donation). Despite some success, efforts to immobilize homogeneous oxidation catalysts onto functionalized silica gels generally result in catalytic systems with limited lifetimes due to the inevitable oxidation of organic tethers.

5.4.3 Schiff-base complexes. In 1990, Jacobsen and coworkers reported one of the first Mn–salen complexes that was active for the epoxidation of several olefins (*e.g.*, 1-methyl cyclohexene, styrene, 2-phenyl propene, *trans*-stilbene) with a wide range of yields (36–93%) and enantioselectivities (20–93% ee) using iodosylmesitylene as the oxidant.[386] The enantioselectivity of epoxidation reactions on Mn–salen complexes reflects the substitution at the diamino bridge on the salen ligand as it controls the approach of olefins to the activated Mn–metal center.[387] Berkessel *et al.* modified the salen ligand to possess an internally tethered imidazole group (Scheme 23) that coordinates to the Mn metal atom (Mn–SalenIM) and helps to epoxidize styrene with styrene oxide yields of 100% using 1 wt% H_2O_2 solutions.[388,389] The imidazole group coordinates to the Mn center and provides additional electron density, which aids in the activation of H_2O_2 in ways similar to those seen for Mn–POR catalysts. This additional electron density is critical because H_2O_2 is more difficult to activate than iodomesitylene. These results have motivated a number of studies that utilize electron-rich additives (*e.g.*, *N*-methylmorpholine *N*-oxide[390] or ammonium acetate[391]) in order to facilitate the activation of H_2O_2 *via* heterolytic O–O bond cleavage of Mn–OOH intermediates to form the active Mn=O species.

The original Mn–salen compounds inspired the recent development of diamino–pyridine (dpb) complexes, which are a new class of catalysts for the epoxidation of olefins with H_2O_2. Miao *et al.* developed a Mn–dbp complex that efficiently epoxidizes cyclic (*e.g.*, cyclooctene, cyclohexene, cycloheptene) and linear (*e.g.*, 1-octene, *trans*-2-heptene, and *cis*-2-heptene) alkenes in relatively high yields (45 to 92%) when H_2SO_4 is used as a co-catalyst.[392] A Mn–OOH intermediate forms upon activation with H_2O_2

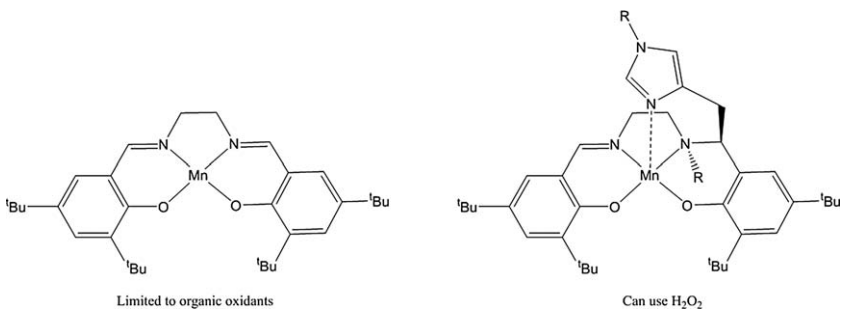

Scheme 23 Jacobsen's Mn–Salen and Berkessel's Mn–SalenIM complexes.

and subsequently undergoes acid-catalyzed heterolysis to form a Mn(v)=O species that is active for epoxidation. As such, the presence of protons (H^+) in solution is necessary for the activation of H_2O_2 with these catalysts. Acid-catalyzed hydration of the epoxides to form the corresponding diols did not occur, because the reaction was conducted at 253 K, where rates of decomposition are slow. Additionally, over 20 olefins (linear, cyclic, conjugated, electron rich, and electron poor) were shown to undergo epoxidation with reasonable yields (45–100%) and excellent enantioselectivities (60–98% ee).[392] Recently, Cussó *et al.* synthesized an Fe(dbp) complex that efficiently epoxidizes 36 different cyclic enones with up to 99% ee using H_2O_2.[393] EPR spectra reveal that carboxylic acids (*i.e.*, typical additives) coordinate to the Fe–metal center and assist in the heterolytic cleavage of Fe–OOH to generate an electrophilic oxidant (*i.e.*, Fe(v)=O, Scheme 24).[394] Despite the recent interested in the dbp-based catalysts, there are few reports that show their immobilization onto solid supports in order to increase their reusability.

In general, homogeneous catalysts tend to be the most reactive and selective catalysts for olefin epoxidation. However, they typically require the use of organic solvents to increase the solubility of the catalysts and co-reactants and additives (*e.g.*, imidazole or carboxylic acids) to activate H_2O_2. As a result, these catalysts have not been widely adopted by industry for the production of epoxides at large scales. Such catalysts have potential for use in the production of fine chemicals, if these complexes can be effectively constrained or immobilized to solid supports without significant loss of reactivity.

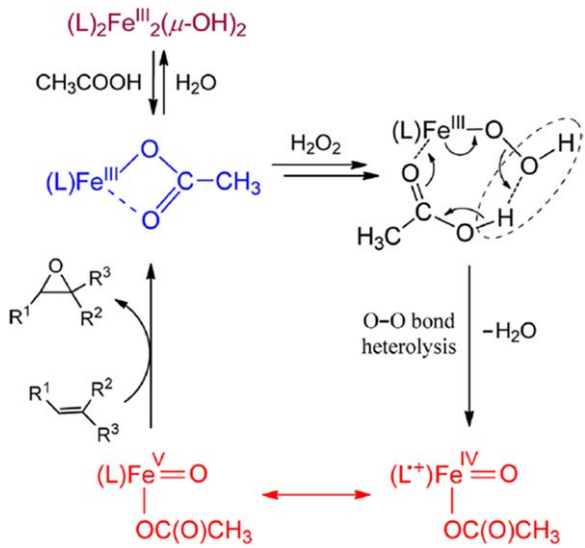

Scheme 24 Proposed mechanism for epoxidation with H_2O_2 over an Fe(dbp) catalyst. Reproduced from O. Y. Lyakin, A. M. Zima, D. G. Samsonenko, K. P. Bryliakov and E. P. Talsi, EPR Spectroscopic Detection of the Elusive Fe[V] = O Intermediates in Selective Catalytic Oxofunctionalizations of Hydrocarbons Mediated by Biomimetic Ferric Complexes, *ACS Catal.*, 2015, **5**, 2702. Copyright 2015 American Chemical Society.

5.5 Detection of active intermediates in epoxidation catalysts

The identity of the reactive intermediate formed by activating H_2O_2 influences the selectivity of the reaction towards specific C=C bonds and also the selectivity towards different competing pathways (*e.g.*, allylic hydrogen abstraction, complete oxidation, *etc.*). Table 7 summarizes the four most commonly discussed reactive intermediates formed upon H_2O_2 activation (*i.e.*, hydroperoxo (M–OOH), superoxo ($M–O_2^-$), peroxo ($M–O_2^{2-}$), and oxo (M=O)), the spectroscopic methods used to detect their presence, and the characteristic features indicative of each type of intermediate. Hydroperoxo species (*e.g.*, Ti–OOH) have been identified on TS-1 after activation of H_2O_2 using a combination of UV-vis,[356] IR,[303] Raman,[304] and EXAFS.[307] These Ti–OOH species were found to have epoxidation rates that increased with the electron-richness of C=C bonds (*e.g.*, Table 5, allyl chloride > allyl alcohol > 1-pentene),[102] which is indicative of the electrophilic nature of the M–OOH moiety.[300] Superoxide species (*e.g.*, Nb-$(O_2)^-$) have been detected as a reactive intermediate by our group using *in situ* UV-vis and IR spectroscopy for cyclohexene epoxidation.[329] Superoxide species likely form with the concomitant cleavage of a M–O bond and are in a dynamic equilibrium with M–OOH

Table 7 Experimental identification of the active intermediate in olefin epoxidation catalysts.

Species	Technique	Characteristic features
Hydroperoxo (M–OOH)	UV-vis	250 nm (Ta–OOH)[356]
	Infrared	837 cm^{-1} (ν(O–O), Ti–OOH)[303]
	Raman	840–843 cm^{-1} (ν(O–O), Ti–OOH)[304]
	EXAFS	2.01 Å (Ti–OOH)[307]
Superoxo ($M–O_2^-$)	UV-vis	330 nm (Nb–$(O_2)^-$)[329]
	Infrared	1024 cm^{-1} (ν(O–O), Nb–$(O_2)^-$)[329]
	EPR	330 mT (Ti–(O_2))[293]
Peroxo ($M–O_2^{2-}$)	UV-vis	385 nm (Ti–OOH)[307]
		370 nm (Nb-$(O_2)^{2-}$)[329]
		252 nm ($[PO_4[W(O)(O_2)_2]_4]^{3-}$)[334]
		320 nm ($CH_3ReO_2(\eta^2–O_2)$)[363]
	Infrared	840 cm^{-1} (ν(O–O), $[PO_4[W(O)(O_2)_2]_4]^{3-}$)[114]
		618 cm^{-1} (ν_s(O–O), Ti-(O_2))[304,306]
		912 cm^{-1} (ν(O–O), Nb-$(O_2)^{2-}$)[329]
		872 cm^{-1} (ν(O–O), $CH_3ReO_2(\eta^2$-$O_2)$)[362]
	Raman	556 cm^{-1} (ν_s(W(O_2)))[334]
		619 cm^{-1} (ν_s(W(O_2)))[334]
	NMR	−500 ppm (^{183}W, W(O_2))[334]
	Single-crystal X-ray structural analysis	Crystal Structures: ($[PO_4[W(O)(O_2)_2]_4]^{3-}$)[112] ($CH_3ReO(\eta^2$-$O_2)_2 \cdot$ diglyme)[361]
Oxo (M=O)	UV-vis	422 nm ((Cl_8TPP)Mn(O))[381]
	Infrared	712 cm^{-1} (ν(Mn=O))[382]
	EPR	$g = 4.5$ (Mn=O)[382]
		Centered $g = 2.05$ (Fe=O)[394]
	Mössbauer	$\delta = 0.08$ mm s^{-1} (Fe=O)[369]
	Mass spectrometry	869 m/z (parent, Mn(TMP)(O)(H_2O))[382]

species prior to epoxidation.[293,329] Peroxo species (*i.e.*, M–$(O_2)^{2-}$) have been detected by UV-vis,[307,329,336,363] IR,[114,304,306,336,363] Raman,[334] NMR,[334] and X-ray crystallography[112,361] and are commonly invoked as the active intermediate for olefin epoxidation on group VI-based polyoxometalates (*i.e.*, W- and Mo-POMS) and methyltrioxorhenium (MTO).[112,114,332,334,361,362] These M-$(O_2)^{2-}$ species are easily paired with phase-transfer catalysts (PTCs) to devise clever bi-phasic catalytic systems that allow for the recovery and reuse of these expensive and traditionally homogeneous catalysts.[332] Metal-bound oxo species (*i.e.*, M=O) have been identified using UV-vis,[381] IR,[382] EPR,[382,394] Mössbauer,[369] and mass spectrometry[382] and are generally believed to be the active intermediate for oxidations over Fe– and Mn–porphyrin and Schiff-base complexes following the heterolytic cleavage of an O–O bond. The addition of electron-donating additives (*e.g.*, imidazole)[378,379] has been shown to accelerate the heterolytic cleavage of the O–O bond, which lends itself to the design of novel catalytic systems that employ electron-donating substituents covalently linked to a solid support to tether these catalysts to increase their recyclability and be incorporated into flow-chemistry processes. Thus, the design of more active, selective, and reusable catalysts for epoxidations hinges on the understanding of how the olefin of interest coordinates and reacts with the active intermediate to identify the best category of catalyst to begin with (*e.g.*, type of catalyst, metal identity, coordinating structure). Only once the active intermediate and its general reactivity is known, can systems be devised to better stabilize this reactive intermediate and increase its propensity to react with specific olefins under tunable reaction conditions.

6 Oxidation schemes that use H_2O_2 formed *in situ*

Few epoxidation catalysts can utilize O_2 as the oxidant for olefin epoxidation (with the notable exception of ethylene oxide production over supported Ag catalysts).[17,18] Concurrently, most industrially practiced epoxidation reactions achieve high site time yields by being practiced at high temperature at the gaseous interface with heterogeneous catalysts, which complicate the efficient use of H_2O_2. Liquid H_2O_2 cannot be easily fed into the inlet of the reactors for these processes without significant decomposition, therefore, a number of research groups (both industrial and academic) have made extensive efforts to create catalytic systems that generate H_2O_2 *in situ* using bifunctional systems that combine metal catalysts (*e.g.*, PtPd bimetallics, Pd, or Au) for H_2O_2 formation and metal oxide catalysts (*e.g.*, TS-1, TiO_2) for olefin epoxidation.

6.1 Bimetallic platinum and palladium on TS-1

The discovery of Pd as an efficient direct synthesis ($H_2 + O_2 \rightarrow H_2O_2$, Section 3) catalyst prompted its incorporation into TS-1 (a well-known catalyst for epoxidations, Section 5.1) to create a catalytic system that utilizes H_2 and O_2 to form and use an active oxidant *in situ*.[395] In the late 1990s, Meier and Hölderich reported the synthesis and use of TS-1 containing PtPd bimetallic clusters (PdPt/TS-1) to epoxidize propylene to PO

(12% yield, 46% PO selectivity) using reactant streams of propylene, H_2, and O_2.[396,397] The PdPt/TS-1 catalyst (1 wt% Pd, 0.1 wt% Pt) was prepared through the incipient wetness impregnation of commercially available TS-1, followed by high-temperature oxidative and reductive treatments (423 K) with the intent to grow the PdPt clusters and reduce the resulting clusters to a metallic state.[396,397] The PtPd clusters produce H_2O_2 *in situ via* direct synthesis from H_2 and O_2 (7 bar H_2, 10 bar O_2, aqueous methanol solvent, 316 K), while framework Ti-atoms of TS-1 utilize the H_2O_2 to epoxidize the propylene charged into the batch reactor.

Unfortunately, the use of PtPd/TS-1 forms a variety of products and the typical PO selectivity is low (*i.e.*, <20% with respect to propylene consumption).[395] Studies by Baiker and coworkers showed that similar PtPd/TS-1 catalysts produce a slate of light oxygenated products including PO, acetone, acrolein, acrylic acid, and methyl formate upon reaction of propylene with H_2O_2 in aqueous methanol.[398] The catalyst initially forms PO with a selectivity of 99% at 3.5% conversion, and methyl formate is the major by-product and forms by the oxidation of the methanol solvent to formic acid, which undergoes subsequent esterification reactions. PO formation rates increase by 20% (2.8 mmol PO h^{-1} to 3.5 mmol PO h^{-1}) when supercritical CO_2 (120 bar) was substituted for the N_2 diluent used with the H_2 and O_2 gas mixtures (to avoid explosive mixtures, Section 3). The increased rates were attributed to increased rates of mass transfer to the catalyst surface, but the non-polar supercritical CO_2 may also preferentially stabilize a critical intermediate in the catalytic cycle. A number of light oxygenate byproducts form by secondary decomposition and oxidation reactions of PO, and must lead to significant yield losses at higher conversions. The decreasing yields of PO formation (at propylene conversions greater than 3.5%) are attributed to Pt coordinating and activating methanol, which then reacts to form methyl formate (the most abundant side product). Additionally, Pt is known to activate O_2 and various alcohols (*e.g.*, methanol) for aerobic oxidation processes and likely reacts with methanol to form surface methoxide species which then react with propylene and PO to form the products observed.[398] Unfortunately, protic solvents (*i.e.*, water, alcohols) are needed for the direct synthesis of H_2O_2,[148] so solvent oxidation is likely to be an issue for Pt-containing catalytic systems that produce H_2O_2 *in situ* for propylene epoxidation. Beckman studied the effect of adding ammonium acetate and other inhibitors (*i.e.*, pH buffers and acid titrants) to the aqueous methanol solvent to neutralize defect sites (*i.e.*, solid-acid sites) on TS-1 that catalyze hydration and decomposition of PO.[295,399] The addition of ammonium acetate significantly increased PO yields from 9 to 24% and PO selectivities from 22 to 82%, which demonstrated the effectiveness of this approach.

PtPd/TS-1 catalysts are one system with the potential to utilize H_2 and O_2 reactants as a source for producing H_2O_2 *in situ* for the epoxidation of olefins. However, defect sites in the TS-1 and the minority Pt site on the metal clusters catalyze a variety of side reactions that reduce the yields of epoxides significantly. The reaction conditions (*i.e.*, solvent choice, use of additives) will need to be optimized in order to increase the conversion

of propylene and the yields and selectivities for PO formation. The complexity of these systems may provide such opportunities, yet developing stable versions of these catalysts, especially in the presence of complex solvents, remains a challenge.

6.2 Gold on TS-1 and TiO_2

In the late 1990s, Haruta *et al.* reported the selective epoxidation of propylene to PO with reactant mixtures of H_2 and O_2 over Au–TiO_2 (Fig. 16). Au and TiO_2 do not catalyze the formation of PO or H_2O_2 independently,[401] which suggests that unique reactivity of the Au–TiO_2 catalyst arises from a synergistic interaction between the Au clusters and the TiO_2 surface. The reaction between O_2* and H atoms is thought to occur at the exposed boundaries between Au clusters and the TiO_2 support, where Au and Ti atoms cooperatively bind O_2 to create a Au–O_2–Ti intermediate that forms an activated Ti–OOH* species following reduction.[400] In this pivotal paper, Haruta reported greater than 90% selectivity for the formation of PO from propylene at 1–2% conversion of propylene. However, the selectivity to PO decreases sharply when the loading of Au is lowered below 0.2 wt%.[400] The authors hypothesized that at low weight loadings, the Au clusters become flat (as opposed to hemispherical in topology), and thus possesses reactivity similar to Pt (a known hydrogenation catalyst).[400] Such a comparison seems to be based primarily on chemical intuition and does not include a fundamental explanation for this change in reactivity.

Since the initial reporting of the Au–TiO_2 epoxidation catalyst, there have been numerous efforts made to create alternative Au–TiO_2 and Au–TS-1 catalysts for the epoxidation of propylene.[305,402–406] For example, Ribeiro and Delgass have synthesized Au–TS-1 catalysts by the electroless deposition of Au onto TS-1.[401,407] Au–TS-1 was found to have maximum

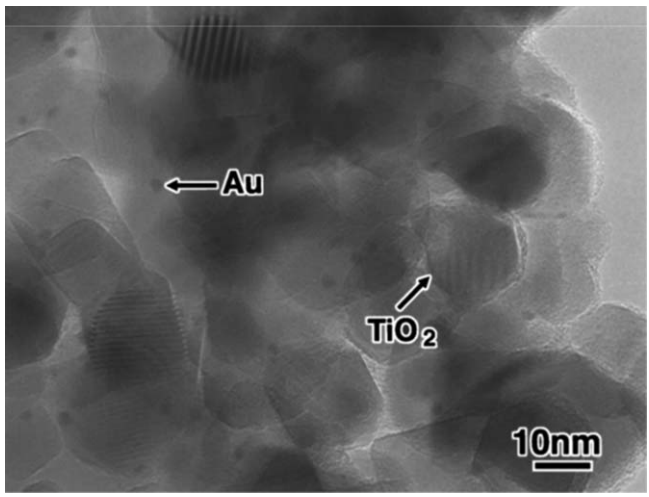

Fig. 16 Transmission electron micrograph of Au–TiO_2 catalysts with 0.98 wt% Au loading. Reproduced from T. Hayashi, K. Tanaka and M. Haruta, Selective Vapor-Phase Epoxidation of Propylene over Au/TiO2 Catalysts in the Presence of Oxygen and Hydrogen, *J. Catal.*, **178**, 566. Copyright 1998 with permission from Elsevier.

PO formation rates (*i.e.*, 160 $g_{PO}\ kg_{cat}^{-1}\ h^{-1}$) at low Au loadings (0.1 wt%), where Au clusters were not observable by high-resolution TEM, which suggests that the average cluster diameter was less than 1 nm. The high dispersity of the Au clusters may increase PO formation rates by maximizing the number of Au atoms adjacent to Ti-atoms. Accordingly, the high reaction rates can be attributed to the increased number of exposed Au–Ti sites, which are believed to be an active site for the reduction of O_2. It has proven to be difficult to create robust Au–TS-1 catalysts that retain activity and selectivity over long times on stream (>15 days), and consequently, Au–TS-1 has not been implemented in any industrial processes, despite the appeal of this chemistry.

In situ diffuse reflectance UV-vis spectroscopy,[65] X-ray absorption near-edge structure (XANES),[408] and EPR spectroscopy[409] were used to study the formation of Ti–OOH species during the gas-phase epoxidation of propylene with H_2 and O_2 over Au–TiO_2 catalysts. EPR spectra did not reveal a Ti-$(O^2)^-$ superoxide anion, but rather suggest that O_2^- species form on Au atoms, which are likely located at the perimeter of clusters (*i.e.*, border of Au cluster and TiO_2). *In situ* UV-vis experiments show a broad peak at 360 nm that indicates a Ti–OOH* intermediate is formed (Section 5.1).[65] Together these results suggest that H_2O_2 is formed *in situ* over the Au clusters and activates over a Ti atom to create Ti–OOH*, which subsequently epoxidizes propylene, as depicted in Scheme 25. Neurock and Yates combined DFT and IR spectroscopy to study the

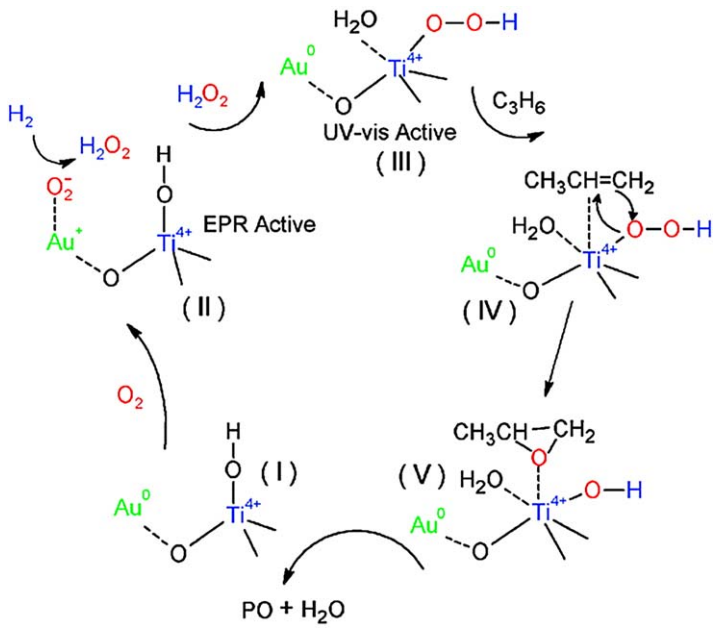

Scheme 25 Proposed catalytic cycle for the activation of H_2 and O_2 (to generate H_2O_2 *in situ*) over Au–TiO_2 catalysts for propylene epoxidation. Reproduced from J. J. Bravo-Suarez, K. K. Bando, J. Lu, M. Haruta, T. Fujitani and S. T. Oyama, Transient Technique for Identification of True Reaction Intermediates: Hydroperoxide Species in Propylene Epoxidation on Gold/Titanosilicate Catalysts by X-ray Absorption Fine Structure Spectroscopy, *J. Phys. Chem. C*, 2008, **112**, 1115. Copyright 2008 American Chemical Society.

oxidation of CO over Au–TiO_2 with H_2O_2, and their findings suggest that O_2 activates at perimeter sites where Au and TiO_2 contact and form a Au–O–O–Ti complex, which was seen to be an active intermediate for CO oxidation.[410] DFT calculated binding energies of O_2 on Au clusters (−0.16 to −0.51 eV) were much weaker than for O_2 binding at the Au–Ti^{4+} perimeter site (−1.01 eV). Consequently, O_2 likely binds and activates preferentially at perimeter sites rather than on the terraces of the TiO_2 or Au clusters. The intrinsic activation energy to form the reactive Au–O–O–Ti species from physisorbed O_2 is relatively low (0.16 eV), which further suggests that this species is a plausible reactive intermediate.[410] In any case, Au–TiO_2 catalysts with small Au clusters are preferential to larger Au clusters (as they lead to higher reaction rates and epoxide selectivities), as the ratio of perimeter sites to total Au used increases, which results in more sites that are active for O_2 activation and subsequent epoxidation reactions.

In the Au–TiO_2 and Au–TS-1 systems discussed above, H_2 was used as a sacrificial reductant to activate O_2 to produce H_2O and an epoxide. H_2O has also been shown to activate O_2 over Au–TiO_2 catalysts, albeit at lower rates, which reduces the need for H_2 (and associated cost). Iglesia *et al.* showed that reactions of H_2O with O_2 over Au–TiO_2 catalysts create intermediates that epoxidize propylene to form PO.[411] Mixtures of H_2O and O_2 co-reactants give PO formation rates that are an order of magnitude lower than the rates observed using comparable mixtures of H_2 and O_2. These lower rates result from a lower thermodynamic driving force for O_2 activation (likely *via* reduction) from reaction with H_2O as compared to H_2. These results suggest that H_2O and O_2 can form active surface intermediates over Au–TiO_2 despite the fact that the formation of H_2O_2 is highly unfavorable.[411] These findings were supported by recent experiments and DFT calculations from Chandler and Grabow that strongly suggest that reactions between adsorbed H_2O and O_2 molecules (*i.e.*, $Au \cdot H_2O \cdot O_2$*) near Au perimeter atoms form Au–OOH* species, which can react with CO to form CO_2[412] and may be responsible for increased rates of PO formation when H_2O is added to H_2–O_2 mixtures. Chang and coworkers employed DFT to show that Au–OOH* species form on Au–TiO_2 by reactions of H_2O and O_2 through a Langmuir–Hinshelwood mechanism, after which, Au–OOH* produces PO by direct reaction with propylene.[413] Additionally, a recent mini-review by Chandler and Grabow[414] highlights the importance of H_2O on O_2 activation over Au–TiO_2 catalysts for small-molecule oxidations. The authors note that PO formation was optimized to yield 90% PO selectivity over Au–TiO_2 catalysts, but that formation is not observed in the absence of H_2O. This is particularly interesting as it suggests that following O_2 adsorption, protons are necessary for hydroperoxide (*i.e.*, Au–OOH) formation, which is strikingly similar to the requirement of a protic solution for the direct synthesis of H_2O_2 over Pd clusters.[148]

While Au–TiO_2 and Au–TS-1 catalysts appear to be promising epoxidation catalysts, they tend to deactivate irreversibly over time or have low rates of epoxide (typically PO) formation. Additionally, the cost of Au can

be prohibitive which presents the opportunity and challenge of finding similar catalytic systems that can activate O_2 with H_2O and maintain high selectivities and rates for PO (or other epoxide) formation.

7 Conclusions

H_2O_2 is an environmentally benign oxidant with the potential to replace chlorinated oxidants for many important industrial processes. Currently, industrial-scale H_2O_2 production is dominated by the anthraquinone auto-oxidation process, which involves many energy intensive steps such as separation and concentration, necessitating large scale facilities and resulting in H_2O_2 prices higher than those for chlorinated oxidizers. Direct synthesis of H_2O_2 avoids these separation and concentration steps, and therefore, has the potential to make cheaper H_2O_2 (and at smaller scales) than anthraquinone auto-oxidation. Economic analysis of industrial scale direct synthesis indicates that the primary costs, and thus the main factor affecting its competitiveness as an industrial process, stem from the cost of H_2. This cost holds back direct synthesis because H_2O is the thermodynamically favored product of direct synthesis, making it difficult to obtain H_2O_2 selectivities comparable to anthraquinone auto-oxidation. As such, research on direct synthesis has focused on improving H_2O_2 selectivity through mechanistic understanding of the reaction, catalyst design, and reaction systems engineering.

Selectivity towards H_2O_2 in direct synthesis has improved over the past two decades through studies of the mechanism, the benefits of acid and halide additives, alloying of metals, and post-synthetic treatments of the catalyst support. Both Langmuir–Hinshelwood and Eley–Rideal mechanisms have been proposed with experimental evidence and DFT calculations supporting both mechanisms, indicating that direct synthesis is a complicated reaction to fully understand. Improved understanding of secondary decomposition of H_2O_2 and selective reaction conditions have led to more accurate and thorough studies of the reaction mechanism, therefore, each mechanistic study improves significantly upon previous analyses. This growing body of knowledge on the mechanism, as well as improved interest in this field of study, suggest that complete understanding of the mechanism can be expected in the future, allowing for the design of more selective catalysts. It has already been discovered that modification of the catalyst surface, by the adsorption of strongly binding ions (*e.g.*, Cl^-, Br^-) or through alloying of metals (*e.g.*, AuPd, PdSn), as well as post-synthetic modification of the support with acids can lead to high selectivities. These toxic and caustic additives and expensive alloys are not the complete solution, but instead guide the synthesis of cheap, selective, and environmentally benign catalysts and reaction conditions. Once H_2O_2 can be made more cheaply, it can lead to cheaper and more environmentally conscious oxidations of various compounds such as simple alkanes (*e.g.*, methane and ethane), alcohols, and sulfides to important industrial precursors and commodity chemicals, many of which have already been investigated on many different transition metal

(*e.g.*, Cu, Fe, W) containing zeolite catalysts. In general, all the oxidation reactions involving H_2O_2 are operationally straightforward, clean, and safe, making it a great replacement for the harmful and toxic oxidants which are currently in use. Future work should identify and improve upon catalysts that perform these oxidations, and concomitantly the direct synthesis of H_2O_2, with high yields and selectivities.

The biggest advances in making economically viable H_2O_2 for industrial oxidation chemistries have come from understanding the fundamental factors governing olefin epoxidation. Epoxides are important precursors for the production of pharmaceuticals, commodity chemicals, plastics, and epoxy resins. The current production of many industrially relevant epoxides is through reaction with a chlorine-containing acid followed by treatment with a strong base. However, in the case of oxidation chemistry, chlorine is not located in the final product and so waste produced contains toxic halogen-containing molecules. To remedy this, extensive efforts have been made to devise catalysts and catalytic systems that selectively activate H_2O_2 for olefin epoxidation as the only byproduct is H_2O. Extensive work has been conducted to understand the mechanisms of H_2O_2 activation through spectroscopic/kinetic measurements over transition-metal substituted zeolites, polyoxometalates, supported transition metal oxides, and homogeneous (*i.e.*, methyltrioxorhenium, porphyrin-ligated Fe and Mn compounds, and Schiff-base complexes) catalysts. Currently, there is no ''ideal'' catalyst for the epoxidation of olefins with H_2O_2 as the reactivity (*i.e.*, reaction rates) and selectivities can be tuned depending on the reaction conditions (*e.g.*, reactant concentrations, temperature), presence of additive molecules, and immobilization of the catalyst onto a solid support. Alternative catalysts (*e.g.*, Au–TS-1/TiO_2 or Pt/Pd–TS-1) have been devised that activate O_2 with the use of H_2 or H_2O as a sacrificial reductant. These catalysts have been mainly studied for the epoxidation of propylene to PO, but tend to have low yields and selectivities. Additionally, there is much work that needs to be done in identifying the mechanism for epoxidation, especially in the case of heterogeneous catalysts, such that more efficient catalysts can be designed both through experimentation and *in silico* to aid in the discovery of increasingly effective catalysts.

The large body of research on direct synthesis of H_2O_2 and subsequent oxidation reactions show that there is significant interest in economic and environmental improvements to industrial oxidations. This interest in H_2O_2 can be seen from the increase in global H_2O_2 production as well as implementation of new, more energy-efficient processes such as HPPO. The next step will be to achieve direct synthesis selectivities comparable to AO under benign conditions, leading to the construction of industrial scale direct synthesis facilities, and eventually, the epoxidation of olefins following *in situ* direct synthesis of H_2O_2. Implementation of more efficient processes for huge global industries, such as epoxidation, will lead to improved conservation of a significant portion of the energy resources available globally.

Acknowledgements

The authors gratefully acknowledge financial support from the National Science Foundation, grant number CBET-1553137, and the U. S. Army Research Office under grant number W911NF-16-1-0128. DTB was supported in part by a National Defense Science and Engineering Graduate (NDSEG) Fellowship.

References

1 G. Sienel, R. Rieth and K. T. Rowbottom, *Ullmann's Encyclopedia of Industrial Chemistry: Epoxides*, Wiley-VCH, Weinheim, Germany, 2000.
2 R. A. Sheldon, *Stud. Surf. Sci. Catal.*, 1991, **66**, 573.
3 M. Hey, *Pap. Conservator*, 1977, **2**, 10.
4 O. Tünay, I. Kabdaşı, I. Arslan-Alaton and T. Ölmez-Hanı, *Chemical Oxidation Applications for Industrial Wastewaters*, IWA Publishing, London, UK, 2010.
5 W. H. Glaze, *Ullmann's Encyclopedia of Industrial Chemistry: Water, 6. Treatment by Oxidation Processes*, Wiley-VCH, Weinheim, Germany, 2011.
6 B. Singh, G. K. Prasad, K. S. Pandey, R. K. Danikhel and R. Vijayaraghavan, *Def. Sci. J.*, 2010, **60**, 428.
7 P. Schmittinger, T. Florkiewicz, L. C. Curlin, B. Lüke, R. Scannell, T. Navin, E. Zelfel and R. Bartsch, *Ullmann's Encyclopedia of Industrial Chemistry: Chlorine*, Wiley-VCH, Weinheim, Germany, 2011.
8 The World Chlorine Council and Sustainable Development, http://www.worldchlorine.org/wp-content/themes/brickthemewp/pdfs/report.pdf, (accessed July 2016).
9 The Chlorine Insitute, Inc., *Water and Wastewater Operators Chlorine Handbook*, http://hdoa.hawaii.gov/pi/files/2013/01/Pamphlet155Ed2-January-2008.pdf, (accessed July 2016).
10 EPA Fact Sheet: The Pulp and Paper Industry, the Pulping Process, and Pollutant Releases to the Environment, Technical Report EPA-821-F-97-011, U.S. Environmental Protection Agency (EPA), Office of Water, Washington, DC, 1997.
11 M. Ragnar, G. Henriksson, M. E. Lindström, M. Wimby, J. Blechschmidt and S. Heinemann, *Ullmann's Encyclopedia of Industrial Chemistry: Pulp*, Wiley-VCH, Weinheim, Germany, 2014.
12 D. L. Sedlak and U. von Gunten, *Science*, 2011, **331**, 42.
13 W. H. Casey, *Science*, 2002, **295**, 985.
14 G. T. F. Wong and J. A. Davidson, *Water Res.*, 1977, **11**, 971.
15 J. Thornton, *Pandora's Poison: Chlorine, Health, and a New Environmental Strategy*, MIT Press, Cambridge, Massachusetts, 2000.
16 C. Kurt and J. Bitner, *Ullmann's Encyclopedia of Industrial Chemistry: Sodium Hydroxide*, Wiley-VCH, Weinheim, Germany, 2012.
17 S. Linic and M. A. Barteau, *J. Am. Chem. Soc.*, 2003, **125**, 4034.
18 J. G. Serafin, A. C. Liu and S. R. Seyedmonir, *J. Mol. Catal. A: Chem.*, 1998, **131**, 157.
19 G. Strukul, *Catalytic Oxidations with Hydrogen Peroxide as Oxidant*, Springer, Netherlands, 1992, vol. 9.
20 J. M. Campos-Martin, G. B. Blanco-Brieva and J. L. G. Fierro, *Angew. Chem., Int. Ed.*, 2006, **45**, 6962.

21 Chlorine Replacement Applications with Hydrogen Peroxide, http://www.h2o2.com/municipal-applications/wastewater-treatment.aspx?pid=134&, (accessed July 2016).
22 W. Eul, A. Moeller and N. Steiner, *Kirk-Othmer Encyclopedia of Chemical Technology: Hydrogen Peroxide*, John Wiley & Sons, Inc., Hoboken, New Jersey, 2001.
23 G. Käbisch and H. Wittmann, *US Pat.* US 3 488 150, 1970.
24 G. Goor, J. Glennberg and S. Jacobi, *Ullmann's Encyclopedia of Industrial Chemistry: Hydrogen Peroxide*, Wiley-VCH, Weinheim, Germany, 2012.
25 C. Samanta, *Appl. Catal., A*, 2008, **350**, 133.
26 V. Russo, R. Tesser, E. Santacesaria and M. Di Serio, *Ind. Eng. Chem. Res.*, 2013, **52**, 1168.
27 K. Otsuka and I. Yamanaka, *Electrochim. Acta*, 1990, **35**, 319.
28 Z. Qiang, J.-H. Chang and C.-P. Huang, *Water Res.*, 2002, **36**, 85.
29 A. Verdaguer-Casadevall, D. Deiana, M. Karamad, S. Siahrostami, P. Malacrida, T. W. Hansen, J. Rossmeisl, I. Chorkendorff and I. E. L. Stephens, *Nano Lett.*, 2014, **14**, 1603.
30 S. Siahrostami, A. Verdaguer-Casadevall, M. Karamad, D. Deiana, P. Malacrida, B. Wickman, M. Escudero-Escribano, E. A. Paoli, R. Frydendal, T. W. Hansen, I. Chorkendorff, I. E. L. Stephens and J. Rossmeisl, *Nat. Mater.*, 2013, **12**, 1137.
31 I. Yamanaka, T. Onisawa, T. Hashimoto and T. Murayama, *ChemSusChem*, 2011, **4**, 494.
32 J. S. Jirkovský, I. Panas, E. Ahlberg, M. Halasa, S. Romani and D. J. Schiffrin, *J. Am. Chem. Soc.*, 2011, **133**, 19432.
33 H. Goto, Y. Hanada, T. Ohno and M. Matsumura, *J. Catal.*, 2004, **225**, 223.
34 C. Korman, D. W. Bahnemann and M. R. Hoffmann, *Environ. Sci. Technol.*, 1988, **22**, 798.
35 K. Morinaga, *Bull. Chem. Soc. Jpn.*, 1962, **35**, 345.
36 D. Bianchi, R. Bortolo, R. D'Aloisio and M. Ricci, *Angew. Chem., Int. Ed.*, 1999, **38**, 706.
37 J. García-Serna, T. Moreno, P. Biasi, M. J. Cocero, J.-P. Mikkola and T. O. Salmi, *Green Chem.*, 2014, **16**, 2320.
38 U.S. Energy Information Adminitration Annual Energy Outlook 2016 Early Release: Annotated Summary of Two Cases, http://www.eia.gov/forecasts/aeo/er/pdf/0383er(2016).pdf, (accessed July 2016).
39 J. N. Gerard, *Chem. Eng. News*, 2016, **94**, 26.
40 Q. Liu, J. C. Bauer, R. E. Schaak and J. H. Lunsford, *Appl. Catal., A*, 2008, **339**, 130.
41 P. Biasi, F. Menegazzo, F. Pinna, K. Eranen, P. Canu and T. O. Salmi, *Ind. Eng. Chem. Res.*, 2010, **49**, 10627.
42 R. Noyori, M. Aoki and K. Sato, *Chem. Commun.*, 2003, 1977.
43 K. Sato, M. Hyodo, M. Aoki, X.-Q. Zheng and R. Noyori, *Tetrahedron*, 2001, **57**, 2469.
44 M. Hudlicky, *Oxidations in Organic Chemistry*, American Chemical Society, Washington, DC, 1990.
45 O. Badr and D. Probert, *Appl. Energy*, 1993, **44**, 197.
46 V. N. Parmon, G. I. Panov, A. Uriarte and A. S. Noskov, *Catal. Today*, 2005, **100**, 115.
47 S. Dash, S. Patel and B. K. Mishra, *Tetrahedron*, 2009, **65**, 707.
48 M. Deborde and U. von Gunten, *Water Res.*, 2008, **42**, 13.
49 S. W. Krasner, *Philos. Trans.: Math., Phys. Eng. Sci.*, 2009, **367**, 4077.

50 B. Puértolas, A. K. Hill, T. García, B. Solsona and L. Torrente-Murciano, *Catal. Today*, 2015, **248**, 115.
51 M. M. Forde, R. D. Armstrong, C. Hammond, Q. He, R. L. Jenkins, S. A. Kondrat, N. Dimitratos, J. A. Lopez-Sanchez, S. H. Taylor, D. Willock, C. J. Kiely and G. J. Hutchings, *J. Am. Chem. Soc.*, 2013, **135**, 11087.
52 M. M. Forde, R. D. Armstrong, R. McVicker, P. P. Wells, N. Dimitratos, Q. He, L. Lu, R. L. Jenkins, C. Hammond, J. A. Lopez-Sanchez, C. J. Kiely and G. J. Hutchings, *Chem. Sci.*, 2014, **5**, 3603.
53 C. Hammond, R. L. Jenkins, N. Dimitratos, J. A. Lopez-Sanchez, M. H. ab Rahim, M. M. Forde, A. Thetford, D. M. Murphy, H. Hagen, E. E. Stangland, J. M. Moulijn, S. H. Taylor, D. J. Willock and G. J. Hutchings, *Chemistry*, 2012, **18**, 15735.
54 K. Sato, M. Aoki and R. Noyori, *Science*, 1998, **281**, 1646.
55 K. Sato, M. Aoki, M. Ogawa, T. Hashimoto and R. Noyori, *J. Org. Chem.*, 1996, **61**, 8310.
56 K. Sato, M. Aoki, M. Ogawa, T. Hashimoto, D. Panyella and R. Noyori, *Bull. Chem. Soc. Jpn.*, 1997, **70**, 905.
57 K. Sato, J. Takagi, M. Aoki and R. Noyori, *Tetrahedron Lett.*, 1998, **39**, 7549.
58 R. Armstrong, G. Hutchings and S. Taylor, *Catalysts*, 2016, **6**, 71.
59 R. D. Armstrong, S. J. Freakley, M. M. Forde, V. Peneau, R. L. Jenkins, S. H. Taylor, J. A. Moulijn, D. J. Morgan and G. J. Hutchings, *J. Catal.*, 2015, **330**, 84.
60 N. V. Beznis, A. N. C. van Laak, B. M. Weckhuysen and J. H. Bitter, *Microporous Mesoporous Mater.*, 2011, **138**, 176.
61 M. M. Forde, B. C. Grazia, R. Armstrong, R. L. Jenkins, M. H. A. Rahim, A. F. Carley, N. Dimitratos, J. A. Lopez-Sanchez, S. H. Taylor, N. B. McKeown and G. J. Hutchings, *J. Catal.*, 2012, **290**, 177.
62 M. G. Clerici and P. Ingallina, *J. Catal.*, 1992, **140**, 71.
63 E. G. Derouane, G. J. Hutchings, W. F. Mbafor and S. M. Roberts, *New J. Chem.*, 1998, **22**, 797.
64 K. Yamaguchi, K. Mori, T. Mizugaki, K. Ebitani and K. Kaneda, *J. Org. Chem.*, 2000, **65**, 6897.
65 I. W. C. E. Arends and R. A. Sheldon, *Appl. Catal., A*, 2001, **212**, 175.
66 M. G. Clerici, G. Bellussi and U. Romano, *J. Catal.*, 1991, **129**, 159.
67 M. Santonastaso, S. J. Freakley, P. J. Miedziak, G. L. Brett, J. K. Edwards and G. J. Hutchings, *Org. Process Res. Dev.*, 2014, **18**, 1455.
68 K. Sato, M. Aoki, J. Takagi and R. Noyori, *J. Am. Chem. Soc.*, 1997, **119**, 12386.
69 K. Sato, M. Hyodo, J. Takagi, M. Aoki and R. Noyori, *Tetrahedron Lett.*, 2000, **41**, 1439.
70 D. J. Robinson, L. Davies, N. McGuire, D. F. Lee, P. McMorn, J. Willock, G. W. Watson, P. C. Bulman Page, D. Bethell and G. J. Hutchings, *Phys. Chem. Chem. Phys.*, 2000, **2**, 1523.
71 N. R. Foster, *Appl. Catal.*, 1985, **19**, 1.
72 Y. H. Hu and E. Ruckenstein, *Adv. Catal.*, 2004, **48**, 297.
73 C. Hammond, N. Dimitratos, R. L. Jenkins, J. A. Lopez-Sanchez, S. A. Kondrat, M. H. ab Rahim, M. M. Forde, A. Thetford, S. H. Taylor, H. Hagen, E. E. Stangland, J. H. Kang, J. M. Moulijn, D. J. Willock and G. J. Hutchings, *ACS Catal.*, 201, **3**, 689.
74 E. Davy, *Philos. Trans. R. Soc.*, 1820, **110**, 108.
75 J. Brinksma, M. T. Rispens, R. Hage and B. L. Feringa, *Inorg. Chim. Acta*, 2002, **337**, 75.
76 B.-Z. Zhan and A. Thompson, *Tetrahedron*, 2004, **60**, 2917.

77 A. E. J. de Nooy, A. C. Besemer and H. Bekkum, *Carbohydr. Res.*, 1995, **269**, 89.
78 L. J. Davies, P. McMorn, D. Bethell, P. C. B. Page, F. King, F. E. Hancock and G. J. Hutchings, *J. Catal.*, 2001, **198**, 319.
79 A. Ghaemi, S. Rayati, S. Zakavi and N. Safari, *Appl. Catal., A*, 2009, **353**, 154.
80 J. M. Khurana, A. K. Panda, A. Ray and A. Gogia, *Org. Prep. Proced. Int.*, 1996, **28**, 234.
81 S. Patai and Z. Rappoport, *Synthesis of Sulfones, Sulfoxides and Cyclic Sulfides*, John Wiley and sons ltd., West Sussex, England, 1994.
82 G. V. Breton, J. D. Fields and P. J. Kropp, *Tetrahedron Lett.*, 1995, **36**, 3825.
83 B. M. Trost and R. Braslau, *J. Org. Chem.*, 1988, **53**, 532.
84 V. Chandra Srivastava, *RSC Adv.*, 2012, **2**, 759.
85 G. Grigoropoulou, J. H. Clark and J. A. Elings, *Green Chem.*, 2003, **5**, 1.
86 B. S. Lane and K. Burgess, *Chem. Rev.*, 2003, **103**, 2457.
87 N. Mizuno, K. Yamaguchi and K. Kamata, *Coord. Chem. Rev.*, 2005, **249**, 1944.
88 W. J. Choi and C. Y. Choi, *Biotechnol. Bioprocess Eng.*, 2005, **10**, 167.
89 H. Xie, Y. Fan, C. Zhou, Z. Du, E. Min, Z. Ge and X. Li, *Chem. Biochem. Eng. Q.*, 2008, **22**, 25.
90 A. T. Nijhuis, M. Makkee, J. A. Moulijn and B. M. Weckhuysen, *Ind. Eng. Chem. Res.*, 2006, **45**, 3447.
91 C. H. Hamblet and A. McAlevy, *US Pat.* US 2 439 513, 1948.
92 K. A. Jorgensen, *Chem. Rev.*, 1989, **89**, 431.
93 H. Nur, S. Ikeda and B. Ohtani, *J. Catal.*, 2001, **204**, 402.
94 M. E. Ali, M. M. Rahman, S. M. Sarkar and S. B. A. Hamid, *J. Nanomater.*, 2014, **2014**, 1.
95 R. Xu, W. Pang, J. Yu, Q. Huo and J. Chen, *Chemistry of Zeolites and Related Porous Materials*, John Wiley & Sons, Singapore, 2007.
96 J. C. van der Waal, M. S. Rigutto and H. van Bekkum, *Appl. Catal., A*, 1998, **167**, 331.
97 A. Corma, P. Esteve, A. Martinez and S. Valencia, *J. Catal.*, 1995, **152**, 18.
98 C. B. Dartt and M. E. Davis, *Appl. Catal., A*, 1996, **143**, 53.
99 T. G. Traylor, S. Tsuchiya, Y. S. Byun and C. Kim, *J. Am. Chem. Soc.*, 1993, **115**, 2775.
100 D. Mandelli, M. C. A. van Vliet, R. A. Sheldon and U. Schuchardt, *Appl. Catal., A*, 2001, **219**, 209.
101 A. J. Kauian, *US Pat.* US 3 122 569, 1964.
102 M. Clerici and P. Ingallina, *J. Catal.*, 1993, **140**, 71.
103 N. E. Thornburg, A. B. Thompson and J. M. Notestein, *ACS Catal.*, 2015, **5**, 5077.
104 F. Somma, P. Canton and G. Strukul, *J. Catal.*, 2005, **229**, 490.
105 G. J. Hutchings and J. C. Vedrine, in *Basic Principles in Applied Catalysis*, ed. M. Baerns, Springer-Verlag GmbH, Berlin, Germany, 2004, p. 215.
106 K. Gadamasetti, *Process Chemistry in the Pharmaceutical Industry*, CRC Press, Boca Raton, Florida, 1999, vol. 1.
107 R. J. Ouellette and J. D. Rawn, *Organic Chemistry: Structure, Mechanism, and Synthesis*, Elsevier, San Diego, California, 2014.
108 J. M. Notestein, E. Iglesia and A. Katz, *J. Am. Chem. Soc.*, 2004, **126**, 16478.
109 R. Neumann and M. Gara, *J. Am. Chem. Soc.*, 1994, **116**, 5509.
110 U. Kortz, A. Müller, J. van Slageren, J. Schnack, N. S. Dalal and M. Dressel, *Coord. Chem. Rev.*, 2009, **253**, 2315.
111 D. L. Long, R. Tsunashima and L. Cronin, *Angew. Chem., Int. Ed.*, 2010, **49**, 1736.
112 C. Venturello, R. D'Aloisio, J. Bart and M. Ricci, *J. Mol. Catal.*, 1985, **32**, 107.

113 K. Yamaguchi, C. Yoshida, S. Uchida and N. Mizuno, *J. Am. Chem. Soc.*, 2005, **127**, 530.
114 X. Zuwei, Z. Ning and L. Kunlan, *Science*, 2001, **292**, 1139.
115 J. Hartwig, *Organotransition Metal Chemistry: From Bonding to Catalysis*, University Science Books, 2009.
116 W. Dai, G. Li, B. Chen, L. Wang and S. Gao, *Org. Lett.*, 2015, **17**, 904.
117 Solvay, *Solvay to Expand Peroxides Production to Serve Growing North American Markets*, http://www.solvay.us/en/media/press_releases/2015-03-25-Solvay-Longview-Expansion.html, (accessed May 2016).
118 Evonik, http://h2o2.evonik.com/product/h2o2/en/about-hydrogen-peroxide/pages/default.aspx, (accessed May 2016).
119 Arkema, *Arkema to double production capacity at its Leuna hydrogen peroxide facility*, http://www.arkema.com/en/media/news/news-details/Arkema-to-double-production-capacity-at-its-Leuna-hydrogen-peroxide-facility, (accessed May 2016).
120 M. Johansson, E. Skúlason, G. Nielsen, S. Murphy, R. M. Nielsen and I. Chorkendorff, *Surf. Sci.*, 2010, **604**, 718.
121 Evonik, http://corporate.evonik.com/en/media/search/pages/news-details.aspx?newsid=45021, (accessed May 2016).
122 H. Riedl, G. Pfleiderer and H. W. Duiseberg, *US Pat.* US 2 215 883, 1940.
123 W. R. Holmes and C. W. Le Feuvre, *US Pat.* US 2 914 382, 1959.
124 L. H. Dawsey, C. K. Muehlhausser and R. R. Umhoefer, *US Pat.* US 2 537 655, 1951.
125 E. Suokas and R. Aksels, *US Pat.* US 5 114 701, 1992.
126 L. G. Vaughan, *US Pat.* US 4 046 868, 1977.
127 M. Nystrom and M. Siverstrom, *Eur Pat.* EP 0778085, 1997.
128 A. Biffis, R. Ricoveri, S. Campestrini, M. Kralik, K. Jerabek and B. Corain, *Chem. – Eur. J.*, 2002, **8**, 2962.
129 X. Chen, H. Hu, B. Liu, M. Qiao, K. Fan and H. He, *J. Catal.*, 2003, **220**, 254.
130 M. Kralik and A. Biffis, *J. Mol. Catal. A: Chem.*, 2001, **177**, 113.
131 B. Liu, M. Qiao, J. Wang and K. Fan, *Chem. Commun.*, 2002, 1236.
132 E. Santacesaria, M. Di Serio, A. Russo, U. Leone and R. Velotti, *Chem. Eng. Sci.*, 1999, **54**, 2799.
133 J. Kemnade and B. Maurer, *World Pat.* WO 1 986 006 710, 1986.
134 I. Turunen and E. Mustonen, *German Pat.* DE 40 297 841 999, 1991.
135 G. Goor and E. Staab, *US Pat.* US 20 050 063 896, 2005.
136 G. Goor, E. Staab and J. Glennberg, *US Pat.* US 7 238 335, 2007.
137 B. R. Henry, *US Pat.* US 3 043 658, 1962.
138 L. F. C. William, R. H. William and S. W. William, *US Pat.* US 2 914 382, 1959.
139 American Energy Indepdendence, *Hydrogen Peroxide*, http://www.americanenergyindependence.com/peroxide.aspx, (accessed May 2016).
140 Dow, *New BASF and Dow HPPO Plant in Antwerp Completes Start-Up*, http://www.dow.com/propyleneoxide/news/20090305a.htm, (accessed May 2016).
141 Dow, *BASF, Dow, Solvay partnership breaks new groun with innovative HPPO technology in Antwerp*, http://urethaneblog.typepad.com/my_weblog/2008/10/basf-dow-solvay-hppo-plant-in-antwerp.html, (accessed July 2016).
142 A. H. Tullo and P. L. Short, *Chem. Eng. News*, 2006, **84**, 22.
143 P. L. Short, *Chem. Eng. News*, 2009, **87**(11), 21.
144 S. K. Ritter, *Chem. Eng. News*, 2010, **88**(19), 12–17.
145 A. H. Tullo, *Chem. Eng. News*, 2005, **83**(44), 7.
146 J. Kemsley, *Chem. Eng. News*, 2008, **86**(34), 9.
147 D. W. Leyshon, R. J. Jones and R. N. Cochran, *US Pat.* US 5 254 326, 1993.
148 N. M. Wilson and D. W. Flaherty, *J. Am. Chem. Soc.*, 2016, **138**, 574.

149 N. Gemo, T. Salmi and P. Biasi, *React. Chem. Eng.*, 2016, **1**, 300.
150 P. Biasi, N. Gemo, J. R. H. Carucci, K. Eränen, P. Canu and T. O. Salmi, *Ind. Eng. Chem. Res.*, 2012, **51**, 8903.
151 P. Landon, P. J. Collier, A. F. Carley, D. Chadwick, A. J. Papworth, A. Burrows, C. J. Kiely and G. J. Hutchings, *Phys. Chem. Chem. Phys.*, 2003, **5**, 1917.
152 D. Hâncu and E. J. Beckman, *Green Chem.*, 2001, **3**, 80.
153 V. R. Choudhary and C. Samanta, *J. Catal.*, 2006, **238**, 28.
154 S. Chinta and J. H. Lunsford, *J. Catal.*, 2004, **225**, 249.
155 S. J. Freakley, M. Piccinini, J. K. Edwards, E. N. Ntainjua, J. A. Moulijin and G. J. Hutchings, *ACS Catal.*, 201, **3**, 487.
156 Y. Voloshin and A. Lawal, *Appl. Catal., A*, 2009, **353**, 9.
157 V. Paunovic, V. Ordomsky, M. F. N. D'Angelo, J. C. Schouten and T. A. Nijhuis, *J. Catal.*, 2014, **309**, 325.
158 T. Inoue, M. A. Schmidt and K. F. Jensen, *Ind. Eng. Chem. Res.*, 2007, **46**, 1153.
159 T. Inoue, K. Ohtaki, J. Adachi, M. Lu and S. Murakami, *Catal. Today*, 2015, **248**, 169.
160 L. Shi, A. Goldbach, G. Zeng and H. Xu, *Catal. Today*, 2010, **156**, 118.
161 S. Abate, G. Centi, S. Melada, S. Perathoner, F. Pinna and G. Strukul, *Catal. Today*, 2005, **104**, 323.
162 V. R. Choudhary, A. G. Gaikwad and S. D. Sansare, *Angew. Chem., Int. Ed.*, 2001, **40**, 1776.
163 L. Wang, S. Bao and J. Yi, *Appl. Catal., B*, 2008, **79**, 157.
164 X. Wang and C. K. Law, *J. Chem. Phys.*, 2013, **138**, 134305.
165 J. K. Edwards, A. F. Carley, A. A. Herzig, C. J. Kiely and G. J. Hutchings, *Faraday Discuss.*, 2008, **138**, 225.
166 P. Biasi, F. Menegazzo, F. Pinna, K. Eränen, T. O. Salmi and P. Canu, *Chem. Eng. J.*, 2011, **176–177**, 172.
167 L. Ouyang, G. Da, P. Tian, T. Chen, G. Liang, J. Xu and Y.-F. Han, *J. Catal.*, 2014, **311**, 129.
168 J. K. Edwards, B. Solsona, N. E. Ntainjua, A. F. Carley, A. A. Herzig, C. J. Kiely and G. J. Hutchings, *Science*, 2009, **323**, 1037.
169 S. J. Freakley, Q. He, J. H. Harrhy, L. Lu, D. A. Crole, D. J. Morgan, E. N. Ntainjua, J. . K. Edwards, A. F. Carley, A. Y. Borisevich, C. J. Kiely and G. J. Hutchings, *Science*, 2016, **351**, 965.
170 H. Henkel and W. H. C. Weber, *US Pat.* 1 108 752, 1914.
171 H.-J. Riedl and G. Pfiederer, *US Pat.* 2 158 525, 1939.
172 D. P. Dissanayake and J. H. Lunsford, *J. Catal.*, 2003, **214**, 113.
173 Y. Izumi, H. Miyazaki and S.-I. Kawahara, *US Pat.* 4 009 252, 1977.
174 H.-N. Sun, J. J. Leonard and H. Shalit, *US Pat.* 4 393 038, 1983.
175 L. W. Gosser and J. T. Schwartz, *US Pat.* 4 772 458, 1988.
176 J. V. Weynbergh, J.-P. Schoebrechts and J.-C. Colery, *US Pat.* 5 447 706, 1995.
177 Business Roundup, *Chem. Eng. News*, 2015, **93**, 28.
178 M. Taramasso, G. Perego and B. Notari, *US Pat.* 4 410 501, 1983.
179 S. B. Kumar, S. P. Mirajkar, G. C. G. Pais, P. Kumar and R. Kumar, *J. Catal.*, 1995, **156**, 163.
180 A. Thangaraj, R. Kumar and P. Ratnasamy, *J. Catal.*, 1991, **131**, 294.
181 P. Bassler, H.-G. Göbbel and M. Weidenbach, *Chem. Eng. Trans.*, 2010, **21**, 571.
182 P. Landon, P. J. Collier, A. J. Papworth, C. J. Kiely and G. J. Hutchings, *Chem. Commun.*, 2002, 2058.
183 E. Ntainjua, J. K. Edwards, A. F. Carley, J. A. Lopez-Sanchez, J. A. Moulijn, A. A. Herzing, C. J. Kiely and G. J. Hutchings, *Green Chem.*, 2008, **10**, 1162.

184 G. Blanco-Brieva, M. P. F. Escrig, J. M. Campos-Martin and J. L. G. Fierro, *Green Chem.*, 2010, **12**, 1163.
185 S. Park, J. C. Jung, J. G. Seo, T. J. Kim, Y.-M. Chung, S.-H. Oh and I. K. Song, *Catal. Lett.*, 2009, **130**, 604.
186 A. C. Alba-Rubio, A. Plauck, E. E. Strangland, M. Mavrikakis and J. A. Dumesic, *Catal. Lett.*, 2015, **145**, 2057.
187 M. O. Nutt, K. N. Heck, P. Alvarez and M. S. Wong, *Appl. Catal., B*, 2006, **69**, 115.
188 S. Sterchele, P. Biasi, P. Centomo, P. Canton, S. Campestrini, T. Salmi and M. Zecca, *Appl. Catal., A*, 2013, **468**, 160.
189 Y. Voloshin, R. Halder and A. Lawal, *Catal. Today*, 2007, **125**, 40.
190 C. A. Farberow, A. Godinez-Garcia, G. Peng, J. F. Perez-Robles, O. Solorza-Feria and M. Mavrikakis, *ACS Catal.*, 2013, **3**, 1622.
191 A. Plauck, E. E. Strangland, J. A. Dumesic and M. Mavrikakis, *Proc. Natl. Acad. Sci.*, 2016, **113**, E1973.
192 M. Piccinini, E. Ntainjua, J. K. Edwards, A. F. Carley, J. A. Moulijn and G. J. Hutchings, *Phys. Chem. Chem. Phys.*, 2010, **12**, 2488.
193 D. C. Ford, A. U. Nilekar, Y. Xu and M. Mavrikakis, *Surf. Sci.*, 2010, **604**, 1565.
194 R. Todorovic and R. J. Meyer, *Catal. Today*, 2011, **160**, 242.
195 Q. Liu and J. H. Lunsford, *Appl. Catal., A*, 2006, **314**, 94.
196 *NASA Safety Standard for Hydrogen and Hydrogen Systems: Guidelines for Hydrogen System Design, Materials Selection, Operations, Storage, and Transportation*, https://www.hq.nasa.gov/office/codeq/doctree/canceled/871916.pdf, (accessed July 2016).
197 Q. Liu and J. H. Lunsford, *J. Catal.*, 2006, **239**, 237.
198 Y.-F. Han and J. H. Lunsford, *J. Catal.*, 2005, **230**, 313.
199 L. Ouyang, P.-F. Tian, G.-J. Da, H.-C. Xu, C. Ao, T.-Y. Chen, R. Si, J. Xu and Y.-F. Han, *J. Catal.*, 2015, **321**, 70.
200 P. J. Brandhuber and G. Korshin, *Methods for the Detection of Residual Concentrations of Hydrogen Peroxide in Advanced Oxidation Processes*, Water Reuse Foundation, Alexandria, Virginia, 2009.
201 A. N. Baga, G. R. A. Johnson, N. B. Nazhat and R. A. Saadalla-Nazhat, *Anal. Chim. Acta*, 1988, **204**, 349.
202 E. L. Cussler, *Diffusion Mass Transfer in Fluid Systems*, Cambridge University Press, New York, New York, 2nd edn, 2007.
203 R. J. Madon and M. Boudart, *Ind. Eng. Chem. Fundam.*, 1982, **21**, 438.
204 K. F. Jensen, *AIChE J.*, 1999, **45**, 2051.
205 B. Zhou and L.-K. Lee, *US Pat.* US 6 919 065, 2005.
206 P. P. Olivera, E. M. Patrito and H. Sellers, *Surf. Sci.*, 1994, **313**, 25.
207 R. B. Rankin and J. Greeley, *ACS Catal.*, 2012, **2**, 2664.
208 Y. Voloshin and A. Lawal, *Chem. Eng. Sci.*, 2010, **65**, 1028.
209 T. A. Pospelova, N. I. Kobozev and E. N. Eremin, *Russ. J. Phys. Chem.*, 1961, **35**, 143.
210 N. Gemo, S. Sterchele, P. Biasi, P. Centomo, P. Canu, M. Zecca, A. Shchukarev, K. Kordàs, T. O. Salmi and J.-P. Mikkola, *Catal. Sci. Technol.*, 201, **5**, 3543.
211 Q. Liu, K. K. Gath, J. C. Bauer, R. E. Schaak and J. H. Lunsford, *Catal. Lett.*, 2009, **132**, 342.
212 L. C. Grabow, B. Hvolbaek, H. Falsig and J. K. Norskov, *Top. Catal.*, 2012, **55**, 336.
213 H. C. Ham, G. S. Hwang, J. Han, S. W. Nam and T. H. Lim, *J. Phys. Chem. C*, 2010, **113**, 12943.

214 T. Deguchi and M. Iwamoto, *J. Phys. Chem. C*, 2013, **117**, 18540.
215 F. A. Lewis, *Platinum Met. Rev.*, 1960, **4**, 132.
216 H. C. Ham, J. A. Stephens, G. S. Hwang, J. Han, S. W. Nam and T. H. Lim, *Catal. Today*, 2011, **165**, 138.
217 S. S. Stahl, J. L. Thorman, R. C. Nelson and M. A. Kozee, *J. Am. Chem. Soc.*, 2001, **123**, 7188.
218 J. A. Keith and T. Jacob, *Angew. Chem., Int. Ed.*, 2010, **49**, 9521.
219 J. A. Keith and T. Jacob, *Theory and Experiment in Electrocatalysis*, Springer-Verlag, New York, New York, 2010, vol. 50.
220 V. R. Choudhary, C. Samanta and P. Jana, *Appl. Catal., A*, 2007, **332**, 70.
221 V. V. Krishnan, A. G. Dokoutchaev and M. E. Thompson, *J. Catal.*, 2000, **196**, 366.
222 N. E. Ntainjua, M. Piccinini, J. C. Pritchard, J. K. Edwards, A. F. Carley, J. A. Moulijn and G. J. Hutchings, *ChemSusChem*, 2009, **2**, 575.
223 J. K. Edwards and G. J. Hutchings, *Angew. Chem., Int. Ed.*, 2008, **47**, 9192.
224 Y.-F. Han, Z. Zhong, K. Ramesh, F. Chen, L. Chen, T. White, Q. Tay, S. N. Yaakub and Z. Wang, *J. Phys. Chem. C*, 2007, **111**, 8410.
225 F. Menegazzo, M. Manzoli, M. Signoretto, F. Pinna and G. Strukul, *Catal. Today*, 2015, **247**, 18.
226 J. K. Edwards, A. Thomas, A. F. Carley, A. A. Herzing, C. J. Kiely and G. J. Hutchings, *Green Chem.*, 2008, **10**, 388.
227 M. Hohenegger, E. Bechtold and R. Schennach, *Surf. Sci.*, 1998, **412/413**, 184.
228 I. Chorkendorff and J. W. Niemantsverdriet, *Concepts of Modern Catalysis and Kinetics*, Wiley-VCH, Weinheim, Germany, 2nd edn, 2007.
229 W. Erley, *Surf. Sci.*, 1980, **94**, 281.
230 W. Erley, *Surf. Sci.*, 1982, **114**, 47.
231 T. Fukushima, M.-B. Song and M. Ito, *Surf. Sci.*, 2000, **464**, 193.
232 V. R. Choudhary, Y. V. Ingole, C. Samanta and P. Jana, *Ind. Eng. Chem. Res.*, 2007, **46**, 8566.
233 V. R. Choudhary, C. Samanta and A. G. Gaikwad, *Chem. Commun.*, 2004, 2054.
234 F. Menegazzo, M. Signoretto, G. Frison, F. Pinna, G. Strukul, M. Manzoli and F. Boccuzzi, *J. Catal.*, 2012, **290**, 143.
235 S. Kim, D.-W. Lee, K.-Y. Lee and E. A. Cho, *Catal. Lett.*, 2014, **144**, 905.
236 R. van Hardeveld and F. Hartog, *Surf. Sci.*, 1969, **15**, 189.
237 F. Liu, D. Wechsler and P. Zhang, *Chem. Phys. Lett.*, 2008, **461**, 254.
238 T.-U. Nahm, R. Jung, J.-Y. Kim, W.-G. Park, S.-J. Oh, J.-H. Park, J. W. Allen, S.-M. Chung, Y. S. Lee and C. N. Whang, *Phys. Rev. B: Condens. Matter Mater. Phys.*, 1998, **58**, 9817.
239 P. A. P. Nascente, S. G. C. de Castro, R. Landers and G. G. Kleiman, *Phys. Rev. B: Condens. Matter Mater. Phys.*, 1991, **43**, 4659.
240 J. Xu, T. White, P. Li, C. He, J. Yu, W. Yuan and Y.-F. Han, *J. Am. Chem. Soc.*, 2010, **132**, 10398.
241 S. Marx and A. Baiker, *J. Phys. Chem. C*, 2009, **113**, 6191.
242 A. M. Venezia, V. L. Parola, G. Deganello, B. Pawelec and J. L. G. Fierro, *J. Catal.*, 2003, **215**, 317.
243 L. D. Lloyd, R. L. Johnston, S. Salhi and N. T. Wilson, *J. Mater. Chem.*, 2004, **14**, 1691.
244 I. E. L. Stephens, A. S. Bondarenko, U. Grønjberg, J. Rossmeisl and I. Chorkendorff, *Energy Environ. Sci.*, 2012, **5**, 6744.
245 S. J. Tauster, *Acc. Chem. Res.*, 1987, **20**, 389.

246 S. Galvagno, J. Schwank, G. Parravano, F. Garbassi, A. Marzi and G. R. Tauszik, *J. Catal.*, 1981, **69**, 283.
247 R. Burch and P. R. Ellis, *Appl. Catal., B*, 2003, **42**, 203.
248 V. Paunovic, V. V. Ordomsky, V. L. Sushkevich, J. C. Schouten and T. A. Nijhuis, *ChemCatChem*, 2015, **7**, 1161.
249 A. Pashkova and R. Dittmeyer, *Catal. Today*, 2015, **248**, 128.
250 K.-Y. Yeh, S. A. Wasileski and M. J. Janik, *Phys. Chem. Chem. Phys.*, 2009, **11**, 10108.
251 M. J. Janik, C. D. Taylor and M. Neurock, *J. Electrochem. Soc.*, 2009, **156**, B126.
252 E. Marco Aieta and J. D. Berg, *J. – Am. Water Works Assoc.*, 1986, **78**, 62.
253 Z. Wang, R. Yuan, Y. Guo, L. Xu and J. Liu, *J. Hazard. Mater.*, 2011, **190**, 1083.
254 D. W. Goheen and C. F. J. Bennett, *J. Org. Chem.*, 1961, **26**, 1331.
255 K. E. Pfitzner and J. G. Moffatt, *J. Am. Chem. Soc.*, 1963, **85**, 3028.
256 N. Rahimi and R. Karimzadeh, *Appl. Catal., A*, 2011, **398**, 1.
257 S. R. Golisz, T. B. Gunnoe, W. A. Goddard, J. T. Groves and R. A. Periana, *Catal. Lett.*, 2010, **141**, 213.
258 G. W. Huber, S. Iborra and A. Coma, *Chem. Rev.*, 2006, **106**, 4044.
259 N. R. Hunter, H. D. Gesser, L. A. Morton, P. S. Yarlagadda and D. P. C. Fung, *Appl. Catal.*, 1990, **57**, 45.
260 K. Narsimhan, K. Iyoki, K. Dinh and Y. Román-Leshkov, *ACS Cent. Sci.*, 2016, **2**, 424.
261 K. Narsimhan, V. K. Michaelis, G. Mathies, W. R. Gunther, R. G. Griffin and Y. Roman-Leshkov, *J. Am. Chem. Soc.*, 2015, **137**, 1825.
262 C. J. Jones, D. Taube, V. R. Ziatdinov, R. A. Periana, R. J. Nielsen, J. Oxgaard and W. A. Goddard 3rd, *Angew. Chem., Int. Ed.*, 2004, **43**, 4626.
263 M. F. Fellah and I. Onal, *J. Phys. Chem. C*, 2010, **114**, 3042.
264 H. F. Liu, R. S. Liu, K. Y. Liew, R. E. Johnson and J. H. Lunsford, *J. Am. Chem. Soc.*, 1984, **106**, 4117.
265 J. A. Labinger, *J. Mol. Catal. A: Chem.*, 2004, **220**, 27.
266 J. A. Labinger and J. E. Bercaw, *Nature*, 2002, **417**, 507.
267 Columbia, http://www.ehs.columbia.edu/NitrousOxideHealthHazards.pdf, (accessed July 2016).
268 EPA, https://www3.epa.gov/climatechange/ghgemissions/gases/n2o.html, (accessed July 2016).
269 J. Xu, R. D. Armstrong, G. Shaw, N. F. Dummer, S. J. Freakley, S. H. Taylor and G. J. Hutchings, *Catal. Today*, 2016, **270**, 93.
270 G. Centi, S. Perathoner, F. Pino, R. Arrigo, G. Giordano, A. Katovic and V. Pedulà, *Catal. Today*, 2005, **110**, 211.
271 P. Vanelderen, B. E. Snyder, M. L. Tsai, R. G. Hadt, J. Vancauwenbergh, O. Coussens, R. A. Schoonheydt, B. F. Sels and E. I. Solomon, *J. Am. Chem. Soc.*, 2015, **137**, 6383.
272 J. S. Woertink, P. J. Smeets, M. H. Groothaert, M. A. Vance, B. F. Sels, R. A. Schoonheydt and E. I. Solomon, *Proc. Natl. Acad. Sci.*, 2009, **106**, 18908.
273 S. Grundner, W. Luo, M. Sanchez-Sanchez and J. A. Lercher, *Chem. Commun.*, 2016, **52**, 2553.
274 S. Grundner, M. A. Markovits, G. Li, M. Tromp, E. A. Pidko, E. J. Hensen, A. Jentys, M. Sanchez-Sanchez and J. A. Lercher, *Nat. Commun.*, 2015, **6**, 7546.
275 G. Bellussi and C. Perego, *Catal. Sci. Technol.*, 2000, **4**, 4.

276 C.-Y. Cheng, K.-J. Lin, M. R. Prasad, S.-J. Fu, S.-Y. Chang, S.-G. Shyu, H.-S. Sheu, C.-. H. Chen, C.-H. Chuang and M.-T. Lin, *Catal. Commun.*, 2007, **8**, 1060.
277 W. Zhu, H. Li, X. He, Q. Zhang, H. Shu and Y. Yan, *Catal. Commun.*, 2008, **9**, 551.
278 H. Wei, H. Li, Y. Liu, P. Jin, X. Wang and B. Li, *ACS Appl. Mater. Interfaces*, 2012, **4**, 4106.
279 M. Vafaeezadeh, M. M. Hashemi and M. Shakourian-Fard, *Catal. Commun.*, 2012, **26**, 54.
280 K. Sato, M. Aoki, J. Takagi, K. Zimmermann and R. Noyori, *Bull. Chem. Soc. Jpn.*, 1999, **72**, 2287.
281 T. Mallat and A. Baiker, *Chem. Rev.*, 2004, **104**, 3037.
282 C. Djerassi and R. R. Engle, *J. Am. Chem. Soc.*, 1953, **75**, 3838.
283 S. E. Jacobson, D. A. Muccigrosso and F. Mares, *J. Org. Chem.*, 1979, **44**, 921.
284 A. O. Chong and K. B. Sharpless, *J. Org. Chem.*, 1976, **42**, 1587.
285 A. F. Ghiron and R. C. Thompson, *Inorg. Chem.*, 1988, **27**, 4766.
286 J. D. Lydon, L. M. Schwane and R. C. Thompson, *Inorg. Chem.*, 1987, **26**, 2606.
287 E. N. Prilezhaeva, *Russ. Chem. Rev.*, 2000, **69**, 367.
288 A. Mckillip and J. A. Tarbin, *Tetrahedron Lett.*, 1983, **24**, 1505.
289 K. Kim, O. G. Tsay, D. A. Atwood and D. G. Churchill, *Chem. Rev.*, 2011, **111**, 5345.
290 Y. Yang, J. A. Baker and J. R. Ward, *Chem. Rev.*, 1992, **92**, 1729.
291 G. W. Wagner, L. R. Procell, Y. Yang and C. A. Bunton, *Langmuir*, 2001, **17**, 4809.
292 F. Carniato, C. Bisio, R. Psaro, L. Marchese and M. Guidotti, *Angew. Chem., Int. Ed.*, 2014, **53**, 10095.
293 E. Lorençon, D. C. B. Alves, K. Krambrock, E. S. Ávila, R. R. Resende, A. S. Ferlauto and R. M. Lago, *Fuel*, 2014, **132**, 53.
294 M. A. Cortes-Jácome, M. Morales, C. Angeles Chavez, L. F. Ramirez-Verduzco, E. Lopez-Salinas and J. A. Toledo-Antonio, *Chem. Mater.*, 2007, **19**, 6605.
295 J. Zhuang, Z. Yan, X. Liu, X. Liu, X. Han, X. Bao and U. Mueller, *Catal. Lett.*, 2002, **83**, 87.
296 J. Aubry and S. Bouttemy, *J. Am. Chem. Soc.*, 1997, **119**, 5286.
297 I. Schmidt, A. Krogh, K. Wienberg, A. Carlsson, M. Brorson and C. Jacobsen, *Chem. Commun.*, 2000, 2157.
298 A. Wroblewska, A. Fajdek, E. Milchert and B. Grzmil, *Pol. J. Chem.*, 2010, **1**, 29.
299 E. L. First, C. E. Founaris, J. Wei and C. E. Floudas, *Phys. Chem. Chem. Phys.*, 2011, **13**, 17339.
300 B. Notari, *Catal. Today*, 1993, **18**, 163.
301 X. Wang, X. Guo and G. Li, *Catal. Today*, 2002, **74**, 65.
302 E. V. Anslyn and D. A. Dougherty, *Modern Physical Organic Chemistry*, University Science, 2nd edn, 2005.
303 W. Lin and H. Frei, *J. Am. Chem. Soc.*, 2002, **124**, 9292.
304 S. Bordiga, D. Alessandro, F. Bonino, G. Ricchiardi, C. Lamberti and A. Zecchina, *Angew. Chem., Int. Ed.*, 2002, **41**, 4734.
305 J. J. Bravo-Suarez, J. Lu, C. G. Dallos, T. Fujitani and S. T. Oyama, *J. Phys. Chem. C*, 2007, **111**, 17427.
306 S. Bordiga, A. Damin, F. Bonino, G. Ricchiardi, A. Zecchina, R. Tagliapietra and C. Lamberti, *Phys. Chem. Chem. Phys.*, 2003, **5**, 4390.

307 F. Bonino, A. Damin, G. Ricchiardi, M. Ricci, G. Spano, R. D'Aloisio, A. Zecchina, C. Lamberti, C. Prestipino and S. Bordiga, *J. Phys. Chem. B*, 2004, **108**, 3573.
308 S. Krifnen, P. Sanchez, B. T. F. Jakobs and J. H. C. van Hooff, *Microporous Mesoporous Mater.*, 1999, **31**, 163.
309 B. Tang, W. Dai, X. Sun, N. Guan, L. Li and M. Hunger, *Green Chem.*, 2014, **16**, 2281.
310 J. Li, C. Zhou, H. Xie, Z. Ge, L. Yuan and X. Li, *J. Nat. Gas Chem.*, 2006, **15**, 164.
311 O. Kholdeeva, A. Derevyankin, A. Shmakov, N. Trukhan, A. Paukshtis, A. Tuel and V. Romannikov, *J. Mol. Catal. A: Chem.*, 2000, **158**, 417.
312 O. Kholdeeva, M. Mel'gunov, A. Shmakov, N. Trukhan, V. Kriventsov, V. Zaikovskii, M. Malyshev and V. Romannikov, *Catal. Today*, 2004, **91–92**, 205.
313 A. Corma, A. Camblor, P. Esteve, A. Martinez and J. Perez-Pariente, *J. Catal.*, 1994, **145**, 151.
314 P. Wu, T. Tatsumi, T. Komatsu and T. Yashima, *J. Catal.*, 2001, **202**, 245.
315 F. Tielens, T. Shishido and S. Dzwigaj, *J. Phys. Chem. C*, 2010, **114**.
316 S. Dzwigaj, M. Peltre, P. Massiani, A. Davidson, M. Che, T. Sen and S. Sivasankar, *Chem. Commun.*, 1998, 87.
317 C. Hammond, S. Conrad and I. Hermans, *Angew. Chem., Int. Ed.*, 2012, **51**, 11736.
318 E. Nikolla, Y. Román-Leshkov, M. Moliner and M. E. Davis, *ACS Catal.*, 2011, **1**, 408.
319 P. Wolf, M. Valla, A. J. Rossini, A. Comas-Vives, F. Nunez-Zarur, B. Malaman, A. Lesage, L. Emsley, C. Coperet and I. Hermans, *Angew. Chem., Int. Ed.*, 2014, **53**, 10179.
320 V. L. Sushkevich, D. Palagin and I. I. Ivanova, *ACS Catal.*, 2015, **5**, 4833.
321 P. Wolf, C. Hammond, S. Conrad and I. Hermans, *Dalton Trans.*, 2014, **43**, 4514.
322 Y. Wang, J. D. Lewis and Y. Román-Leshkov, *ACS Catal.*, 2016, **6**, 2739.
323 G. J. Hutchings, C. Langham, P. Piaggio, S. Taylor, P. McMorn, D. J. Willock, D. Bethell, P. C. Bulman Page, C. Sly, F. Hancock and F. King, *Stud. Surf. Sci. Catal.*, 2000, **130**, 521.
324 Q. Zhang, Y. Wang, S. Itsuki, T. Shishido and K. Takehira, *Chem. Lett.*, 2001, 946.
325 M. Nielsen, R. Y. Brogaard, H. Falsig, P. Beato, O. Swang and S. Svelle, *ACS Catal.*, 201, **5**, 7131.
326 B. M. Chandra Shekara, B. S. Jai Prakash and Y. S. Bhat, *ACS Catal.*, 2011, **1**, 193.
327 Y. Wang, Q. Zhang, T. Shishido and K. Takehira, *J. Catal.*, 2002, **209**, 186.
328 N. Morlanes and J. M. Notestein, *Appl. Catal., A*, 2010, **387**, 45.
329 D. T. Bregante, P. Priyadarshini and D. W. Flaherty, *J. Catal*, 2016, in review.
330 N. M. Gresley, W. Griffith, A. C. Laemmel, H. Nogueira and B. C. Parkin, *J. Mol. Catal. A: Chem.*, 1997, **117**, 185.
331 W. Griffith, B. C. Parkin, A. J. P. White and D. J. Williams, *J. Chem. Soc., Dalton Trans.*, 1995, 3131.
332 Y. Ishii, K. Yamawaki, T. Ura, H. Yamada, T. Yoshida and M. Ogawa, *J. Org. Chem.*, 1988, **53**, 3587.
333 K. Sato, M. Aoki, M. Ogawa, T. Hashimoto and R. Noyori, *J. Org. Chem.*, 1996, **61**, 8310.
334 C. Aubry, G. Chottard, N. Platzer, J. M. Bregeault, R. Thouvenot, F. Chauveau, C. Huet and H. Ledon, *Inorg. Chem. Commun.*, 1991, **30**, 4409.

335 A. L. Villa De P, B. Sels, D. E. De Vos and P. A. Jacobs, *J. Org. Chem.*, 1999, **64**, 7267.
336 A. L. Villa De P, F. Taborda and C. Montes de Correa, *J. Mol. Catal. A: Chem.*, 2002, **185**, 269.
337 F. Jalilian, B. Yadollahi, M. Riahi Farsani, S. Tangestaninejad, H. Amiri Rudbari and R. Habibi, *RSC Adv.*, 2015, **5**, 70424.
338 I. C. M. S. Santos, M. M. Q. Simões, M. M. M. S. Pereira, R. R. L. Martins, M. G. P. M. S. Neves, J. A. S. Cavaleiro and A. M. V. Cavaleiro, *J. Mol. Catal. A: Chem.*, 2003, **195**, 253.
339 E. Ishikawa and T. Yamase, *J. Mol. Catal. A: Chem.*, 1999, **142**, 61.
340 S. R. Amanchi, A. M. Khenkin, Y. Diskin-Posner and R. Neumann, *ACS Catal.*, 2015, **5**, 3336.
341 C. Nozaki, I. Kiyoto, Y. Minai, M. Misono and N. Mizuno, *Inorg. Chem.*, 1999, **38**, 5724.
342 N. Mizuno, C. Nozaki, I. Kiyoto and M. Misono, *J. Am. Chem. Soc.*, 1998, **120**, 9267.
343 C. Chen, H. Yuan, H. Wang, Y. Yao, W. Ma, J. Chen and Z. Hou, *ACS Catal.*, 2016, **6**, 3354.
344 R. Ben-Daniel, A. M. Khenkin and R. Neumann, *Chem. – Eur. J.*, 2000, **6**, 3722.
345 V. Mirkhani, M. Moghadam, S. Tangestaninejad, I. Mohammadpoor-Baltork, E. Shams and N. Rasouli, *Appl. Catal., A*, 2008, **334**, 106.
346 E. Tebandeke, H. Ssekaalo and O. F. Wendt, *Afr. J. Pure Appl. Chem.*, 2013, **7**, 50.
347 A. Wroblewska, *Molecules*, 2014, **19**, 19907.
348 P. Wu, T. Tatsumi, T. Komatsu and T. Yashima, *Chem. Mater.*, 2002, **14**, 1657.
349 S. K. Thorimbert and W. F. Maier, *J. Catal.*, 1996, **163**, 476.
350 N. Moussa, A. Ghorbel and P. Grange, *J. Sol-Gel Sci. Technol.*, 2005, **33**, 127.
351 C. Tiozzo, C. Bisio, F. Carniato, L. Marchese, A. Gallo, N. Ravasio, R. Psaro and M. Guidotti, *Eur. J. Lipid Sci. Technol.*, 2013, **115**, 86.
352 I. D. Ivanchikova, N. V. Maksimchuk, I. Y. Skobelev, V. V. Kaichev and O. A. Kholdeeva, *J. Catal.*, 2015, **332**, 138.
353 F. Somma, A. Puppinato and G. Strukul, *Appl. Catal., A*, 2006, **309**, 115.
354 P. Célestin Bakala, E. Briot, L. Salles and J.-M. Brégeault, *Appl. Catal., A*, 2006, **300**, 91.
355 D. A. Ruddy and T. D. Tilley, *Chem. Commun.*, 2007, 3350.
356 D. A. Ruddy and T. D. Tilley, *J. Am. Chem. Soc.*, 2008, **130**, 11088.
357 N. Morlanés and J. M. Notestein, *J. Catal.*, 2010, **275**, 191.
358 J. Tang, L. Wang, G. Liu, Y. Liu, Y. Hou, W. Zhang, M. Jia and W. R. Thiel, *J. Mol. Catal. A: Chem.*, 2009, **313**, 31.
359 R. F. de Farias, U. Arnold, L. Martínez, U. Schuchardt, M. J. D. M. Jannini and C. Airoldi, *J. Phys. Chem. Solids*, 2003, **64**, 2385.
360 Q. H. Xia, H. Q. Ge, C. P. Ye, Z. M. Liu and K. X. Su, *Chem. Rev.*, 2005, **105**, 1603.
361 W. A. Herrmann, R. W. Fischer, W. Scherer and M. U. Rauch, *Angew. Chem., Int. Ed.*, 1993, **32**, 1157.
362 W. A. Herrmann, R. W. Fischer and D. W. Marz, *Angew. Chem., Int. Ed.*, 1991, **30**, 1638.
363 B. R. Goldsmith, T. Hwang, S. Seritan, B. Peters and S. L. Scott, *J. Am. Chem. Soc.*, 2015, **137**, 9604.
364 J. Rudolph, K. L. Reddy, J. P. Chang and K. B. Sharpless, *J. Am. Chem. Soc.*, 1997, **119**, 6189.

365 H. Adolfsson, C. Coperet, J. P. Chiang and A. K. Yudin, *J. Org. Chem.*, 2000, **65**, 8651.
366 S. Yamazaki, *Org. Biomol. Chem.*, 2007, **5**, 2109.
367 G. S. Owens and M. M. Abu-Omar, *Chem. Commun.*, 2000, 1165.
368 W. Adam and C. M. Mitchell, *Angew. Chem., Int. Ed.*, 2003, **35**, 533.
369 J. T. Groves, R. C. Haushalter, M. Nakamura, T. E. Nemo and B. J. Evans, *J. Am. Chem. Soc.*, 1981, **103**, 2884.
370 A. Chefson and K. Auclair, *Mol. Biosyst.*, 2006, **2**, 462.
371 J. T. Groves and R. S. Myer, *J. Am. Chem. Soc.*, 1983, **105**, 5791.
372 D. Mansuy, P. Battioni, J. P. Ranud and P. Gueroin, *Chem. Commun.*, 1985, 155.
373 W. Nam, M. H. Lim, H. J. Lee and C. Kim, *J. Am. Chem. Soc.*, 2000, **122**, 6641.
374 D. Ostovic and T. C. Bruice, *Acc. Chem. Res.*, 1991, **25**, 314.
375 N. A. Stephenson and A. T. Bell, *J. Mol. Catal. A: Chem.*, 2007, **275**, 54.
376 F. S. Vinhado, P. R. Martins, A. P. Masson, D. G. Abreu, E. A. Vidoto, O. R. Nascimento and Y. Iamamoto, *J. Mol. Catal. A: Chem.*, 2002, **188**, 141.
377 T. Niwa and M. Nakada, *J. Am. Chem. Soc.*, 2012, **134**, 13538.
378 J. P. Renaud, P. Battioni, J. F. Bartoli and D. Mansuy, *Chem. Commun.*, 1985, 888.
379 P. Battioni, J. P. Renaud, J. F. Bartoli, M. Reina-Artiles, M. Fort and D. Mansuy, *J. Am. Chem. Soc.*, 1988, **110**, 8462.
380 S. Banfi, F. Legramandi, F. Montanari, G. Pozzi and S. Quici, *Chem. Commun.*, 1991, 1285.
381 R. D. Arasasingham, G. X. He and T. C. Bruice, *J. Am. Chem. Soc.*, 1993, **115**, 7985.
382 J. T. Groves and M. K. Stern, *J. Am. Chem. Soc.*, 1987, **109**, 3812.
383 W. Dai, S. Shang, B. Chen, G. Li, L. Wang, L. Ren and S. Gao, *J. Org. Chem.*, 2014, **79**, 6688.
384 S. L. H. Rebelo, A. R. Gonçalves, M. M. Pereira, M. M. Q. Simões, M. G. P. M. S. Neves and J. A. S. Cavaleiro, *J. Mol. Catal. A: Chem.*, 2006, **256**, 321.
385 R. De Paula, I. C. M. S. Santos, M. M. Q. Simões, M. G. P. M. S. Neves and J. A. S. Cavaleiro, *J. Mol. Catal. A: Chem.*, 2015, **404–405**, 156.
386 W. Zhang, J. L. Loebach, S. R. Wilson and E. N. Jacobsen, *J. Am. Chem. Soc.*, 1990, **112**, 2801.
387 E. N. Jacobsen, E. Zhang, A. R. Muci, J. R. Ecker and L. Deng, *J. Am. Chem. Soc.*, 1991, **113**, 7063.
388 A. Berkessel, M. Farauenkron, T. Schwenkreis, A. Steinmetz, G. Baum and D. Fenske, *J. Mol. Catal. A: Chem.*, 1996, **113**, 321.
389 T. Schwenkreis and A. Berkessel, *Tetrahedron Lett.*, 1993, **34**, 4785.
390 P. Pietikainen, *J. Mol. Catal. A: Chem.*, 2001, **165**, 73.
391 R. I. Kureshy, N. H. Khan, S. H. R. Abdi, S. T. Patel and R. V. Jasra, *Tetrahedron: Asymmetry*, 2001, **12**, 433.
392 C. Miao, B. Wang, Y. Wang, C. Xia, Y. M. Lee, W. Nam and W. Sun, *J. Am. Chem. Soc.*, 2016, **138**, 936.
393 O. Cussó, M. Cianfanelli, X. Ribas, R. J. Klein Gebbink and M. Costas, *J. Am. Chem. Soc.*, 2016, **138**, 2732.
394 O. Y. Lyakin, A. M. Zima, D. G. Samsonenko, K. P. Bryliakov and E. P. Talsi, *ACS Catal.*, 2015, **5**, 2702.
395 Q. Chen and E. J. Beckman, *Green Chem.*, 2008, **10**, 934.
396 R. Meiers and W. F. Holderich, *Catal. Lett.*, 1999, **59**, 161.
397 R. Meiers, U. Dingerdissen and W. F. Holderich, *J. Catal.*, 1998, **176**, 376.

398 G. Jenzer, T. Mallat, M. Maciejewski, F. Eigenmann and A. Baiker, *Appl. Catal., A*, 2001, **208**, 125.
399 R. S. Drago, S. C. Dias, J. M. McGilvray and L. M. L. Mateus, *J. Phys. Chem. B*, 1998, **102**, 1508.
400 T. Hayashi, K. Tanaka and M. Haruta, *J. Catal.*, 1998, **178**, 566.
401 W.-S. Lee, L. Lai, M. C. Akatay, E. A. Stach, F. H. Ribeiro and W. N. Delgass, *J. Catal.*, 2012, **296**, 31.
402 T. A. Nijhuis, T. Visser and B. M. Weckhuysen, *J. Phys. Chem. B*, 2005, **109**, 19309.
403 T. A. Nijhuis, B. J. Huizinga, M. Makkee and J. A. Moulijn, *Ind. Eng. Chem. Res.*, 1999, **38**, 884.
404 W.-S. Lee, R. Zhang, M. C. Akatay, C. D. Baertsch, E. A. Stach, F. H. Ribeiro and W. N. Delgass, *ACS Catal.*, 201, **1**, 1327.
405 J. Jiang, S. M. Oxford, B. Fu, M. C. Kung, H. H. Kung and J. Ma, *Chem. Commun.*, 2010, **46**, 3791.
406 J. Jiang, H. H. Kung, M. C. Kung and J. Ma, *Gold Bull.*, 2009, **42**, 280.
407 W.-S. Lee, M. C. Akatay, E. A. Stach, F. H. Ribeiro and W. N. Delgass, *J. Catal.*, 2012, **287**, 178.
408 J. J. Bravo-Suarez, K. K. Bando, J. Lu, M. Haruta, T. Fujitani and S. T. Oyama, *J. Phys. Chem. C*, 2008, **112**, 1115.
409 B. Chowdhury, J. J. Bravo-Suarez, N. Mimura, J. Lu, K. K. Bando, S. Tsubota and M. Haruta, *J. Phys. Chem. B*, 2006, **110**, 22995.
410 I. X. Green, W. Tang, M. Neurock and J. T. Yates, *Acc. Chem. Res.*, 2014, **47**, 805.
411 M. Ojeda and E. Iglesia, *Chem. Commun.*, 2009, 352.
412 J. Saavedra, H. A. Doan, C. J. Pursell, L. C. Grabow and B. D. Chandler, *Science*, 2014, **345**, 1599.
413 C.-R. Chang, Y.-G. Wang and J. Li, *Nano Res.*, 2011, **4**, 131.
414 H. V. Tran, H. A. Doan, B. D. Chandler and L. C. Grabow, *Curr. Opin. Chem. Eng.*, 2016, **13**, 100.